Poznan University of Technology

Doctoral Thesis

Non-Orthogonal Multiple Access with Successive Interference Cancellation and its Applications

Hind Salim Ghazi

Supervisor:
Prof. dr hab. inż. Krzysztof Wesołowski

Thesis submitted in fulfillment of the requirements
for the degree of Doctor of Philosophy
in the
Faculty of Computing and Telecommunications

Poznań, 2021

Abstract

Fifth Generation (5G) Mobile Network is the forthcoming revolution of mobile technology beyond 4G standards. Machines, objects, devices in addition to people can be virtually connected by a new network run by 5G technology. Recently 5G wireless communication networks attract a lot of significant research in the era of the increasing demand for connectivity. They offer a set of desirable potential features such as high data rate, ultra-low latency, higher reliability as well as low power consumption.

Non-Orthogonal Multiple Access (NOMA) with Successive Interference Cancellation (SIC) is proposed as one of the candidate radio access technologies for the upcoming 5G networks. In NOMA transmission, multiple users can simultaneously employ common resources in a non-orthogonal manner that can attain high spectral efficiency while some degree of multiple access interference is allowed at receivers.

This dissertation suggests designing of uplink NOMA transmission in multi-carrier wireless communication systems. For simplicity, an example in WiFi application (Standard IEEE 802.11a) was applied aiming to examine NOMA performance in such systems in order to achieve better Quality of Services (QoS) and hence throughput increase.

One of the crucial features of NOMA transmission is the necessity of careful selection of participating users according to their powers and channel conditions. In the context of successive interference cancellation, the research presents an improved detection algorithm, which allows for using the NOMA transmission for much smaller power differences between the users sharing common radio resources in the uplink, as compared with standard successive cancellation being applied in NOMA. The idea of this proposed algorithm lies in the application of tentative decisions about weaker signals in the detection of stronger ones and then, after improved detection of stronger user signals, achieving more reliable decisions about the weaker ones. This approach can achieve user fairness and enhance the throughput of participating users.

The final scope of this dissertation is the application of the proposed improved detection algorithm in the relay node of two-way relaying system when Physical Network Coding (PNC) is applied. PNC is one of the techniques which aim at improving network throughput. It originates from the network coding idea in which network nodes are equipped not only with routing capabilities but also can perform some mathematical operations. Two-way relaying is one of the

scenarios in which an intermediate node (relay) receives and transmits packets exchanged between two end nodes. Its efficiency can be improved when network coding is applied in the physical layer. Intensive simulations performed for the reference and proposed physical layer network coding algorithms applied in the relay of two-way relaying systems have proven that the proposed PNC detection algorithm applied in the relay can be a valuable alternative to the typical, regular one at the price of higher computational requirements in the relay, mostly in the form of separate channel decoding of both data streams generated by the end users.

Streszczenie

Sieci piątej generacji (5G) stanowią istotną rewolucję w dziedzinie technologii mobilnych względem istniejących obecnie standardów 4G. Maszyny, różne obiekty i urządzenia mogą być oprócz ludzi połączone za pomocą nowej sieci działającej zgodnie z technologią 5G. W czasach wzrastających wymagań dostępu do sieci telekomunikacyjnych sieci bezprzewodowe 5G stały się obiektem istotnych badań. Sieci te potencjalnie oferują zbiór korzystnych cech takich jak: wysoka przepływność danych, szczególnie niskie opóźnienia, wyższa niezawodność jak i niskie zapotrzebowanie na moc.

Wielodostęp nieortogonalny (NOMA – *Non-Orthogonal Multiple Access*) wraz z sukcesywną kompensacją interferencji (SIC – *Successive Interference Cancellation*) został zaproponowany jako jedna z kandydujących technologii wielodostępu we wprowadzanych sieciach 5G. W transmisji NOMA wielu użytkowników może równocześnie stosować wspólne zasoby radiowe w sposób nieortogonalny, co ma zapewnić wysoką sprawność spektralną przy pozwoleniu na pewien stopień interferencji między użytkownikami.

Niniejsza rozprawa przedstawia projekt transmisji NOMA w łączu w górę w systemach telekomunikacyjnych z wieloma podnośnymi. W celu zachowania prostoty badań symulacyjnych, zastosowano przykład w postaci systemu WiFi zgodnego ze standardem IEEE 802.11a mający na celu sprawdzenie jakości działania metody transmisji NOMA w takich systemach i zapewnienie wyższej jakości usług QoS i wzrostu przepływności.

Jedną z kluczowych cech transmisji NOMA jest konieczność ostrożnego doboru użytkowników na podstawie ich mocy i warunków propagacyjnych w ich kanałach uczestniczących w dostępie do tych samych zasobów. W kontekście sukcesywnej kompensacji interferencji przeprowadzone badania doprowadziły do zaproponowania ulepszonego algorytmu detekcji, który pozwala na zastosowanie transmisji NOMA w przypadku znacznie mniejszych różnic w poziomach mocy pomiędzy użytkownikami współdzielącymi wspólne zasoby radiowe w łączu w górę w porównaniu z tym, co zapewnia standardowa sukcesywna kompensacja interferencji stosowana w transmisji NOMA. Ideą zaproponowanego w rozprawie algorytmu jest zastosowanie tymczasowych (wstępnych) decyzji dotyczących słabszych sygnałów w detekcji silniejszych a wtedy po ulepszonej detekcji sygnałów silniejszych, uzyskanie bardziej niezawodnych decyzji dotyczących sygnałów słabszych. Takie podejście zapewnia uczciwe traktowanie użytkowników i podnosi przepustowość uczestniczących w transmisji użytkowników.

Końcowym zakresem niniejszej dysertacji jest zastosowanie zaproponowanego ulepszonego algorytmu detekcji w węźle przekaźnikowym systemu dwukierunkowej wymiany danych w przypadku, gdy zastosowano kodowanie sieciowe w warstwie fizycznej (PNC – *Physical Layer Network Coding*).

PNC jest jedną z technik mających na celu podniesienie przepustowości sieci. Pochodzi ona od idei kodowania sieciowego, w którym węzły sieci są wyposażone nie tylko w możliwości określania trasy pakietów, ale także wykonują na nich określone operacje matematyczne. Dwukierunkowa transmisja z pośrednictwem przekaźnika jest jednym ze scenariuszy, w którym węzeł pośredniczący (przekaźnik) odbiera i nadaje pakiety wymieniane pomiędzy dwoma węzłami (terminalami) końcowymi. Jej efektywność może zostać podniesiona, gdy kodowanie sieciowe jest zastosowane w warstwie fizycznej. Przeprowadzono intensywne symulacje dla określenia jakości systemu PNC w jego standardowej wersji i w wersji z zaproponowanym algorytmem detekcji w przekaźniku, które pokazały, że zaproponowany algorytm detekcji działający w przekaźniku może być wartościową alternatywą dla typowego algorytmu za cenę wyższych wymagań obliczeniowych w przekaźniku w większości z postaci osobnego dekodowania kodów kanałowych zastosowanego w obu strumieniach danych generowanych przez użytkowników końcowych.

Acknowledgements

Firstly, I would like to express my special thanks to my patient and supportive supervisor, Professor Krzysztof Wesołowski. His support, guidance and overall insights in this field have made this an inspiring experience for me.

My biggest thanks to my husband Mohammed Khafaji for providing guidance, and for his patience and encouragement, without which I would have stopped these studies a long time ago. I also thank my lovely son Aiham who encouraged me by his beautiful smiles and innocent words.

I cannot forget to thank my family and friends especially my kind mum Rajaa. Your love, support and encouragement that gave me the strength to complete this dissertation.

I also wish to thank my brother-in-law Adnan for his encouragement and for his kind words that supported me for completing the study.

Finally, many thanks to all participants that took part in the study and enabled this research to be possible.

Table of Contents

List of Figures

List of Tables

List of Abbreviations

1G	First Generation of Mobile Cellular Systems
2G	Second Generation of Mobile Cellular Systems
3G	Third Generation of Mobile Cellular Systems
3GPP	3rd Generation Partnership Project
3GPP2	3rd Generation Partnership Project number 2
4G	Fourth Generation of Mobile Cellular Systems
5G	Fifth Generation of Mobile Cellular Systems
AP	Access Point
AWGN	Additive White Gaussian Noise
BC	Broadcast
BCs	broadcast channels
BER	Bit Error Rate
BS	Base Station
CA	Collision Avoidance
CDMA	Code Division Multiple Access
CEPT	Telecommunications Commission of the European Conference of Postal and Telecommunication Administrations
CIR	Committed Information Rate
CoMP	Coordinated Multi-Point
CPU	Central Processing Unit
CSI	Channel State Information
CSIT	Channel State Information at Transmitter
CSMA	Carrier Sense Multiple Access
CSS-PA	Channel State Sorting-Pairing Algorithm
D2D	Device-to-Device
DECT	Digital Enhanced Cordless Telephony
DoF	Degrees of Freedom
DPA	Determinant Pairing Algorithm

DS-SS	Direct Sequence Spread Spectrum
EDGE	Enhanced Data Rates for GSM Evolution
eMBB	enhanced Mobile Broadband
EPA	Expectation Propagation Algorithm
ESE	Elementary Signal Estimators
FDM	Frequency Division Multiplexing
FDMA	Frequency Division Multiple Access
FFT	Fast Fourier Transform
FH	Frequency Hopping
FH-CDMA	Frequency Hopping Code Division Multiple Access
FHSS	Frequency Hopping Spread Spectrum
FM	Frequency Modulation
FN	Factor Nodes
FPA	Fixed Power Allocation
FTPA	Fractional Transmit Power Allocation
GPRS	General Packet Radio Services
GSM	Global System for Mobile Communications
IC	Interference Cancellation
IDMA	Interleave Division Multiple Access
IEEE	Institute of Electrical and Electronic Engineers
IFFT	Inverse Fast Fourier Transform
IMT-2000	International Mobile Telephony by the Year 2000
IoT	Internet of Things
IRC	Interference Rejection Combining
ISI	Inter-Symbol Interference
ITU-R	International Telecommunications Union Radio Communications
ITU-T	International Telecommunications Union Radio Telecommunications
IWPA	Iterative Water Power Allocation
JD	Joint Detection
LAN	Local Area Network
LDS	Low-Density Spreading

LFSR	Linear Feedback Shift Registers
LLR	log-Likelihood Ratio
LTE	Long Term Evolution
MAC	Medium Access Control
MACs	Multiple Access Channels
MAI	Multiple Access Interference
MC-NOMA	Multi-Carrier NOMA
MCS	Modulation and Coding Schemes
MIMO	Multi-Input Multi-Output
ML	Maximum Likelihood
MMSE	Minimum Mean Square Error
mMTC	massive Machine Type Communications
MPA	Message Passing Algorithm
M-QAM	M element Quadrature Amplitude Modulation
MUD	Multiple User Detection
MUST	Multi-User Superposition Transmission
NC	Network Coding
NMIMO	Network Multiple Input-Multiple Output
NOMA	Non-Orthogonal Multiple Access
NR	New Radio
OFDM	Orthogonal Frequency Division Multiplexing
OFDMA	Orthogonal Frequency Division Multiple Access
OMA	Orthogonal Multiple Access
OPA	Orthogonal Pairing Algorithm
OVSF	Orthogonal Variable Spreading Factor
PDC	Personal Digital Cellular
PDP	Power Delay Profile
PIC	Parallel Interference Cancellation
PN	Pseudo Noise
PNC	Physical Layer Network Coding
PSK	Phase Shift Keying

QoS	Quality of Services
QPSK	Quadrature Phase Shift Keying
RE	Resource Elements
RF	Radio Frequency
RPA	Random Pairing Algorithm
SC	Superposition Coding
SC-FDMA	Single-Carrier Frequency Division Multiple Access
SC-NOMA	Single-Carrier Non-Orthogonal Multiple Access
SIC	Successive Interference Cancellation
SINR	Signal-to-Interference plus Noise Ratio
SIR	Signal-to-Interference Ratio
SISO	Single Input - Single Output
SNR	Signal-to-Noise Ratio
SoI	Signal of Interest
TCMA	Trellis Coded Multiple Access
TDMA	Time Division Multiple Access
TWRC	Two-Way Relaying Channel
UE	User Equipment
UMTS	Universal Mobile Telecommunications System
URLLC	Ultra-Reliable and Low-Latency Communications
V2X	Vehicle-to-Everything
VN	Variable Nodes
WARC	World Administrative Radio Conference
WCDMA	Wideband Code Division Multiple Access
WiMAX	Worldwide Interoperability for Microwave Access
WNC	Wireless Network Coding
WPNC	Wireless Physical Network Coding

Chapter 1

Introduction

1.1 Preface

It has been observed that there is an evolutionary change in mobile communications systems shown clearly every decade. Commercial wireless systems and services have undergone a remarkable development since they started to operate.

The early 1970s saw the emergence of the radio technology that was needed for the deployment of mobile radio systems in the 800/900MHz band at a reasonable cost; the first generation (1G) of mobile cellular systems were introduced in the Scandinavian countries in 1981 and early 1982. Spain, Austria, the United Kingdom, the Netherlands, Germany, Italy, and France followed with their own systems in the period 1982–1985. These systems were based on frequency division multiple access (FDMA) and analog FM technology and designed to carry narrow band circuit switched voice services, but the problem was that they were different from each other and incompatible. This meant communication was generally restricted to one country only [Msh12].

The second generation (2G) of mobile cellular systems were developed in the 1980s and early 1990s, and widely deployed throughout the world in the 1990s. Due to limitation of the first generation of mobile cellular systems in achieving the interoperation between the European countries' networks the Telecommunications Commission of the European Conference of Postal and Telecommunication Administrations (CEPT) established in 1982 a study group called the Groupe Spécial Mobile (GSM) to develop the specifications and define standards for the future Pan-European cellular radio systems. 2G systems were started to operate with the digital transmission and use either time division multiple access (TDMA) or code division multiple access (CDMA) as a multiple access technology. They were operating within several standards such as GSM/DCS1800 standard in Europe, PCS1900 in the USA, the Personal Digital Cellular (PDC) standard in Japan, and the IS-54/136 and IS-95 standards in the USA. The GSM system (newly called "Global System for Mobile Communications") was developed to operate in a new frequency allocation. It offered high spectral efficiency with a better quality of services. Pan-

European roaming and support of data services were the key objectives of GSM system. Originally, besides digital speech transmission, 2G standards started to offer data rates up to 9 kbps. Then some extensions were introduced in order to provide higher data services such as General Packet Radio Service (GPRS) that provided data rates up to 140 kbps, whereas Enhanced Data Rates for GSM Evolution (EDGE) introduced higher speed data transmission (it provides data rates up to 473.6 kbps) by applying a higher-level 8-PSK modulation format and some other improvements in data transmission [Stü17].

Third generation (3G) cellular systems were envisioned as ubiquitous wireless systems that could support voice, multimedia, and high-speed data communication. In March 1992, the World Administrative Radio Conference (WARC) approved a worldwide spectral allocation in support of IMT-2000 (International Mobile Telephony by the Year 2000) in the 1885–2200 MHz band. The IMT-2000 standard was developed by the International Telecommunications Union Radio Communications (ITU-R) and Telecommunications (ITU-T) sectors. It provided different data rates depending on mobility and location of mobile stations from 384 Kbps for pedestrian use to 144 Kbps for vehicular use and to 2 Mbps for indoor office use. IMT-2000 was actually a family of requirements. Two of the standards fulfilling these requirements were based on TDMA approaches, namely EDGE and Digital Enhanced Cordless Telephony (DECT). While, the most predominant forms of IMT-2000 were cdma2000 developed by the *3rd Generation Partnership Project* number 2 (3GPP2) consortium and the Universal Mobile Telecommunications System (UMTS) family of standards developed by 3rd Generation Partnership Project. The latter set of standards includes wideband code division multiple access (WCDMA). The main distinctions between WCDMA and cdma2000 centered around the chip rate that is used, as well as synchronous (cdma2000) vs. asynchronous (WCDMA) network operation [Sch05].

The fourth generation of cellular system is the most innovative wireless technology which gradually replaced the 3G systems. 4G provides access to wide range of telecommunication services, including advanced mobile services, supported by mobile and fixed networks. Fourth generation cellular systems have capabilities defined by the ITU-R in IMT-Advanced requirements. IMT-Advanced specifies peak data rates of 100 Mbps in high mobility applications and 1 Gbps in stationary or low mobility applications. Unlike the 3G cellular systems that have used CDMA technology, the 4G cellular systems utilize multi-carrier based multiple access methods, namely orthogonal frequency division multiple access (OFDMA) and

single carrier frequency division multiple access (SC-FDMA). Commercially, there were two candidates of 4G systems. The first one was Long Term Evolution (LTE) that was standardized by 3GPP although it has not fulfilled all the IMT-Advanced requirements, while the other was IEEE 802.16e (Mobile WiMAX (Worldwide Interoperability for Microwave Access)) standardized by the Institute of Electrical and Electronics Engineers (IEEE). Thereafter more advanced versions of 4G standards were introduced as Long Term Evolution Advanced (LTE-A) and Mobile WiMAX Release 2 (IEEE 802-2012). LTE-A is based on LTE to further increase data rate as defined in 3GPP Releases 10 and 11. From the other hand, WiMAX is a telecommunications protocol that provides fixed and fully mobile Internet access. There are several versions of the WiMAX standard, IEEE 802.16-2004 also known as 802.16d, is sometimes referred to as fixed WiMAX since it does not support the mobility. Whereas IEEE 802.16e-2005 often abbreviated as 802.16e and commonly known as Mobile WiMAX due to its support for mobility among other things, it delivers the mobile broadband services with peak data rates up to 40 Mbps at vehicular speeds greater than 120 kmph [Stü17, KAS13].

The rapid escalation in multimedia devices such as smartphones and tablets, and explosive growth in mobile access to Internet and creation of the Internet of Things (IoT) triggered the design of the next generation of cellular networks that can offer further significant improvements in coverage and user experience [MHL19]. The fifth generation of mobile communications (5G) is is currently in the phase of deployment and it becomes a focal point for academic and industrial communities [AXI14]. The next generation of mobile technology is presently facing a new challenge, giving birth to a hyper-connected society through the emergence of its services. 5G networks will introduce a scenario in which seven trillions of wireless devices will serve seven billions of people sharing the even more scarce physical spectral resources and generating 49 exabytes of global mobile data traffic per month. 5G technology is expected to support three typical usage scenarios, including enhanced mobile broadband (eMBB), massive machine type communications (mMTC) and ultra-reliable low-latency communications (URLLC). It will able to meet the following key features as compared to existing 4G systems: 10–100 times increased data rate, up to 99.99% availability, reduced delays, 10–100 times higher number of connected devices, guaranteed coverage, 10 times reduced energy consumption, and efficient incorporation of existing wireless technologies with new 5G techniques [IAD16]. Non-orthogonal multiple access (NOMA) has been recently recognized as the new candidate of multiple access technique

for 5G networks due to its superior spectral efficiency, although it was already proposed for the 4th generation LTE-Advanced system. NOMA is currently under the consideration by 3GPP. 3GPP release 16 has presented the study on NOMA performance for the new radio (NR). Recall that NR denotes new physical layer transmission standard applied in 5G systems. The key idea behind NOMA transmission is allowing multiple users within the same cell to share simultaneously the same physical resource blocks, e.g., time, frequency, or spreading code. Consequently, NOMA can offer some features, including improved spectral efficiency, massive connectivity, higher cell-edge throughput, low transmission latency, and user fairness. The available NOMA technology can be broadly divided into two categories, namely, power-domain and code-domain NOMA [LNL18].

In this dissertation, the performance of uplink NOMA transmission aided by the principle of successive interference cancellation (SIC) is discussed. In the literature, various channel models were exploited to examine NOMA performance. The proposed model aims to achieve better QoS and hence throughput increase. Selection of participating users depends on the principle of user pairing algorithms, whereas the allocation of transmission power to users is based on the power allocation algorithms. Only Uplink NOMA transmission is investigated, as the implementation of multi-user detection and interference cancellation schemes is performed in a centralized entity (at base station (BS)) and it is relatively uncomplicated.

1.2 Purpose and Theses

Three problems have been investigated by the author of this thesis, namely:

- The spectral efficiency NOMA transmission with appropriately designed receivers,

NOMA can increase the spectral efficiency of digital communications and enhance the users' throughput by allowing several terminals to simultaneously transmit and receive the information upon the same radio resource. We aim to further increase the spectral efficiency by appropriate NOMA receiver design.

- Reducing the range of power differences between the terminals sharing common radio resources in uplink transmission through the use of proposed SIC detection.

The improved SIC detection algorithm has been proposed in order to reduce the range of power differences between the users sharing the same physical resources (time/ frequency). The key idea of improved detection method is represented by employing tentative decisions of weaker signals in the detection process of stronger ones and then, using the improved detection of stronger user signals for achieving more reliable decisions about the weaker ones.

- Improvement of transmission quality in two-way relaying systems using physical layer network coding by NOMA-specific methods.

Application of the proposed SIC receiver can also be applied in two-way relaying in case of employing physical layer network coding (PNC) principle during the transmission. We investigate possibility of achieving higher performance of such transmission using the proposed SIC receiver.

Consequently, theses of this dissertation can be formulated as:

- The performance of uplink NOMA transmission aided by the principle of successive interference cancellation can be significantly improved in digital communications through employing a new detection algorithm which enables the receiver to correctly detect the information of participating users even though the differences in power levels allocated to them are very small.
- The transmission quality of two-way relaying can be enhanced through employing the proposed SIC detection at the relay receiver in such a system.

1.3 Outline of the contents

This thesis is organized in six chapters, as follows:

- ❖ Chapter 2 presents the background information of multiple access techniques that were utilized in each generation of the mobile technologies. Moreover, state-of-the-art literature of the new multiple access (NOMA) technique which fulfills the needs of next generation of wireless communications is surveyed. Some power allocation algorithms namely iterative water power allocation, fixed power allocation, and fractional transmit

power allocation, as well as user pairing algorithms including random pairing algorithm, orthogonal pairing algorithm, determinant pairing algorithm, and channel state sorting-pairing algorithm are presented in the last part of this chapter.

- Chapter 3 introduces the fundamentals and applications of interference cancellation methods and the focus is laid on successive interference cancellation which is proposed as one of the key technologies supporting NOMA transmission. Analysis of successive interference cancellation performance in both downlink and uplink NOMA networks is presented in detail. Furthermore, simulation results are addressed to evaluate the performance of uplink NOMA transmission based on Wi-Fi application.

- In Chapter 4, the concept of the proposed SIC detection algorithm is introduced and its performance analyses are given. BER measurements are investigated to examine the performance of improved SIC detection compared to the standard SIC technique.

- Chapter 5 takes into account the possibility to use the proposed SIC detection algorithm at the relay receiver of two-way relaying in case of employing physical layer network coding during the data transmission. A simple comparison of receiver's performance of both PNC and proposed SIC transmission methods is introduced through presenting some experimental results.

- Chapter 6 concludes the work of this thesis and shows interesting future research directions.

Chapter 2

Non Orthogonal Multiple Access Technique

In wireless communications systems, multicarrier transmission has been found as the one which is able to enhance the bandwidth, efficiency, data rate, and furthermore increase the number of served users within the network cells [RBK14]. The multiple access techniques allow the network nodes (cells) and users to transmit and receive data simultaneously via the shared medium (i.e., channel) with the minimum level of interference [SM14], therefore subsequent generations of mobile communications have employed several multiple access techniques for data exchange between a base station (BS) and mobile users allocated to it [AGS18].

This chapter presents a general view of the multiple access technique fundamentals that are used in each generation of the mobile technologies besides the new promising multiple access technique for the fifth generation of wireless systems.

2.1 General overview of multiple access techniques

In this section, the author refers to the system resources assigned to users to communicate with the network with an acceptable interference level. There are different types of access to these resources, such as Frequency Division Multiple Access (FDMA), Time Division Multiple Access (TDMA), Code Division Multiple Access (CDMA) and Orthogonal Frequency Division Multiple Access (OFDMA).

2.1.1 Frequency Division Multiple Access (FDMA)

It was the first multiple access technique in cellular systems. In this channel access scheme, the principle of frequency division multiplexing (FDM) has been applied [RBK14]. For unidirectional systems such as radio broadcasting and TV several non-overlapping frequency ranges are set for various channels and, in turn, for several users within the same system bandwidth. In bidirectional transmission systems like mobile communication, each user has a pair of different carrier frequencies allocated for transmitting and receiving data. One of them is used for the downlink (communication from a base station to a user) and the other is assigned for the uplink (communication from a user to its assigned base station) [SM14].

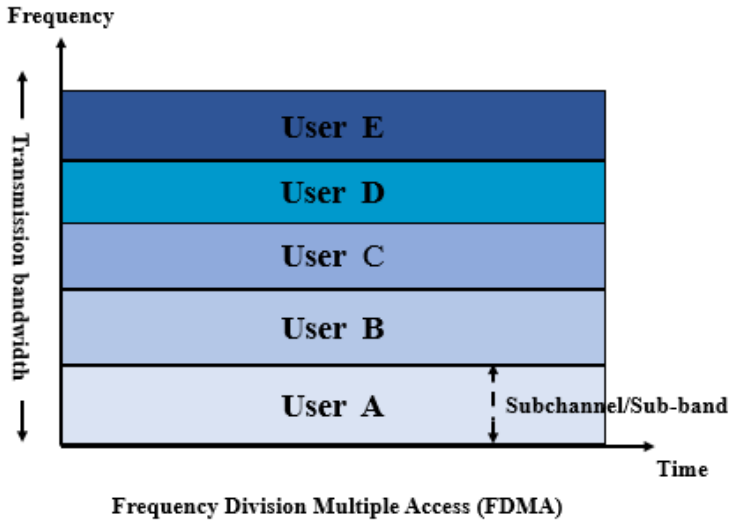

Figure 2.1 Frequency Division Multiple Access scheme [Ahm13]

2.1.2 Time Division Multiple Access (TDMA)

Time Division Multiple Access (TDMA) is the common access technique that has been used in wired and wireless digital transmission systems. In TDMA, the time axis is split into a series of repeating time slots on a regular basis. Each time a slot is assigned for data transmission and allocated for one user only [Wes09]. For example, in a TDMA system with two users they can share the channel on the same carrier frequency according to the following scenario: the first user tries to get access to the frequency with a fixed short time period, then the channel returns to the second user with same time period that has been allocated to the first one. This cycle is repeated again regularly for both users [RBK14]. Organization of the time slots per frame is influenced by many factors such as modulation technique and allocated bandwidth [SM14].

One of the most common advantages of TDMA over FDMA is achievable bit rates of transmission to/from individual user terminals, which can be controlled according to the current user demands through increasing the number of allocated time slots to the user [FAG95]. However, TDMA has also some drawbacks. The first drawback is visible in case of a TDMA system with N users, where each user has $1/N$ duty cycle. It means, a user has a periodically pulsating power envelope which is considered as a challenge for designers to provide portable RF units. The second drawback can be summarized by frequency and time slots assignment and management which in turn add extra complexity to a TDMA system. Furthermore, a TDMA

system may require channel equalization due to *N* times higher bit rates [RBK14, FAG95], so multipath effect becomes visible.

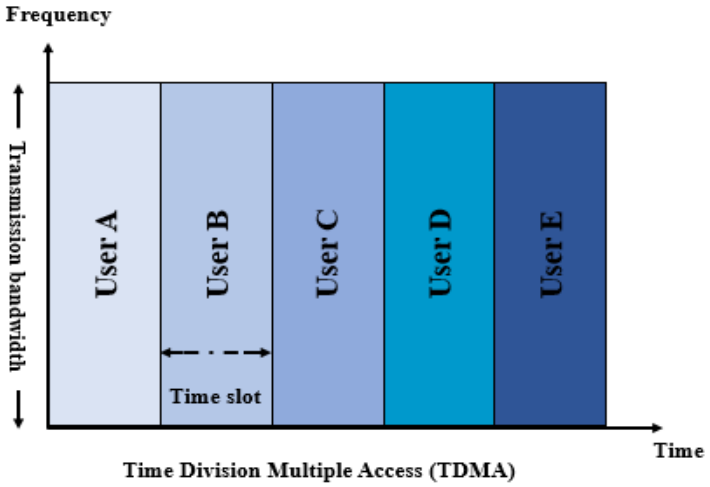

Figure 2.2 Time Division Multiple Access scheme [Ahm13]

2.1.3 Code Division Multiple Access (CDMA)

Code Division Multiple Access **(**CDMA) is the multiple access technology that has been widely used in the cellular and satellite systems. CDMA used in these systems is based on direct sequence spread spectrum (DS-SS) technique and a special coding scheme to authorize multiple users to share the same physical channel [Sin13]. In spread spectrum technique the user data are spread over much larger band than that required by transmitted user data rate [Ilc13]. Bandwidth expansion is carried out by using the spreading code or pseudo-noise (PN) sequence that is independent of message and is known at the receiver side. At the transmitting side, each transmitter is assigned a code different from others, and these codes are selected to be orthogonal or quasi-orthogonal to each other [SM14, Stü17]. Impact of multiplying information bits by the pseudo-random sequence is to transform the binary information stream to a noise-like sequence of much wider spectral width [Sch04].

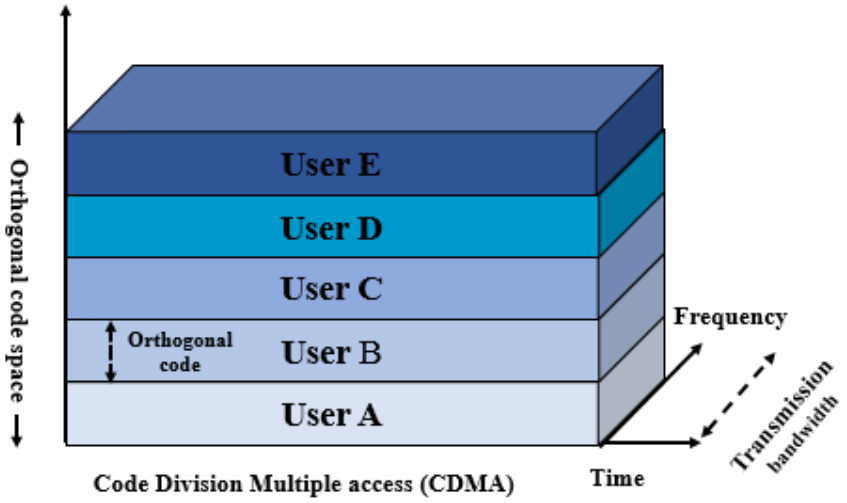

Figure 2.3 Code Division Multiple Access scheme [Ahm13]

At the reception side, the multiplication by the same pseudo-random sequence is implemented to reproduce the original information bit stream. Other coded signals that use the same carrier frequency are dismissed due to the orthogonality of applied spreading codes [SM14, Stü17]. Separation of received signals is implemented by correlating the received coded signal with a synchronized replica of the spreading code for the desired user [Sch04].

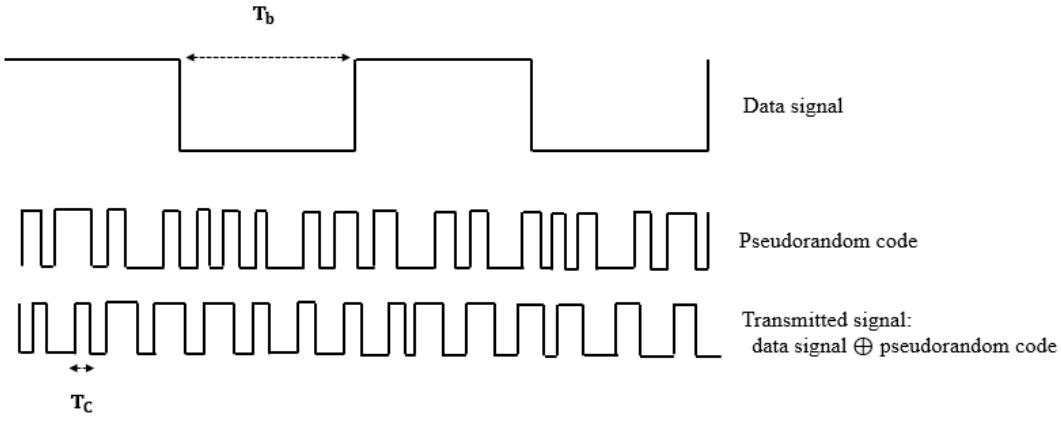

Figure 2.4 Generation of Code Division Multiple Access scheme [Stü17].

There are different types of spread spectrum schemes. Two dominant types are direct sequence spread spectrum (DS-SS) and frequency hopping spread spectrum (FH-SS) methods.

DS-SS-CDMA is accomplished by multiplying the original data by a faster-rate spreading code being a sequence of chips (binary short pulses). The resulting signal modulates a wideband carrier. The chip rate of the spread (coded) signal is much greater than the bit rate of a data signal. At the reception side, a different scenario is applied: the receiver despreads the received signal by using the same code that is used by the transmitting terminal. Synchronization plays an essential role, namely, the locally generated code sequence must be synchronized with the received signal, otherwise, the original signal cannot be retrieved [Kor03].

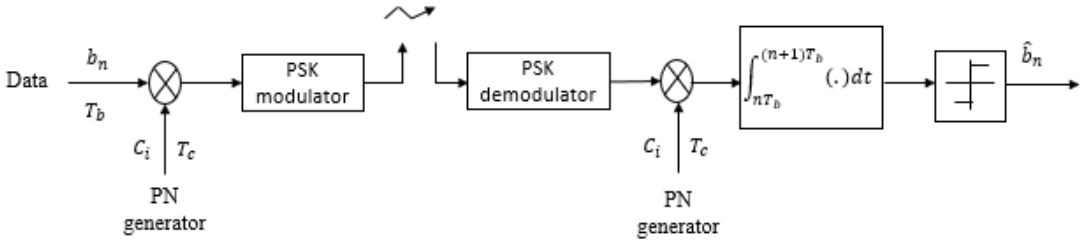

Figure 2.5 Basic scheme of a direct sequence spread spectrum system [Wes09]

Frequency hopping spread spectrum (FH-SS) was formally one of the basis of the baseline IEEE 802.11 standard that was released in 1997 (it utilized PSK modulation with FH-SS or DS-SS), however, it is obsolete now. The basic principle of frequency hopping spread spectrum (FH-SS) is to hop the modulated data signal over a wide bandwidth through changing its carrier frequency according to a spreading code. The spreading code blocks are fed to the frequency synthesizer in order to produce the hopping carrier signal, which in turn feeds the modulator to upconvert the modulated signal to the carrier frequency. This modulator can be either coherent or non-coherent or may be differentially coherent, but a non-coherent modulator is the most common due to the difficulties in maintaining a coherent phase reference during hopping the carrier over a wide bandwidth. At the reception side, the same synchronizer is also employed in order to synchronize incoming signal with the pseudorandom sequence of frequencies that is locally generated. When this synchronization is perfectly obtained, spreading code supplied to the frequency synthesizer creates the hopping pattern of the carrier, which enables the demodulator to down convert the received signal [Gol05].

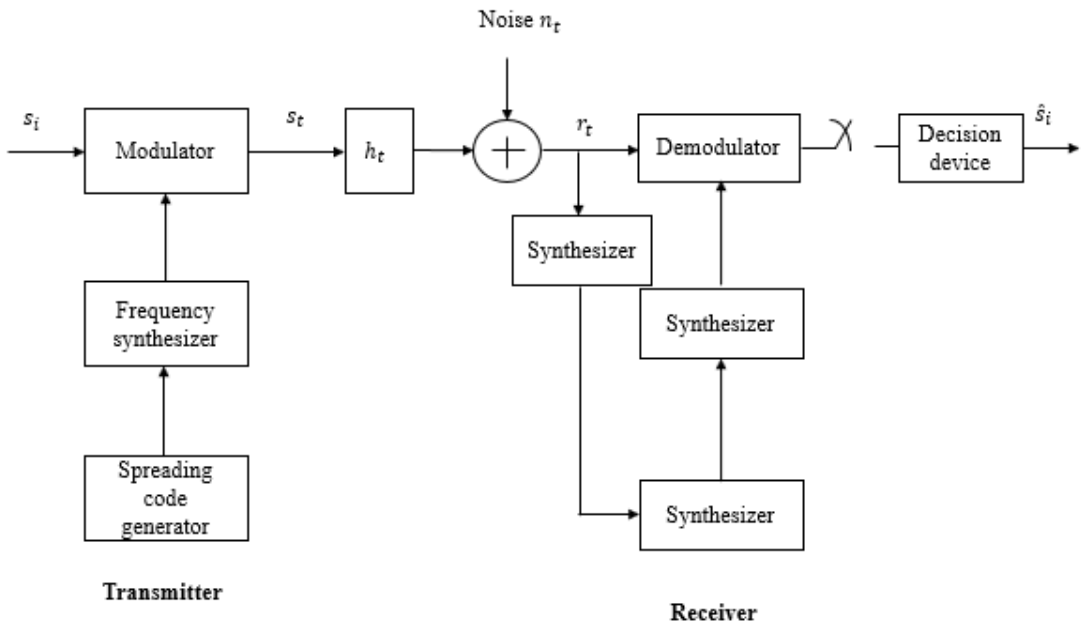

Figure 2.6 Frequency hopping spread spectrum system scheme [Gol05].

In multiuser FH-SS systems, a unique spreading code sequence is assigned to each user to generate his hop pattern. If the users are synchronized in time, and the spreading codes are orthogonal the collisions between users never occur and the performance of each user is similar to that in a single-user FH system. Whereas, the users will collide if they are asynchronous or non-orthogonal codes are employed. Multiuser FH-SS typically utilizes error correction coding to compensate for collisions.

Multiuser FH-SS also referred to as Frequency Hopping-Code Division Multiple Access (FH-CDMA) is the preferred method for military applications due to the anti-jam protection and low probability of interception and detection inherent to FH systems. It was suggested as a candidate for second generation digital cellular systems, but it was not adopted. Moreover, FH-CDMA is also utilized in the Bluetooth system.

Several types of CDMA schemes have been addressed. They are divided into two categories. The first category is a single-carrier CDMA which is based on a single carrier transmission, whereas the second one is represented by a multi-carrier CDMA that employs the multicarrier

transmission as a basis. Both these types are based on spread spectrum techniques [Wes09]. In real wireless 3G cellular systems, a single-carrier CDMA is applied.

2.1.4 Orthogonal Division Multiple Access

Orthogonal Frequency Division Multiple Access (OFDMA) is considered as a special type of FDMA, which can be used for radio transmission and reception in LTE besides several other radio communication systems, such as WiMAX (IEEE 802.16).

OFDMA plays the same role as any other multiple access techniques, namely, it enables the base station to communicate with different mobile users through allocating an individual subcarrier or, more often, a group of subcarriers to various users [Cox12].

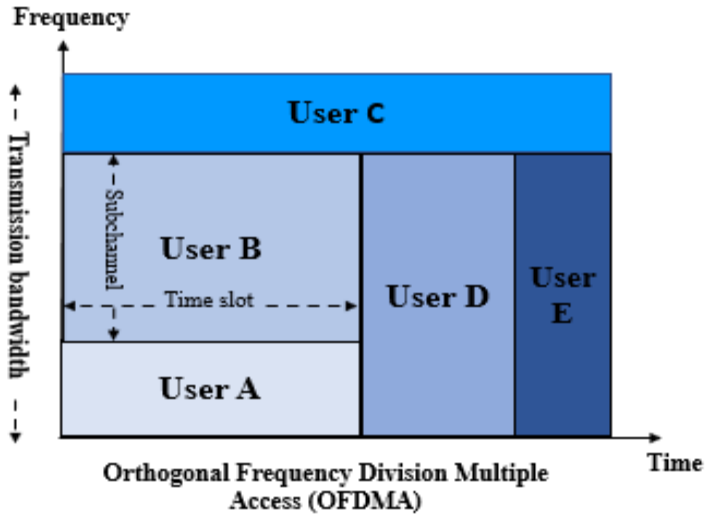

Figure 2.7 Orthogonal Frequency Division Multiple Access scheme [Ahm13]

Different methods have been employed to distribute the subcarriers among users when OFDMA technique is applied. The most popular subcarrier arrangements are represented by the grouped subcarriers and interleaved spread subcarriers.

When the grouped subcarriers method is utilized a group of contiguous subcarriers is assigned for each user. In the second type of subcarrier arrangement a fixed comb pattern of subcarriers is allocated, that means they can be spread over the whole system bandwidth. The grouped subcarrier method can reduce inter-user interference, even though, it is considered to be more sensitive to fading, as a whole group of contiguous subcarriers assigned to a specified user

can suffer from similar deep fading in the channel characteristics. Benefit from using spread subcarrier method is reduction of the sensitivity of the transmission performance to fading, although transmission from several nodes to a single base station is more liable to inter-user interference especially if these users are imperfectly synchronized in frequency and time [Wes09].

OFDMA is derived from Orthogonal Frequency Division Multiplexing (OFDM) transmission therefore a simple explanation of OFDM principle is presented. The basic principle of OFDM is to split the available spectrum into narrowband parallel channels with subcarriers in their middles, and then transmit the information signal on these parallel subcarriers at a reduced signaling rate. The term OFDM turns our attention to the fact that spectra of the signals transmitted on the subcarrier frequencies are overlapped and the subcarrier signals themselves are mutually orthogonal in the selected time intervals. The benefit of applying this technique is to permit each channel to experience almost flat fading which facilitates the simple channel equalization process [Kha09].

In each OFDM symbol interval, modulating symbols are transmitted in parallel on different subcarriers. Any modulation scheme such as QPSK, or *M*-QAM (*M*=16, 64, etc.) can be applied. The subcarrier spacing that is set between neighboring subcarriers depends on type of environment in which the OFDM system operates. It is determined by some parameters such as maximum expected time dispersion and maximum expected Doppler spread [DSJ16].

2.2 Orthogonal versus non-orthogonal multiple access techniques

Multiple access techniques are the key part of radio access technologies for cellular communications. These techniques can be classified into orthogonal and non-orthogonal multiple access methods.

In orthogonal multiple access techniques (OMA), signals transmitted by different users are orthogonal to each other either in frequency, time or code domains in order to mitigate the multiple access interference (MAI) effect. So, their cross-correlation in the appropriate domain is zero. This principle has been simply employed in frequency division multiple access, time division multiple access, code division multiple access, and orthogonal frequency division multiple access [Rum13].

Non-orthogonal strategy in wireless communication schemes allows non-zero cross correlation among the signals from different users, such as in Trellis-Coded Multiple Access (TCMA) and Interleave Division Multiple Access (IDMA) [WJP06].

OMA have failed to fulfill the future communication systems' stringent requirements such as high spectral efficiency, massive connectivity with various QoS, low latency, as well as user fairness. All these requirements are considered as a challenge in the new promising communication systems [WYN16]. Therefore, Non-Orthogonal Multiple Access (NOMA) is proposed as one of promising technologies aiming to fulfill the new requirements.

Non-orthogonal multiple access is the promising technique for designing a new radio access for the fifth generation (5G) of wireless communications networks. NOMA enables high spectral efficiency through combining the concept of Superposition Coding (SC) that is employed at transmitting side with Successive Interference Cancellation (SIC) principle that can be applied at the reception side [DLK17, TI15].

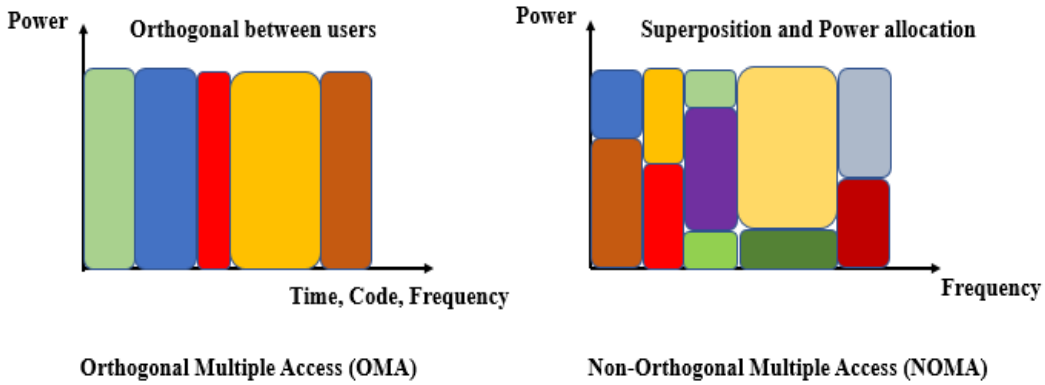

Figure 2.8 Resources allocation in Orthogonal and Non-Orthogonal Multiple Access techniques [WYN16]

2.2.1 CDMA interference limited method with quasi-orthogonality

Code division multiple access based on direct sequence spread spectrum is theoretically orthogonal method of sharing the radio resources in form of channel bandwidth and time. In reality the orthogonality is not perfect. The reasons for it are multifold. If the spreading sequences used by a CDMA system are based on pseudonoise (PN) sequences generated by linear feedback shift registers (LFSR) determined by irreducible polynomials (so called *m*-

sequences), they are quasi-orthogonal only. Cross-correlation of any pair of such PN sequences is not perfectly equal to zero. Moreover, the cross-correlation of a given sequence with its own circular shift (i.e., its autocorrelation) is non-zero either, although its value is small with respect to the peak of the autocorrelation function. The situation becomes even worse when the spreading sequence has its period longer than the data symbol duration what is a typical situation. Therefore, *m*-sequences are not applied in its pure form to play a function of CDMA spreading sequences. In real CDMA systems purely deterministic sequences featuring perfect orthogonality on a transmitter side are applied. They are Walsh functions (in cdmaOne IS-95 2G American CDMA system, or cdma2000), or Orthogonal Variable Spreading Factor (OVSF) sequences (in 3G UMTS systems and its extensions). These sequences determine the channels which are used by different parallel links. For that reason, they are called channelization codes [Mol12]. However, CDMA systems operating in cellular communications require differentiation of neighboring cells in the downlink communication and the users in uplink as well. For that reason, additional spreading sequences are applied which do not extend the spectral width any more (they have the same chip rate as the channelization sequences) but constitute signatures of the given cell or the particular user. The spreading sequences are based on partial *m*-sequences (in cdmaOne system) or segments of Gold sequences (in UMTS). These sequences are not perfectly orthogonal to each other. Additionally, although channelization codes are perfectly orthogonal on the transmitter side, they lose their mutual orthogonality after transmission over a multipath radio channel, as these sequences are not fully orthogonal with respect to their own shifts. The result of these imperfections is interference among users observed on the output of the correlative receiver. More users transmit in parallel, more interference appears on the receiver output, so signal-to-interference+noise ratio (SINR) decreases. In order to ensure the sufficient detection quality, SINR should not fall below a given threshold. Therefore, we can declare that practical CDMA systems are interreference-limited as the number of links running in parallel depends mainly on SINR. In practice not all available channelization codes can be used at the same time, so their number is not practical limitation for the system.

2.2.2 Intentionally non-orthogonal multiple access

During recent intensive development of wireless mobile communication systems, the number of devices connected to them tremendously increases, however, at the same time spectral resources are very limited. Therefore, reusing them a few times for different users and applications is one of the methods to ease the problem of the access to the spectrum. Additionally, demand for Internet of Things (IoT) launched the exigency to connect every person and every object to the network [ATG18].

Current communication systems have some limitations, which in turn restrict any improvements that may occur on the systems to meet the future wireless communication system requirements. This reason leads the researchers to develop suitable techniques and maybe to integrate them in the next-generation of wireless communication systems in order to principally fit the emerging requirements that include very high spectral efficiency, very low latency, massive device connectivity, high achievable data rate, user fairness, high throughput, support for diverse quality of services (QoS), energy efficiency, and low cost [ABC14].

Over the past few decades, wireless communication systems have been employing orthogonal multiple access techniques (OMA) to connect users with the networks. As we have already mentioned above, wireless resources allocated to multiple users are orthogonal either in time, frequency, or code. Separation of users' data can be achieved easily at a low complexity through utilizing relatively cost-efficient receivers.

In fact, these techniques have faced many problems. One of them is the insufficient number of supported users that is limited by the number of available orthogonal resources.

The second problem is the loss of orthogonality in resources that results from channel-induced impairments, which in turn requires invoking some high-complexity measures to restore the orthogonality like multi-user equalizers [DWD18].

OMA faces another limitation represented by spectral inefficiency. It allows user with a poor channel conditions to reserve one of the scarce bandwidth resources in case if that user has high priority data to be sent or that user has not been served for a long time. This problem negatively influences the spectral efficiency and throughput of the overall system [DLK17].

Regarding user fairness, low latency, and massive connectivity in OMA, for example in OFDMA with scheduling, a high priority for serving is returned to the user with a good channel

condition, while the user that has bad channel condition should wait for access. That finally causes a fairness problem and high latency.

All above limitations of OMA made it less applicable and insufficiently suitable to provide the features required by the future generations of wireless communication systems. Consequently, researchers have proposed NOMA as a strong candidate to represent a multiple access technique for the next generations of wireless systems [Lee18].

Two basic terms, namely, Superposition Coding (SC) and Successive Interference Cancellation (SIC) have been addressed to make non-orthogonal multiple access possible to apply. NOMA exploits the principle of superposition coding at the transmitting side to superimpose different users either in power-domain or code-domain, since these users are sharing frequency or spreading code at the same time. Concurrently, the users within the system can be assigned into multiple groups. NOMA is implemented in each group, and thus the orthogonal bandwidth resources have been assigned to these groups. At the receiving side, the principle of successive interference cancellation is applied to detect and decode received messages [KH14, DFP15].

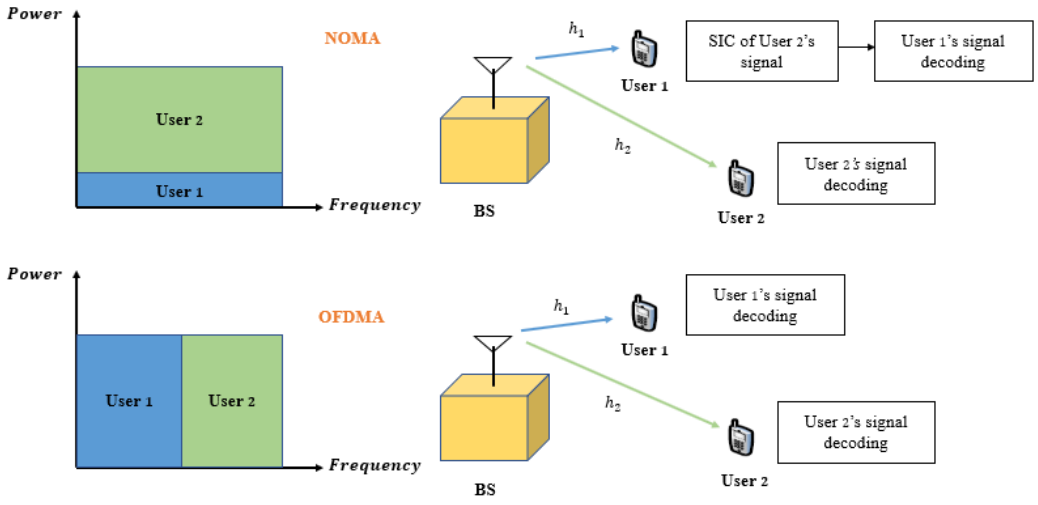

Figure 2.9 Simple comparison between NOMA and OMA that is represented by OFDMA [Kha17]

There are two main schemes of NOMA: a single-carrier NOMA (SC-NOMA) and multi-carrier NOMA (MC-NOMA). In a single-carrier NOMA (SC-NOMA) scheme the base station serves two users simultaneously through assigning the same resource block to them. Multi-carrier NOMA (MC-NOMA) is considered as a special case of hybrid NOMA. The users in a network have been split into multiple groups. Particularly, the users in each group can be served by the same orthogonal resource block through employing the NOMA principle. Different orthogonal resource blocks are assigned to various groups. Intra-group interference is mitigated via using concept of NOMA [WYN16, DLK17].

On the other hand, NOMA can be primarily classified into a pair of categories, called code-domain NOMA and power-domain NOMA. In power-domain NOMA users are allocated different power levels based on certain power allocation algorithms that in turn depend on the users channel conditions, to obtain the maximum gain in the system performance. Power allocation process is also used to separate the different users, so multi-user interference cancellation can be implemented through employing the principle of successive interference cancellation.

Code-domain NOMA is similar to CDMA or multicarrier CDMA. Herein, various users are assigned different codes and then they are multiplexed over the same time/frequency resources. Some techniques such as Code Division Multiple Access (CDMA), Interleave Division Multiple Access (IDMA) [PLW06], and Low-Density Spreading (LDS) [IAT12] allow NOMA to add redundancy via coding/spreading in order to facilitate the users' separation at the receiver. Probably, system spectral efficiency could decrease due to the introduced redundancy [AXI14].

2.3 General description of NOMA in downlink and uplink

In this section basic concepts of NOMA both in downlink and uplink are demonstrated. Uplink or downlink NOMA can be treated as special cases of multiple access channels (MACs) and broadcast channels (BCs). Due to an important role of these multiple access channels in the new generation of communication technologies the author aims to explain the principles of NOMA in downlink and uplink separately and in two parts. The first part will handle basics of NOMA in downlink, while the second part can illustrate NOMA fundamentals in uplink.

2.3.1 Downlink NOMA

A transmission side of the downlink NOMA network is shown in Figure 2.10. Our exemplary network presented in this figure consists of two terminals served by a base station with a single transmitter and receiver antenna. Assume that the overall system transmission bandwidth is one Hertz.

In general, in downlink scenario, the base station broadcasts superposition of K signals to its K users by careful selection of their power levels. BS transmits a signal to user $(i = 1,2, \dots, K)$, which is represented by s_i, where $\mathrm{E}[|s_i|^2] = 1$, with allocated transmission power p_i. Summation of p_i $(i = 1,2, \dots . K)$ is equal to p_{total}.

The principle of superposition coding is applied at the BS side in order to superimpose the components s_i according to the following mathematical expression:

$$x = \sum_i \sqrt{p_i} s_i \qquad i = 1,2, \dots, K \tag{2.1}$$

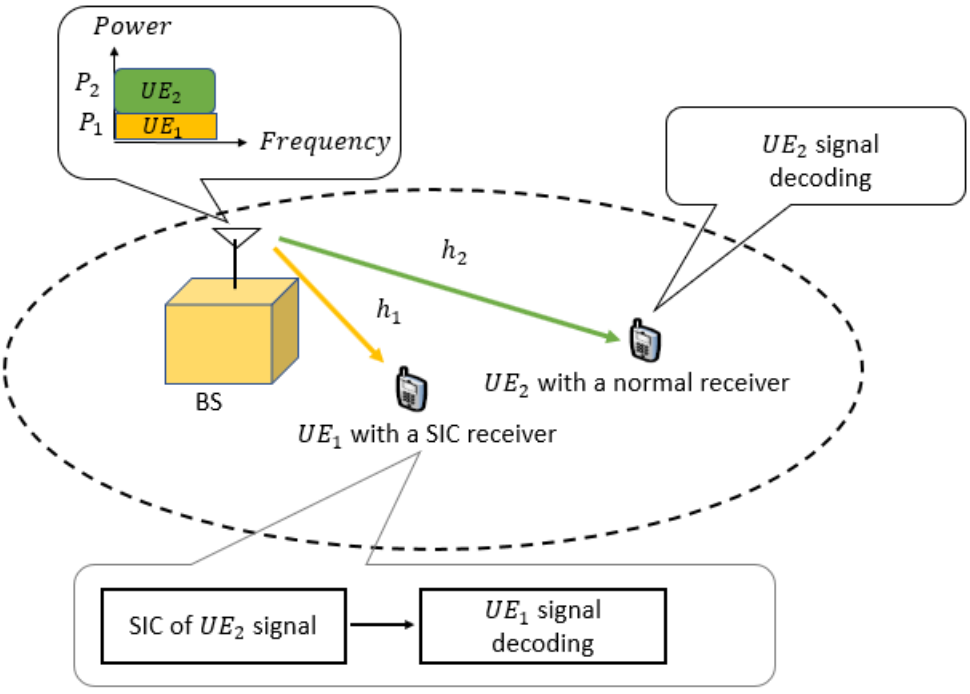

Figure 2.10 Scheme of NOMA in downlink with a power assignment diagram

Then, the signal received by the user i can be represented by the formula:

$$y_i = h_i x + \omega_i \qquad i = 1,2,\dots,K \tag{2.2}$$

where h_i denotes the complex channel coefficient between the base station and the user i, ω_i symbolizes the additive white Gaussian noise including inter-cell interference at the receiver of user i, the power spectral density of ω_i is $N_{0,i}$ [HB15].

At the user terminal, the successive interference cancellation process is applied to eliminate the influence of the undesired received signal components. Users' order in SIC decoding depends on the position of the users in the list ordered according to the increasing of their normalized squared channel gain divided by the noise plus inter-cell interference power, $|h_i|^2/N_{0,i}$. Based on this order, each user can decode its signal correctly, and eliminate the interference coming from the signals of other users whose decoding order in the SIC decoding list comes before the corresponding user's order [DLK17].

Normally, the users that are associated with small normalized channel gains should be assigned higher power levels, in order to improve their received SINR and guarantee high detection reliability. The opposite strategy occurs for the users that have larger normalized channel gains. They are capable of correctly detecting their data with high probability, although they require less power. This benefit turns into using the SIC process in their receivers [YXP17]. Without loss of generality, the author assumes that:

$$|h_1|^2/N_{0,1} > |h_2|^2/N_{0,2} > \cdots > |h_K|^2/N_{0,K} \tag{2.3}$$

Distribution of allocated power among the users can be arranged as:

$$p_1 < p_2 < \cdots < p_K \tag{2.4}$$

More specifically, in case of two users as shown in Figure 2.10, the author assumes that the normalized channel gain by the noise plus inter-cell interference power of the first user is higher than that of the second one, so $|h_1|^2/N_{0,1} > |h_2|^2/N_{0,2}$, and thus $p_1 < p_2$. Therefore, the second user (weak user) tries to decode its own signal directly, so it does not perform the process of interference cancellation due to its position as a first one in the SIC decoding order, whereas the

first user (strong user) retrieves its own signal s_1 through decoding of the second user signal s_2, then subtracting it from the whole received signal y_i through considering it as an interference, as shown in Figure 2.11. According to that, the throughput R_1 of user $i = 1$ can be formulated as [DLK17, YXP17]:

$$R_1 = \log_2\left(1 + p_1|h_1|^2/N_{0,1}\right) \tag{2.5}$$

whereas, for the user 2 it is:

$$R_2 = \log_2\left(1 + p_2|h_2|^2/(p_1|h_1|^2 + N_{0,2})\right) \tag{2.6}$$

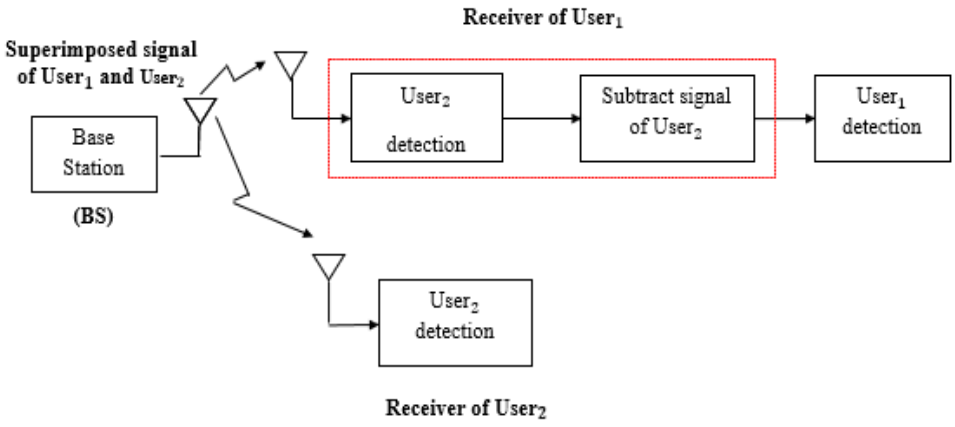

Figure 2.11 Scheme of SIC decoding process at users terminals

2.3.2 Uplink NOMA

Below the author presents a general explanation of uplink NOMA from the perspective of its basic principle, existing schemes, and performance. Operation of the uplink NOMA is quite different from the downlink one.

In the uplink NOMA, each user transmits its own individual signal s_i at the transmission power p_i to BS in the same radio spectrum range which is shared by multiple users as shown in Figure 2.12. The received signal at the BS can be expressed as:

$$x_i = \sqrt{p_i}s_i \qquad\qquad i = 1,2,\dots,K \tag{2.7}$$

$$y = \sum_{i} h_i x_i + \omega \qquad i = 1,2,\dots,K \tag{2.8}$$

where h_i denotes the complex coefficient of the channel between the base station and the user i, ω represents the Gaussian noise plus the inter-cell interference observed at the BS which is associated with the power spectral density N_0 [HB15]. Without loss of generality the author assumes as previously that

$$|h_1|^2/N_{0,1} > |h_2|^2/N_{0,2} > \cdots > |h_K|^2/N_{0,\mathrm{K}} \tag{2.9}$$

Thus, the allocated power levels for the users are assumed as:

$$p_1 > p_2 > \cdots > p_K \tag{2.10}$$

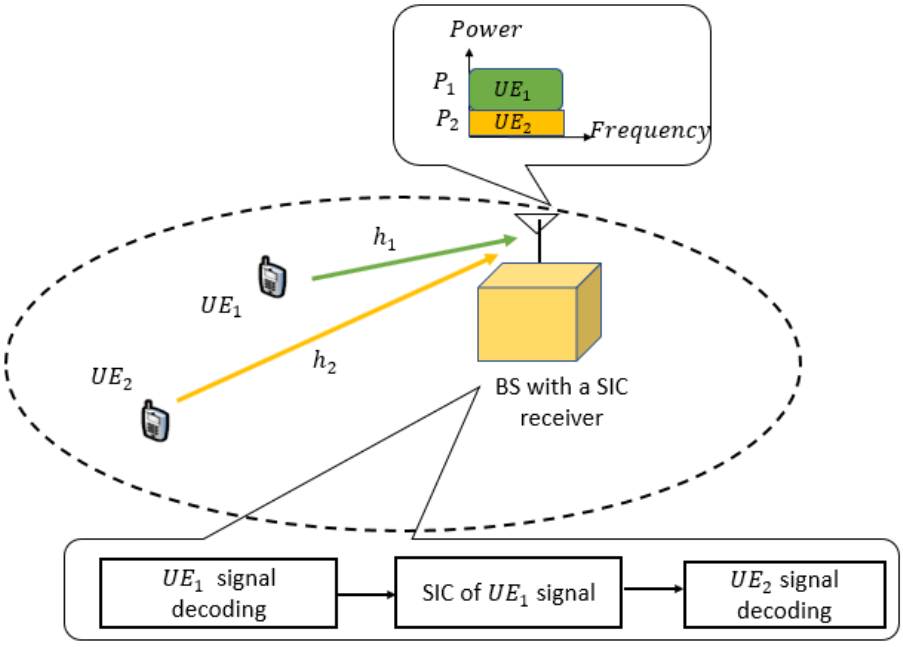

Figure 2.12 Scheme of the uplink NOMA with power assignment

The transmitted power per user is limited by the user's maximum battery power. All users can independently use their battery powers up to the maximum if their channel gains are

sufficiently distinct. When the channel gains become too close to each other, the power control can be utilized to boost up the performance of users that have better channel gains, whereas maintaining the performance of the users with weaker channel gains at a certain level [ATH16, DYF14].

The concept of SIC decoding in the uplink NOMA is quite different from that in the downlink. The optimal order of SIC decoding is based on the order of decreasing of squared channel gains normalized by the noise plus inter-cell interference power $|h_i|^2/N_{0,i}$ [DLK17].

For simplicity, for a moment, two-user uplink NOMA network is considered. The process of SIC is implemented in the BS receiver within two stages.

In the first stage, the BS receiver tries directly to decode the signal s_1 of the strongest user which has the highest channel gain, in the presence of interference resulting from the second one. When s_1 has been retrieved correctly the receiver can subtract s_1 component from the whole received signal y in order to decode s_2.

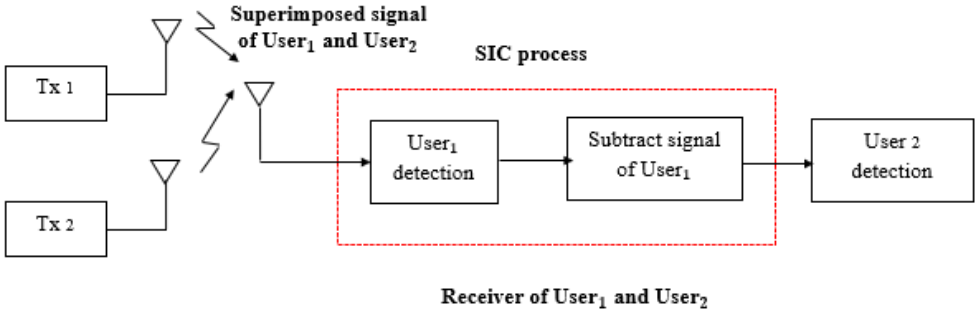

Figure 2.13 Scheme of SIC decoding process at BS

We assume that Rayleigh multipath fading and an additive white Gaussian noise (AWGN) channels are utilized. As a result, achievable data rates per channel bandwidth in two-user system expressed in bits per Hertz are given by the following expressions [TAH16]:

$$R_1 = \log_2(1 + p_1|h_1|^2/(p_2|h_2|^2 + N_0)) \tag{2.11}$$

$$R_2 = \log_2(1 + p_2|h_2|^2/N_0) \tag{2.12}$$

From the 3GPP point of view, there are several types of receivers that can be utilized with uplink NOMA for detecting users' information. They can be summarized as [TR38]:

- Minimum-Mean Squared Error (MMSE) - Interference Rejection Combining (IRC): Inter-cell interference is restrained through MMSE detection; the concept of interference cancellation is not implemented in this receiver. In case of user's data packet decoding, the MMSE detection process and channel decoding is performed only once.

- Minimum-Mean Squared Error (MMSE) - hard Interference Cancellation (IC): In this type of the uplink NOMA receiver the principle of interference cancellation is addressed. Herein, the term "hard" refers to interference cancellation that is based on the hard output of the decoder. Interference cancellation can be managed sequentially, in parallel, or with the hybrid process. In SIC, each user can decode its own signal correctly and then it is removed from the whole signal before processing the signals of the subsequent users. In Parallel Interference Cancellation (PIC), iterative detection and decoding is utilized. All users are decoded in parallel, and successfully decoded users have their signal cancelled and are then removed from the pool of users to decode in every iteration.

- Minimum-Mean Squared Error (MMSE) - Soft Interference Cancellation (IC): MMSE-soft IC cancellation contrasts with MMSE-hard IC in the output of the decoder. MMSE-soft IC includes soft information, which is employed to recreate symbols. As a result, soft interference cancellation is achieved. Interference cancellation can be implemented successively, in parallel, or in the hybrid process. In SIC, each user can decode its own signal correctly and then it can be removed from the whole signal before processing the signals for the subsequent users. While, in PIC iterative detection and decoding is utilized. Signals of all users are decoded in parallel and successfully decoded users have their signal cancelled and are then removed from the pool of users to decode in every iteration.

- Elementary Signal Estimator (ESE) + Soft-Input-Soft-Output decoder (SISO): In this scheme iterative detection and decoding are used. The update of the statistics

information, including mean and variance, can be performed in each outer iteration of the detector.

- Expectation Propagation Algorithm (EPA) + hybrid Interference Cancellation (IC): In this scheme iterative detection and decoding are utilized as well. Message passing between the factor nodes/resource elements (FN/RE) and the variable nodes (VN)/users is typically needed inside EPA for each outer iteration between the EPA and the channel decoder. The interference cancellation can be performed sequentially, in parallel, or with hybrid process. As in MMSE hybrid soft and hard IC, signals from all users are decoded in parallel and the user whose signals have been successfully decoded are removed from the pool of users to decode in every iteration.

There are some key distinctions between downlink and uplink NOMA networks and they can be listed as [LQE18]:

- Transmit power: Users' transmit power in uplink NOMA is not quite different from that of downlink NOMA. It depends on the channel conditions of each user. If the users' channel conditions are significantly distinct, their received SINR can be rather different at the BS, regardless of their transmit power.

- SIC operations: Basics of SIC operations and interference associated by the users in the uplink are quite different from those in the downlink. For sake of simplicity and in order to explain this concept perfectly, the author refers to Figures 2.11, and 2.13 as references. In the downlink NOMA the concept of the SIC process is accomplished in the strong user's terminal which has good channel condition, whereas, interference imposed by the weak user is eliminated through decoding information of the weak user, re-modulating it and then subtracting from the composite signal. On the other hand, the weak user can decode its signal directly without implementing interference cancellation process. The opposite scenario occurs in the uplink NOMA. The SIC process is carried out at the base station to decode information of the strong user treating the weak user's signal as interference. When signal of the strong user is recovered correctly re-modulation and subtraction from the whole received signal are implemented in order to retrieve information of the weak user.

- Performance gain: There is a difference in NOMA performance gain over OMA in both uplink and downlink networks. Using the downlink NOMA results in superior performance in terms of throughput, whereas features of the uplink NOMA are mainly in terms of fairness, especially if compared to OMA with power control.

2.4 NOMA in view of the proposals stated in EU projects

As we have already mentioned, NOMA schemes have recently received a wide interest. However, so far the basic multiple access scheme for the 5G New Radio (NR) is orthogonal for both downlink and uplink data transmissions what means that time and frequency physical resources of different users are not overlapped, as in LTE. The 3GPP, Rel-13 Study Item addressed downlink Multi-User Superposition Transmission (MUST), whereas, some NOMA initial studies in 3GPP, Rel-14 Study Item on NR were performed. The latter was stopped before completion, to concentrate on more urgent features for Rel-15 NR[RP-18].

In 3GPP, Rel-16 Study Item [TR38], many schemes of non-orthogonal multiple access were evaluated. From the results of the evaluated scenarios, a significant benefit of employing non-orthogonal multiple access in NR has been proved, especially in terms of uplink link-level throughput, overloading capability, as well as improvement in the system capacity in terms of supported packet arrival rate at a given system outage.

Non-orthogonal transmission can be used in both grant-based and grant-free modes. Grant-based transmission means that a user can send a scheduling request to the base station at first. Based on the received request, the BS will perform the scheduling for the uplink transmission and send a grant over the downlink channel. When large number of users is served by a network, grant-based transmission would cause high signalling overhead and transmission delay, which significantly reduces the spectral efficiency of the transmissions [DWY15, YYY16]. On the other hand, grant-free transmission is highly expected in uplink non-orthogonal schemes. It has been proposed as a promising multiple access protocol to fulfill the massive connectivity and low latency requirements for the future machine type communications. Grant-free transmission allows several users randomly to transmit at any time slot without transmitting or receiving the (scheduling/or grant) request to broadcast their data [YYL16]. Therefore, NOMA can be proposed as a generic scheme which allows grant-free operation, which may be beneficial for

supporting large number of users requesting intermittent transmissions of small data packets. Beside that, NOMA can provide a benefit in various aspects of scenarios, including enhanced Mobile BroadBand (eMBB), Ultra Reliable Low Latency Communication (URLLC), massive Machine Type Communication (mMTC), etc. [YXP17]. Furthermore, non-orthogonal multiple access schemes are using an advanced receiver that has little or no performance loss. Moreover, some of non-orthogonal MA results can be combined with narrowband and/or repetition operations to achieve the coverage requirement for NR [R1-18].

From an information-theoretical point of view shown in the EU FP7 METIS project [LL13], NOMA can be seen as a proposed multiple access technique for future radio access. METIS was one of the crucial EU projects entitled *Mobile and wireless communications Enablers for the Twenty-twenty Information Society*. The main objective of this project was laying the foundation of the fifth generation mobile and wireless communications system, and at the same time extending wireless communication systems for new usage cases [PMR14]. Researchers activities in the METIS project reported the suggested solutions related to network-level for the future wireless communication networks.

In the METIS project a large variety of scenarios was considered, and many solutions have been approached to fulfill the needs envisioned for the year 2020 and beyond [PMR14]. One of these proposed solutions was NOMA, due to some following motivations [LL13, Pop13]:

- Bandwidth is one of the scarce resources, therefore future systems should accomplish all possibilities that lead to the idea of relaxing the orthogonality constraints.
- Non-orthogonal multiple access employs the principle of superposition coding at transmitting side. NOMA can superimpose signals of multiple users in a power/code domain. Separation of users' information achieved in reception side, can be performed via utilizing the concept of successive interference cancellation. From an information-theoretical point of view, it is well-known that non-orthogonal user multiplexing not only outperforms orthogonal multiplexing, but also it is optimal in the sense of achieving the capacity region of the downlink broadcast channel through employing superposition coding at the transmitter and SIC at the receiver.
- NOMA exploits difference in the channel gains among users. There is an increase in performance gain of NOMA over OFDMA, especially when difference between users’

channel gains is large. At the same time, NOMA can translate the channel gains difference among users into user multiplexing gains through utilizing the user superposition in power-domain, whereas OFDMA translates this channel gain difference into a multi-user diversity by appropriate multi-user scheduling metric.

- NOMA employs channel state information (CSI) in both transmitting and receiving sides. At the transmitter side, CSI is necessary in terms of SINR, for user pairing and power allocation purposes. At the receiver side, the benefit of utilizing the concept of CSI improves the spectrum efficiency. Hence, it is opposed to the schemes which depend on more accurate CSI at the transmitting side, like Multi-Input Multi-Output (MIMO), or CoMP (Coordinated Multi-Point Transmission/reception). As a result, NOMA can provide performance gains that are robust to mobility.

2.5 Increase in traffic efficiency due to NOMA

Use of non-orthogonal multiple access has been envisioned as one of the key technologies in 5th generation mobile systems, as NOMA is a potential multiple access solution that has a superior spectral efficiency resulting from exploiting smart reuse of the network resources. NOMA enables each user to have access to all subcarrier channels. Hence, the bandwidth resources which are allocated to those users that have poor channel conditions can be exploited in parallel by the users with strong channel conditions. This can enhance the system spectral efficiency and increase the cell-edge throughput [DLC17]

NOMA transmission techniques intend to share the limited degrees of freedom (DoF) among users via employing the superposition concept. For this reason, multiple user detection (MUD) technique is requested for separating interfering users that share the same DoF. NOMA can also enhance the latency and fairness by allowing multiple users that have different types of traffic request, to multiplex and transmit simultaneously on the same DoF [WYN16].

NOMA has the potential to support massive connectivity, where non-orthogonal resource allocation in NOMA refers that the number of supportable users/devices is not strictly dependent on or limited by the number of orthogonal resources available. Therefore, NOMA can enlarge number of concurrent connections in some scenarios [DLK17].

Moreover, NOMA allows the multiple users within the same cell to transmit upon the same frequency resource simultaneously and offers a number of advantages, one of them is low transmission latency (no scheduling request from users to base station is required) [IAD16].

The maximal instantaneous sum-rate can be achieved through proposing the optimal resource allocation for multiple input multiple-output (MIMO) NOMA systems. However, in most of the papers in the existing literature devoted to resource allocation of NOMA perfect Channel State Information at Transmitter (CSIT) is assumed which is difficult to obtain in practice [WNY16].

2.6 User Pairing Algorithms

The principle of user pairing performed at the transmitting side has an essential role, since the employing of this principle can improve user fairness as well as system capacity. In this section, some common users pairing methods are presented in order to explain this principle.

2.6.1 Random pairing algorithm (RPA)

Random pairing algorithm [ZZM16] represents a simplest user pairing method. BS nominates the users arbitrarily from a set of multiple users to pair. The information of user's channel state is not used in this method, therefore RPA has a poor performance.

At the transmitter side of a multicarrier system, the users' selection is based by the committed information rate (CIR) that assigns the users to a certain system sub-channel according to the desired bandwidth of its specific business. Due to the lowest complexity of this strategy, its performance is often considered as a reference if compared with other pairing algorithms.

2.6.2 Orthogonal pairing algorithm (OPA)

Assume that the user multi-carrier transmitters have N_t=2 antennas and the system receiver has N_r=1 antenna. The number N of potential users is higher than N_t. Therefore the user pairing process in fact is realization of the MISO (multiple input single output) transmission. Assuming flat fading channels on each subcarrier the joint channel on the m-th subcarrier for a given pair of users is characterized by the channel matrix $\mathbf{H}_m$, and

$$\mathbf{H}_m = \begin{bmatrix} h_{11} & h_{12} \\ h_{21} & h_{22} \end{bmatrix}$$

where $h_{1,i}$ (i=1,2) are the channel coefficients of the first selected user, whereas $h_{2,i}$ (i=1,2) characterize the channel of the second user. This algorithm seeks to pair the users that achieve the best channel orthogonality. Paper [ZZM16] is devoted to explaining the principle of this algorithm. The users are orthogonal to each other if their channel matrix is an orthogonal matrix. This means that $\mathbf{H}_m^H \mathbf{H}_m$ is a diagonal matrix. Therefore the degree of orthogonality can be measured by defining the matrix:

$$\mathbf{F}_m = \mathbf{H}_m^H \cdot \mathbf{H}_m = \begin{pmatrix} f_{11} & f_{12} \\ f_{21} & f_{22} \end{pmatrix} \tag{2.13}$$

Orthogonal factor G_m is a measure of the degree of orthogonality and is determined by the formula:

$$G_m = \frac{(f_{11} + f_{22}) - (f_{12} + f_{21})}{tr(\mathbf{F}_m)} \tag{2.14}$$

where $tr(\mathbf{F}_m)$ represents trace of the matrix $\mathbf{F}_m$.
Accordingly, the better channel orthogonality of a certain user is achieved when it has the bigger value of G_m, hence it gains the higher possibility of pairing.

2.6.3 Determinant pairing algorithm (DPA)

The same criteria as in the OPA method is applied in the DPA algorithm. The only difference is represented by the calculation of the coefficient D_m that is defined below in (2.14). High possibility of the pairing is given to the users that have the smallest value of D_m [ZZM16].

$$D_m = \frac{\det(\mathbf{F}_m)}{tr(\mathbf{F}_m)} \tag{2.15}$$

2.6.4 Channel state sorting-pairing algorithm (CSS-PA)

An increase in the system capacity on the basis of user fairness is obtained in this method. This algorithm depends on the results of users' channel states sorting in which we can pair a user that

has a good channel condition with another user who experiences a poor channel condition [CFJ20].

As a result, the benefit of using CSS-PA is the correct receiving of poor channel conditions users at the reception side, as well as, improving the system fairness while raising system capacity [DFP15].

This algorithm can be implemented by the following steps:

In the first step the candidate users are arranged ascendingly according to their channel gains. Then the sorted users are paired according to the binary dislocation principle (BDP) explained below. For example, if a network consists of K users referred by indices $1, \dots, K$, placed in the ascending order, BDP tries to pair the first user with the $K/2$-th user, the second user with the $(K/2+1)$-st user, and so on until no user is left. If K is an odd number, the left user can be individually allocated [ZZM16]. There is another strategy which can be applied to pair the users by the binary dislocation principle depending on the difference of their SINR as it was introduced in [DFP15]. When compared CSS-PA with other algorithms such as RPA, we can conclude that complexity of this method is still not quite high.

2.7 Power allocation to the user participating in NOMA transmission

In NOMA, the power allocation level of one user can influence the achievable throughput of the corresponding user as well as the throughput of other users due to the power domain multiuser multiplexing.

In this section, some proposed power allocation algorithms are formulated, which can be applied for allocating the power to several users participating in NOMA transmission. These algorithms are listed as: Iterative Water Power Allocation (IWPA), Fixed Power Allocation (FPA) and Fractional Transmit Power Allocation (FTPA).

2.7.1 Iterative water power allocation

One of the main advantages of this method is attaining high level of performance in power allocation through maximizing the channel capacity, but at the same time this method requires multiple iterations of operation in order to get the optimal solution which results a high complexity [CFJ20].

2.7.2 Fixed power allocation

In this algorithm, the users are sorted in a descending order according to their normalized squared channel gain divided by the noise plus inter-cell interference power, $|h_i|^2/N_{0,i}$. Denoting the k-th sorted user as $UE_k, (i = 1,2, \dots, K)$, the allocated power level $P(UE_k)$ of UE_k can be described by the following formula:

$$P(UE_k) = \alpha_{FPA} P(UE_{k+1}) \tag{2.16}$$

where α_{FPA} denotes the power allocation factor of FPA algorithm, and its value is in the range $0 \leq \alpha_{FPA} \leq 1$.

Obviously, high power levels are assigned to the users who experience poor channel conditions. Moreover, the power difference among users gets smaller when the value of α_{FPA} is increased. It is important to mention that the same value of α_{FPA} should be used for all transmitted data packets in an established link. Finally, the main feature of this algorithm is the reduced system complexity [LBC14].

2.7.3 Fractional transmit power allocation

FTPA is applied for further reduction of the computational complexity. If the network consists of K users, FTPA assigns the transmission power dynamically for the k-th user taking into account the normalized squared channel gain divided by the noise plus inter-cell interference power, $|h_i|^2/N_{0,i}$ of this user as follows:

$$P(UE_k) = \frac{P}{\sum_i (|h_i|^2/N_{0,i})^{\alpha_{FTPA}}} \left(|h_k|^2/N_{0,k}\right)^{\alpha_{FTPA}} \tag{2.17}$$

where α_{FTPA} $(0 \leq \alpha_{FTPA} \leq 1)$ is the power allocation factor of FTPA. P and $P(UE_k)$ represent the total amount of transmission power and the allocated power of k-th user, respectively.

In case of α_{FTPA}=0, equal transmit power is allocated to the users, whereas more power is assigned to the users who experience poor channel conditions when the value of α_{FTPA} is increased. As mentioned before in case of FPA, the same value of α_{FTPA} can be utilized for all transmitted packets in the established link [SBK13, WCC16].

As a result, the power allocation factor in both FPA and FTPA has an effective role for deciding about the difference in users' power level. Moreover, it has a significant influence on balancing the system capacity and fairness.

2.8 Summary

This chapter provided the basic principles of multiple access techniques employed in wireless communications systems. Non-Orthogonal Multiple Access (NOMA) was presented as one of the proposed techniques and key component in the fifth generation of mobile systems. An overview of NOMA system in addition to the main features of NOMA with respect to OMA was described. Furthermore, a brief introduction of user pairing and power allocation algorithms which play important role in NOMA transmission were examined.

Chapter 3

Successive Interference Cancellation

The performance of today's cellular networks is limited by the interference more than by any other single effect, so the interference is considered as one of the most important obstacles for achieving successful communication. As a result, the interference minimization or cancellation is an essential aspect in those networks. They aim to mitigate the interference effect which is caused by multiple users sharing the same resources in the same network. Interference cancellation does that through demodulating and/or decoding the desired information and then using this information along with channel estimates to cancel the received interference from the received signal.

Interference cancellation technologies have played an essential part in improving network performance. Consequently, several interference cancellation and mitigation techniques have been proposed in mobile networks. One of them is Successive Interference Cancellation (SIC), suggested as a promising technique to improve the efficiency of wireless networks with relatively low additional complexity.

The current chapter presents a brief overview of successive interference cancellation fundamentals and its applications. It also analyzes SIC performance in NOMA networks. Simulation results that the author has published in [GW18] addressed in this chapter to give a clear perception of the investigated system performance.

3.1 The idea of successive interference cancellation and its application

One of the most common solutions that meets the increasing throughput demand is reducing the cell size by deploying additional base stations which in consequence results in additional interference. Such networks are called interference limited networks, as thermal noise in them is negligible with respect to interference [WQK13]. The most substantial obstacle to achieving successful communication is represented by the overall network interference. Thus, an improvement in dense networks' performance can be obtained by employing efficient interference management schemes. Orthogonality between transmitted signals, either in

frequency, time, or space, as well as some adaptive spectrum allocation policies have been exploited in these schemes. The effective interference level can be reduced through decoding and cancelling out the signals that significantly interfere with the desired signal being the subject of decoding [CQK12].

There are several approaches to interference cancellation (IC) in wireless communication networks. Most of IC techniques employ differences in the properties of the desired signal and that of the interfering signal to separate the received signals. These differences can be exploited in bandwidth, modulation type, or amplitude or power level. Herein, some classes of IC techniques have been addressed such as Joint Detection (JD) technique which was employed in the 3rd generation of mobile communications system to eliminate the intracell multiple access interference (MAI) and inter-symbol interference (ISI) [BJ09, CS03], and Successive Interference Cancellation (SIC) technique which represents a key technology in 5th generation of mobile communication networks to minimize the interference level and enhance the system performance through decoding and canceling the interfering signals [ZH14].

SIC is a well-known physical layer technique that is utilized at a reception side to enable the receiver to receive two or more signals simultaneously [SSC10].

The key idea behind SIC is decoding different users' information successively. The interference coming from decoded users is stripped away from the aggregate received signal before decoding the information of other users. SIC is predicted to be the most effective IC-based methodology in terms of Bit-Error-Rate (BER) performance. As well as, SIC reception can improve the signal-to-interference ratio (SIR) through ordering the received signals according to descending signal power and then decoding and subtracting the subsequently decoded signals from the received multi-user signal. This process is repeated until the signal of interest (SoI) is decoded [WQK14].

While the accuracy and robustness demand increases, the complexity of iterative detection and decoding process is growing at the same time. Hence, there is a trade-off between the performance of SIC and complexity [MV12]. SIC has been demonstrated to be particularly beneficial if very low-rate codes are utilized or active transmitters are gathered around the receiver [ZH14].

Concerning SIC applications, some research has showed the utilization of SIC in the physical layer communications systems [MV12]. At the same time, some advantages from

applying SIC in the cellular networks have been appeared, one of them is summarized by expected gain in the network performance which is resulting from the use of SIC [HTD18].

One of SIC effective applications is represented by Non-Orthogonal Multiplexing Access (NOMA) in both downlink and uplink communications for 5G systems [ZMX16, DLK17].

In NOMA-based networks, the same frequency resources are allocated to multiple users, and intra-cell multiple user interference is mitigated through utilizing the principle of SIC at the reception side which is decoding two or more packets that have arrived at the same time and caused collisions. Because of employing the uplink power control, there is very little chance left for NOMA to implement intra-cell cancellation in the uplink cellular communications.

3.2 Basic SIC detector

Successive interference cancellation has become one of important techniques in data transmission. Even though SIC is considered suboptimal in general, but at the same time, it is able to mitigate the interference level and attain better performance in interference-limited networks.

To implement SIC, all users are ordered according to their signal strength, the priority of data detection is given to the strongest received signal, then the next strongest, and so on [SSC10]. According to that the signal of the strongest user is first decoded, recovered and then subtracted from the whole combined signal in order to decode other users' signals successively.

The performance of all users can be improved in spite of their disproportionately received powers when SIC is employed. A large part of the total interference could be removed by the time the signals of these users are detected [And05].

3.3 SIC Detector in NOMA Transmission

In this section, the author describes the basic principles of the successive interference cancellation technique in both downlink and uplink NOMA systems. There is a clear difference in SIC concept for each approach. In the following subsections, SIC fundamentals in NOMA systems are separately presented and compared in detail.

3.3.1 SIC detector in downlink NOMA

A downlink NOMA system is introduced in this part using a simple example. The system consists of two UEs and a single-antenna BS that serves these single-antenna users at the same time.

At the transmitting side, BS broadcasts the composite signal (which is a superposition of desired signals of users) with different allocated power coefficients to the participating users simultaneously.

As previously shown in Figure 2.10, BS transmits a signal to user $(i = 1,2)$. This signal is represented by s_i, where $\mathrm{E}[|s_i|^2] = 1$, with allocated transmission power p_i. Note that the summation of all $p_i's$ is equal to p_{total}. Superposition coding (SC) is an effective technique utilized at the BS terminal to superimpose components s_i over the same frequency resource with different power levels. The superimposed signal has been represented by the mathematical expression illustrated in Eq. (2.1), while the received signal at user i has been expressed by Eq. (2.2).

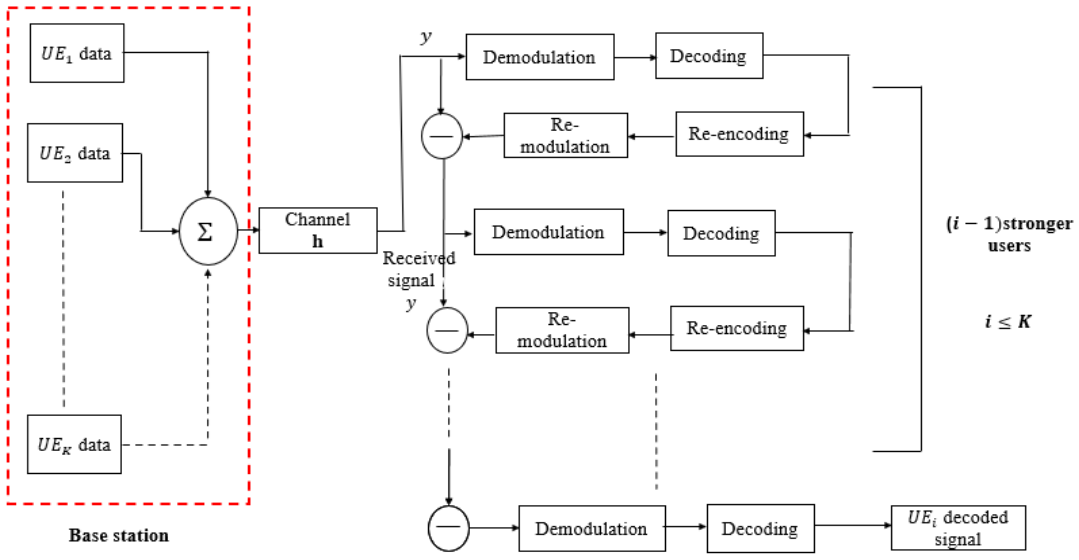

Figure 3.1 Illustrating the principle of successive interference cancellation in downlink communication system consists of *K* users

Referring to Figure 3.1, the concept of successive interference cancellation is employed at the user's receiver to eliminate the multi-user interference. The SIC process is assumed to be

performed successively until the user's signal is retrieved. The amount of allocated power is assigned to the users according to their normalized channel gains, in inversely proportional manner. The signals of high channel gain users are transmitted with low power levels, whereas the signals of low channel gain users can be broadcast with high power levels. Thus, the users with the highest transmission power can detect their signal immediately without implementing any SIC process and treat signals of other users as noise.

As previously explained, users' order in SIC decoding depends on the position of the users in the list ordered according to the increasing of their normalized squared channel gain divided by the noise plus inter-cell interference power, $|h_i|^2/N_{0,i}$. Based on this order, each user can decode their signal correctly, and eliminate the interference coming from the signals of other users whose decoding order on the SIC decoding list comes before the corresponding users' order [ZWZ16].

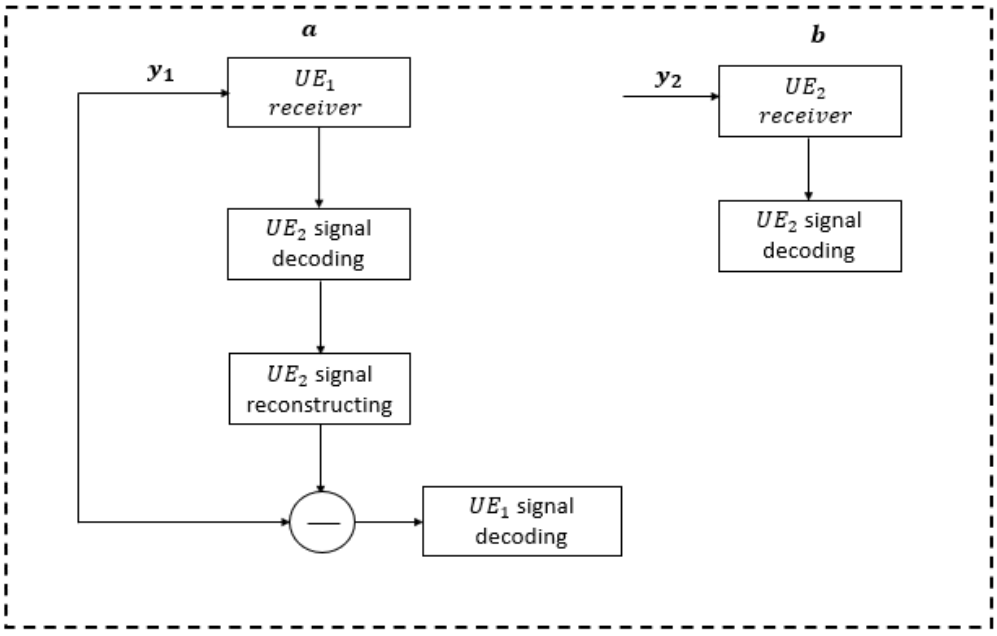

Figure 3.2 Flowchart of SIC process at a two-user terminal

(a) UE_1 receiver operation; (b) UE_2 receiver operation

In this downlink system, the author supposes the following condition $|h_1|^2/N_{0,1} > |h_2|^2/N_{0,2}$ as that shown in Eq. (2.3). As a result, it is not necessary to perform the successive

interference cancellation process at UE_2's receiver, since its order comes first on the SIC decoding list. On the other hand UE_1 aims to employ this concept in its receiver, through decoding component s_2 and subtracting it from the whole received signal y_1 in order to retrieve component s_1 without interference from s_2[BSK13]. This procedure is precisely explained in Figure 3.2.

The achievable rate of user i, R_i, as well as the achievable sum rate of system R have been given by Eq. (2.5) and (2.6) respectively.

3.3.2 SIC Detector in Uplink NOMA

The operation of uplink NOMA is quite different from that of downlink NOMA. In uplink NOMA transmission, multiple users (UEs) broadcast their own signals to a single base station in the same resource block at either maximum transmit power or controlled transmit power**.** All received signals at the BS are the desired signals, even though they cause interference with each other. BS receives transmissions from all users simultaneously and detects data information of users with the aid of the successive interference cancellation principle [ATH16]. Figures 3.3 illustrates the principle of SIC in uplink wireless communication system that consists of *K* users.

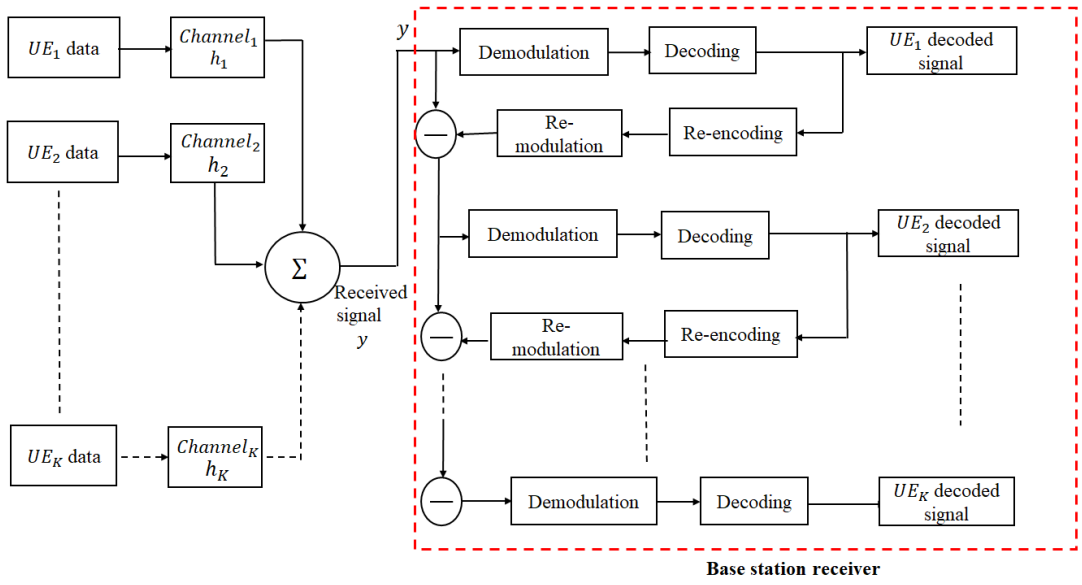

Figure 3.3 Illustrating the diagram of uplink communication system employing the principle of successive interference cancellation

As explained in the previous chapter, the concept of transmitted power in uplink NOMA also differs from that of downlink NOMA. Namely, the transmitted power per user is limited by the user's maximum battery power. All users can independently use their battery powers up to the maximum if their channel gains are sufficiently distinct. When the channel gains become too close to each other, the power control can be utilized to boost up the performance of users that have better channel gains, whereas maintaining the performance of the users with weaker channel gains at a certain level [TAH16].

SIC is performed at the base stations in uplink NOMA transmission, therefore, the users do not need to be aware of the modulation and coding schemes that are utilized by other users. Moreover, the base stations have sufficient processing power to perform SIC [DDC17, DWY15]. The scheme of uplink NOMA system aided by the successive interference cancellation concept has been demonstrated in Figure 2.12.

For simplicity, a two-user uplink NOMA system was temporarily considered. Each user transmits their individual signal s_i with transmission power p_i to a single BS independently. The received signal has been defined in Eq. (2.8).

In order to apply the principle of SIC and decode the users' signals at the BS side, it is important to keep the differences of various signals that are superposed within the received signal *y*. Different channel gains are allocated to the participating users during transmission, so each user's signal experiences distinct channel gain. The received signal from the highest channel gain user is likely the strongest at the BS. Thus, this signal is decoded first at the reception side, with the signals coming from relatively weaker channel users being treated as noise. Accordingly, the signal for the second highest channel gain user can be decoded, and so on [AXI14, ADG17].

In uplink NOMA transmission, as previously shown in Figure 2.12, the author supposes $|h_1|^2/N_{0,1} > |h_2|^2/N_{0,2}$ as that described in E.q. (2.9) As a result, the BS receiver can detect the received signals in subsequent steps.

At the first step, BS receiver detects the component x_1 directly without employing SIC, and treats component x_2 as noise. Once the receiver correctly decodes component x_1, it reconstructs this signal component and subtracts it from the aggregate received signal y to decode x_2, as explained in Figure 3.4.

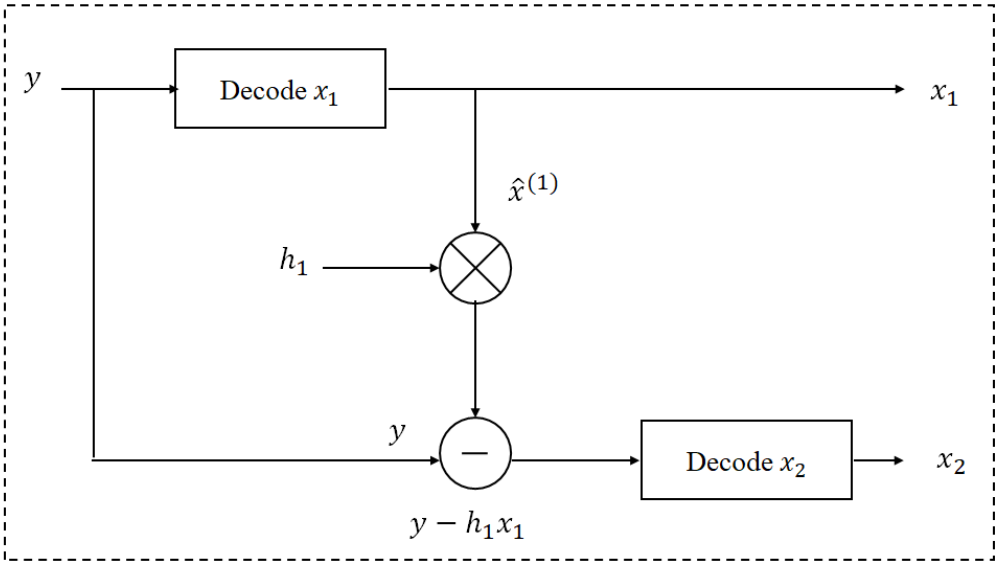

Figure 3.4 Illustrating the flowchart of the SIC process at the reception side of uplink NOMA transmission

The throughput of user i ($i = 1,2$), R_i has been expressed by the mathematical expressions that have already defined in Eq. (2.11) and (2.12) respectively.

3.4 Cooperative Scheme for Uplink NOMA Wi-Fi Transmission

In this section, an uplink NOMA Wi-Fi transmission scheme is presented, aiming to examine NOMA performance in such systems in order to achieve better QoS and hence throughput increase.

For the time being, multicarrier techniques are mainly used in broadband wireless communications, because of their adaptability in resource allocation, in addition to advantages resulting from multiuser diversity.

Due to the growing demand for mobile access to the Internet and the Internet of Things (IoT), the requirements for 5G wireless communications systems, such as high spectral efficiency, massive connectivity, and user fairness have become a challenge. The Internet of Things (IoT) has become a very interesting technology, especially for the industrial and marketing sectors. It represents a proposed expansion of the Internet in the future by achieving a massive jump in the capability of collecting, analyzing and spreading data which can be

converted into information, knowledge, etc. In order to connect things to each other or to the cloud, there are several standards and proper devices can be used for this purpose, such as Wi-Fi, Bluetooth, ZigBee, Active RFID, etc. Because of the Wi-Fi features such as energy consumption and secure network, this type of transmission is considered the most suitable choice to provide Internet connection everywhere in the world. Additionally, Wi-Fi transmission is relatively simple to model and conclusions drawn on the simulated scenarios can be easily extended on other multicarrier systems.

Consequently, the author in [GW18] has proposed a cooperative scheme for uplink NOMA Wi-Fi transmission (according to IEEE 802.11 standards) to allow multiple users with different channel coefficients to transmit or receive their information upon the same resources (e.g., time/frequency) by being allocated in the power domain (PDM). It employs the concept of superposition coding at the transmitting side to superpose the information signals coming from different users with proper transmission power. At the same time, the composite multiuser signal can be separated at the reception side by utilizing the principle of successive interference cancellation.

3.4.1 System Model

A Wi-Fi transmission system model has been used to simply illustrate the concept of NOMA in this application. Let us notice that applying NOMA in this case increases the Wi-Fi network capacity, as the same radio resources are used more than one time. The basic principles of the proposed system are specified below.

3.4.1.1 IEEE 802.11a Wi-Fi Standard

Currently, wireline digital networks are strongly supported by wireless access due to the enormous increase in using mobile communication devices like smartphones, laptops with wireless communication capabilities, etc., at homes, in offices, and in public areas. Wireless LAN technologies have proven to be capable of providing unlimited access for users who were formerly served by wireline networks.

In the early 1990s, the IEEE 802.11 standard was released by the Institute of Electrical and Electronic Engineers (IEEE) for local and metropolitan area networks as an enhancement for

wireless LAN standards. The IEEE 802.11 standard is a set of various standards (e.g., IEEE802.11a, b, g, n, and ac) operating at different frequencies and ranging allotments.

The proposed system model concentrated on IEEE 802.11a for some reasons, one of them being the fact that transmission in conformance to this standard is less liable to interference than IEEE 802.11g, due to the high operating frequency (5 GHz). Moreover, it is more convenient for indoor deployment. IEEE 802.11a standard describes data transmission up to 54 Mbps data rate with the application of Orthogonal Frequency Division Multiplexing (OFDM) as a transmission technique. A single input/single output (SISO) antenna technology is applied.

Table 3.1 shows the specification of the IEEE 802.11a standard chosen to study the performance of the proposed system model.

Table 3.1 Specification of the IEEE 802.11a standard

Parameter	Value
Bandwidth	20 MHz
Cyclic prefix duration	0.8 μsec
Data duration	3.2 μsec
FFT size	64
No. of subcarriers	52
Operating frequency	5 GHz
Sampling rate	40 MHz
Subcarrier spacing	312.5 KHz
Throughput	6 up 54 Mbps
Total symbol duration	4.0 μsec

3.4.1.2 Uplink NOMA Scenario

An uplink scenario with indoor environment is considered in the proposed system model. Consider a single carrier of the OFDM transmission for a moment only. The signal $\mathbf{x}^i$ $(i = 1,2)$ is transmitted by the user equipment UE_i to the access point with allocated transmit power p_i. Its value depends on the channel conditions and the distance between the user and the access point. The author assumes that power distribution is performed according to the Fractional Transmit Power Allocation algorithm (FTPA) which has been described in the previous chapter. Without the loss of generality, the author assumes that $p_1 > p_2$.

Suppose that two NOMA users simultaneously send their signals $\mathbf{x}^{(1)}$ and $\mathbf{x}^{(2)}$ to the access point with allocated powers equal to p_1, and p_2, respectively. These two signals share the same frequency and interfere with each other, as depicted in Figure 3.5.

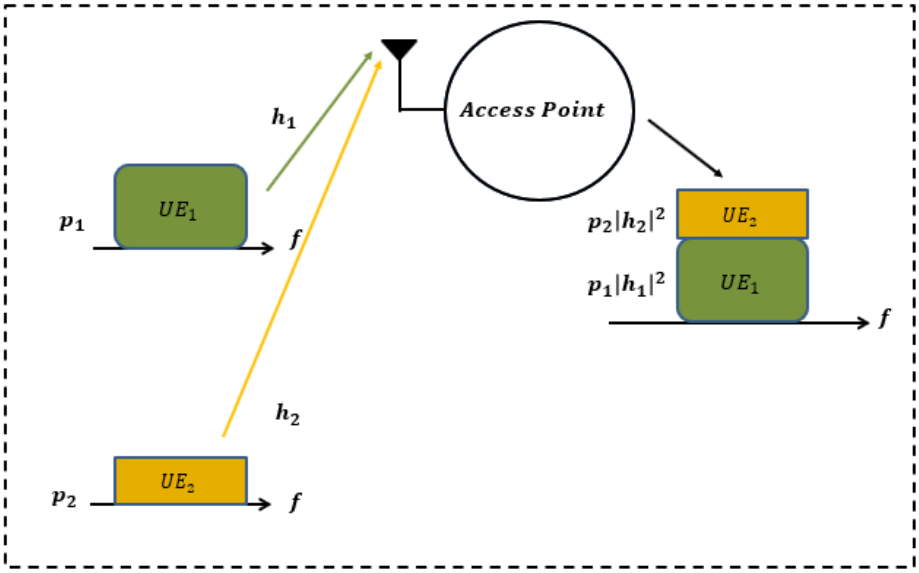

Figure 3.5 Illustrating the diagram of uplink NOMA transmission with users' proper power assignment

SIC technology is implemented at the reception side to decode the information signal of both users consecutively, in which the receiver (access point side) is trying to recover both signals $\mathbf{x}^{(1)}$ and $\mathbf{x}^{(2)}$, respectively, in two steps. In general, the SIC receiver decodes $\mathbf{x}^{(1)}$ and treats $\mathbf{x}^{(2)}$ as noise. After $\mathbf{x}^{(1)}$ being recovered, its influence on the received signal is regenerated and subtracted from the whole received signal y to decode component $\mathbf{x}^{(2)}$. Figure 3.6 illustrates

the information signal decoding rule that is applied inside the access point receiver to retrieve the original data of users.

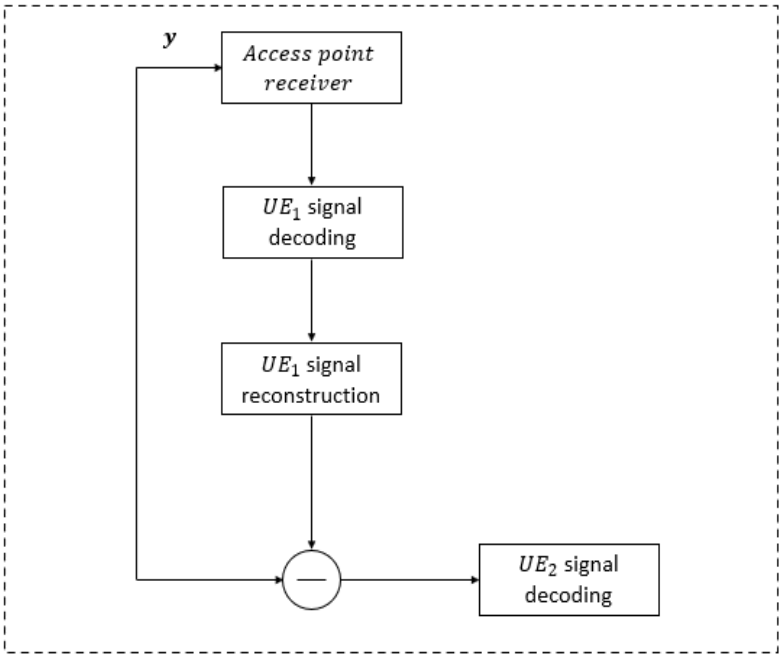

Figure 3.6 Explaining decoding process inside the access point receiver

3.4.1.3 Proposed System

An OFDM-based uplink NOMA system is considered. The investigated system consists of two users co-operating with one access point. The users are transmitting their data simultaneously upon the same frequency resource and their signals interfere with each other. User fairness is satisfied in this model, as NOMA nominates a user terminal with good channel condition and combines it with another user who experiences poor channel condition by applying the Channel State Sorting-Pairing Algorithm (as described in the previous chapter). The strong user (with good channel conditions) is geographically closer to the access point, while the other one is assumed a weak user (it has poor channel conditions) and it is far away from the access point. Figure 3.7 demonstrates a diagram of the proposed system.

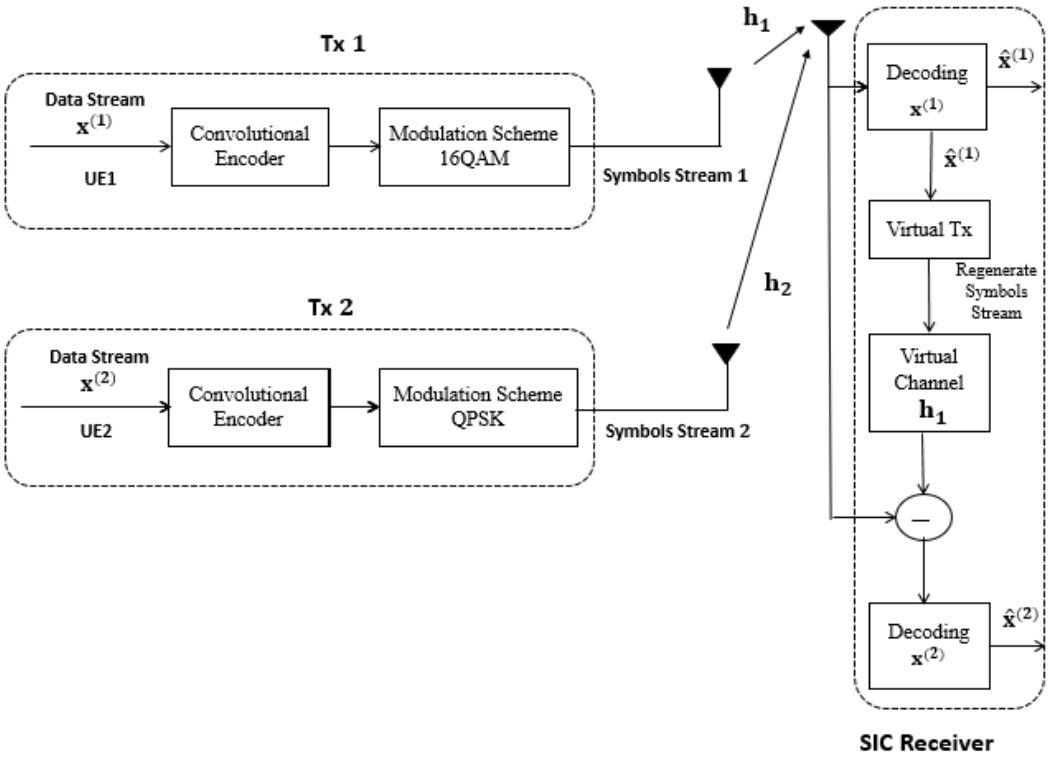

Figure 3.7 Diagram of the considered system

The author assumes the two data streams transmitted by both users are mutually independent. It is also assumed that synchronization is achieved with the accuracy of a fraction of the OFDM cyclic prefix, so that the receiver at the access point can find the OFDM orthogonality period common for both users.

At the transmitting side, the data of each user are first encoded before being transmitted using the convolutional code with coding rate R=1/2. The standard (133,171) code is applied. Different modulation schemes are supported and applied by the users depending on the channel propagation path of each user. Hence, 16-QAM or QPSK is suggested to be used for the strong user, due to its closer position to the access point, as well as good channel conditions experienced by this user. Meanwhile, the weak one uses QPSK as a modulation scheme because of the poor channel conditions resulting from its far position with respect to the access point. Other modulation arrangements are also possible to be applied by the participating users. Figure 3.8 explains the functional blocks sequence inside the transmitter of each user.

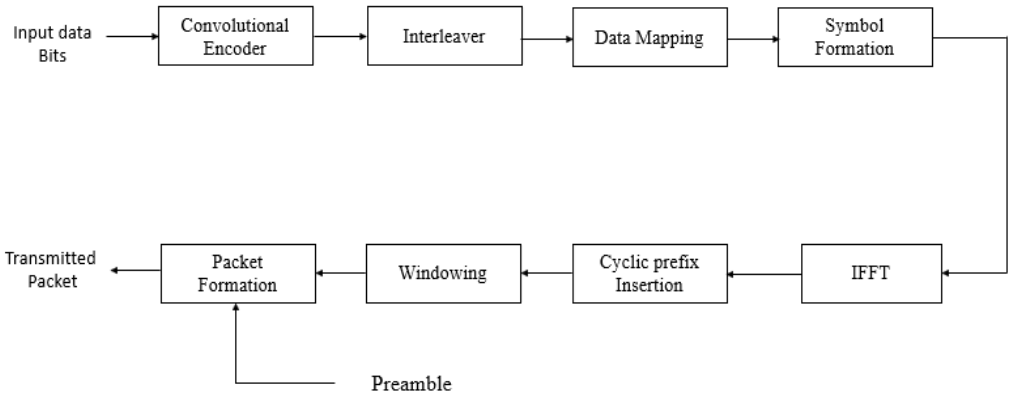

Figure 3.8 Illustrating the functional blocks in the user transmitter

Rayleigh fading channels with complex channel gain coefficient vectors are indicated as $\mathbf{h}_1, \mathbf{h}_2$ represent the channel models between UE_1 and the access point and UE_2 and the access point, respectively. Thereafter, the access point receives a combined version of the signals that have been transmitted by both users.

SIC is implemented at the receiving side in the access point in two stages. First, the data of the strong user $\mathbf{x}^{(1)}$ are decoded, whereas the weak user's data $\mathbf{x}^{(2)}$ are treated as noise. These data constitute the input stream to the local virtual transmitter which, knowing the channel gain coefficients of the strong user, resynthesizes its signal approaching the receiver. Such a stream of samples is subsequently subtracted from the samples of the received joint signal in order to decode the data symbols of the weak user $\mathbf{x}^{(2)}$. Figure 3.9 gives a brief description of SIC process that is implemented inside the access point receiver.

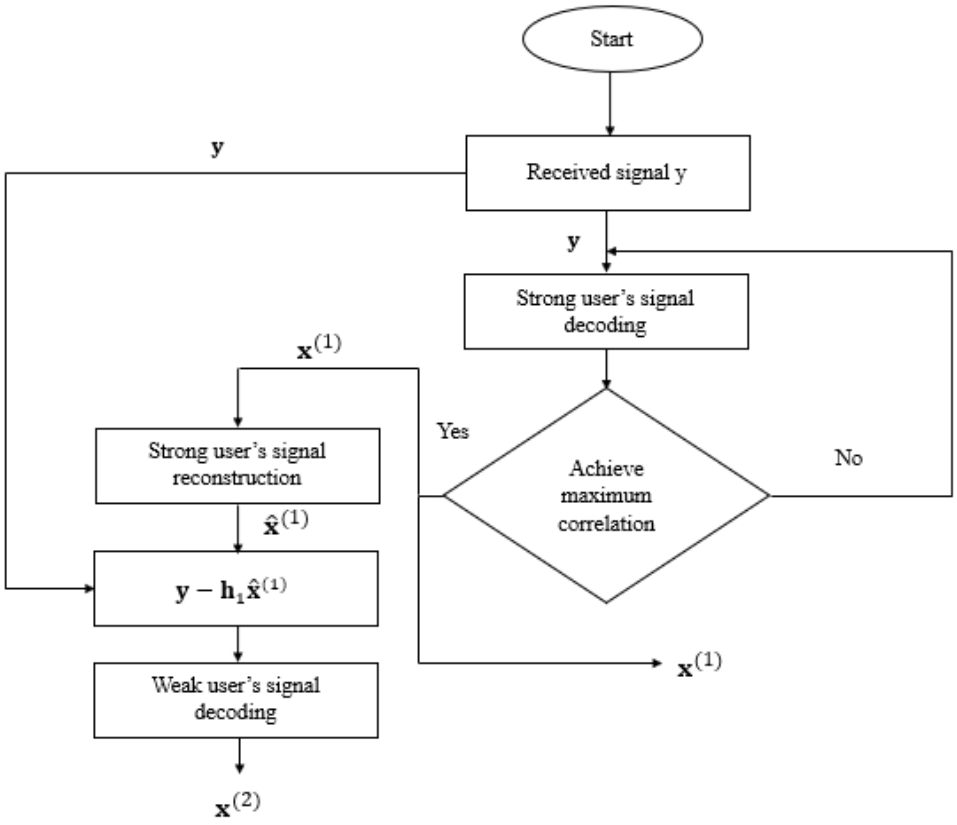

Figure 3.9 Explaining SIC implementation inside the access point receiver

Note that, in contrast to cellular systems, in IEEE 802.11 WiFi the users have access to the transmission medium based on contention according to the CSMA/CA (Carrier Sense Multiple Access/Collision Avoidance) rule. Thus, only a single user is able to transmit their data at a given time and in a given frequency channel, otherwise, collision between different users occurs. In order to enable NOMA in WiFi and potentially increase its spectral efficiency considerably, the radio resource management rule has to be substantially changed. Access point managing uplink and downlink transmissions should arrange appropriate users in pairs after learning from them their wish to transmit data in packets of similar lengths and knowing their propagation path losses. Thus, NOMA transmission in a WiFi cell shown in this system can be treated as a proposal that checks the potential of possible increase in WiFi network capacity due to this technology.

3.4.2 Simulation Results

In this section, some simulation results are presented to show the performance of the analyzed system. BER vs. SNR measurements are considered for that purpose. Certainly, the propagation path loss of the user can be given by:

$$g_i = \sqrt{\frac{p_x}{p_i}} \qquad i = 1,2 \tag{3.1}$$

where p_x represents the received power at the access point. The propagation path loss of the strong user is assumed to be greater than the propagation path loss of the weak user $(g_1 > g_2)$.

In simulation experiments *K* refers to the number of packets that are transmitted by each user (During the data transmission; value of *K* is not a constant, it changes according to the quality of BER), with *L* OFDM symbols inside each packet.

The simulation results are shown for two scenarios determined by the channel models employed, i.e., AWGN and Rayleigh channels. The author describes the experiment results in two parts.

3.4.2.1 Additive White Gaussian Noise (AWGN) channel

The author assumes the channel models between the users and receiving side are AWGN channels. As an example, the propagation path losses are assumed to be $g_1 = 1.0$, $g_2 = 0.3$, respectively.

The system is modelled in two versions with respect to convolutional code decoding: one which employs the hard decision (HD) Viterbi decoder and a second one in which soft decision (SD) 8-level decoder input is applied. For that purpose, the author evaluated log-likelihood ratios for each transmitted bit in a signal constellation and then quantized them into 8 levels.

Various modulation schemes can be assigned for the participating users such as (QPSK, 16-QAM). As a result, the calculation of log-likelihood ratios for these users is different according to their modulation order as follows:

- **In case of 16-QAM modulation:**

The log-likelihood ratios for each transmitted bit can be estimated by using the following approximating formula [KHY06]:

$$LLR(B_j) = \frac{1}{2\sigma^2}\left[\left(\min_{D\in S_{0,j}} |\mathrm{Y}-\mathrm{D}|^2 - \min_{D\in S_{1,j}} |\mathrm{Y}-\mathrm{D}|^2\right], \quad j = 1,2,\dots,4 \tag{3.2}$$

where:

$LLR(B_j)$: evaluated log-likelihood ratios for each transmitted bit in a signal constellation

σ^2 : the variance of AWGN.

Y : the complex received symbol.

$S_{0,j}$: the subset of constellation points with 0 on the j-th position.

$S_{0,j}$: the subset of constellation points with 1 on the j–th position.

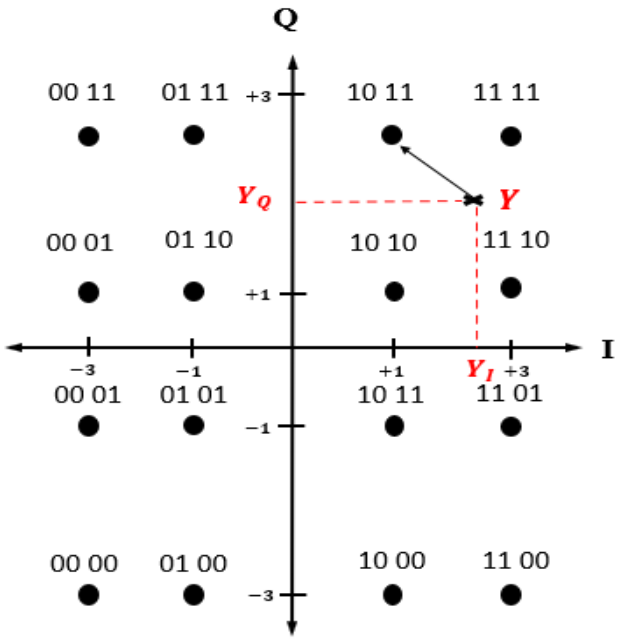

Figure 3.10 Signal constellation for 16-QAM modulation

- **In QPSK modulation case:**

The QPSK signal constellation diagram is shown in Figure (3.10) [KHY06]. The mathematical expression for useful approximation of log-likelihood ratios for each transmitted bit can be represented by Eq. (3.2).

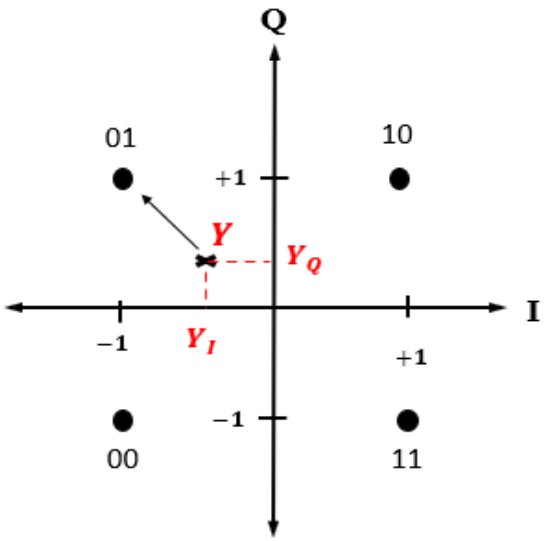

Figure 3.11 QPSK signal constellation diagram

As expected, soft decision decoding (SD) achieved better performance than hard decision decoding (HD). The difference in coding gain is about 2 dB at BER level of 10^{-3}. Therefore, soft decision decoding is adopted in all other investigations.

3.4.2.2 Rayleigh Multipath Fading Channel

In this part of simulation results, the author employed a multipath Rayleigh fading channel as a channel model between users and the receiving side, with different channel gain coefficient vectors which can be represented by $\mathbf{h}_1, \mathbf{h}_2$, respectively. Elements of the channel gain vectors represent subsequent channel path gains in conformance to a typical multipath channel used in WiFi investigations [Sch13]. The channel model applied in these simulations had an exponentially decreasing power delay profile (PDP) with an appropriately selected RMS delay spread, and it is called the Naftali model (it is commonly utilized for wireless LAN applications

such as IEEE 802.11) [NAJ06]. The mathematical representation of Naftali model for the channel is given below [Nab02].

$$h[n] = N\left(0, \frac{1}{2}\sigma_n^2\right) + j \cdot N\left(0, \frac{1}{2}\sigma_n^2\right) \tag{3.3}$$

where $h[n]$ represents impulse response of multipath filter model, $N\left(0, \frac{1}{2}\sigma_n^2\right)$ denotes a zero mean Gaussian distribution with variance equal to $0.5\sigma_n^2$ and M is the number of filter taps. The variance is a function of the tap index n $(0: M-1)$, and it can be described as [Sch13]:

$$\sigma_n^2 = e^{\left(\frac{-n \cdot T_s}{T_{rms}}\right)} \tag{3.4}$$

In Eq. (3.4), T_s referes to the sample period, while T_{rms} is the RMS delay spread of the multipath channel. RMS delay spread is an important single measure for the delay time extent of a multipath radio channel. RMS delay spread is a factor that portrays the time dispersion of the channel. RMS delay spread can be defined as the square root of the second central moment of channel's power delay profile (PDP representing the intensity of a signal received through a multipath channel as a function of time delay, so time delay denotes the difference in travel time between multipath arrivals) [DC00]. Table 3.2 shows several values of RMS delay spread that are assigned for different environments [Sch13].

Table 3.2 Illustrating RMS delay spread values in various environments

RMS delay spread value	Environment
RMS delay spread $< 100\ nsec$	Inside office buildings and residential homes
RMS delay spread $< 200\ nsec$	Large commercial buildings and warehouse
RMS delay spread $= 150\ to\ 400$ nsec	Suburban environments
RMS delay spread $= 1\ to\ 3\ \mu$sec	Dense urban environments like Manhattan

RMS delay spread $= 2\ to\ 25\ \mu$sec	Urban environments (distant large buildings)

Note that for each transmitted packet block, new multipath channel gain coefficient vectors were drawn, and the number of OFDM symbols that are sent inside each packet is $L = 100$.

Figure 3.12 shows BER vs. SNR measurement for the strong user by setting the propagation path loss $g_1 = 1.0$ versus different values of g_2. The RMS delay spread used in this simulation was $(T_{rms} = 50\ nsec)$.

It can be easily observed that there is an improvement in performance (nearly 2 dB gain at BER level of 10^{-2}) with a lower value of propagation path loss g_2 as the signal of the weak user looks more like noise in the strong user's receiver.

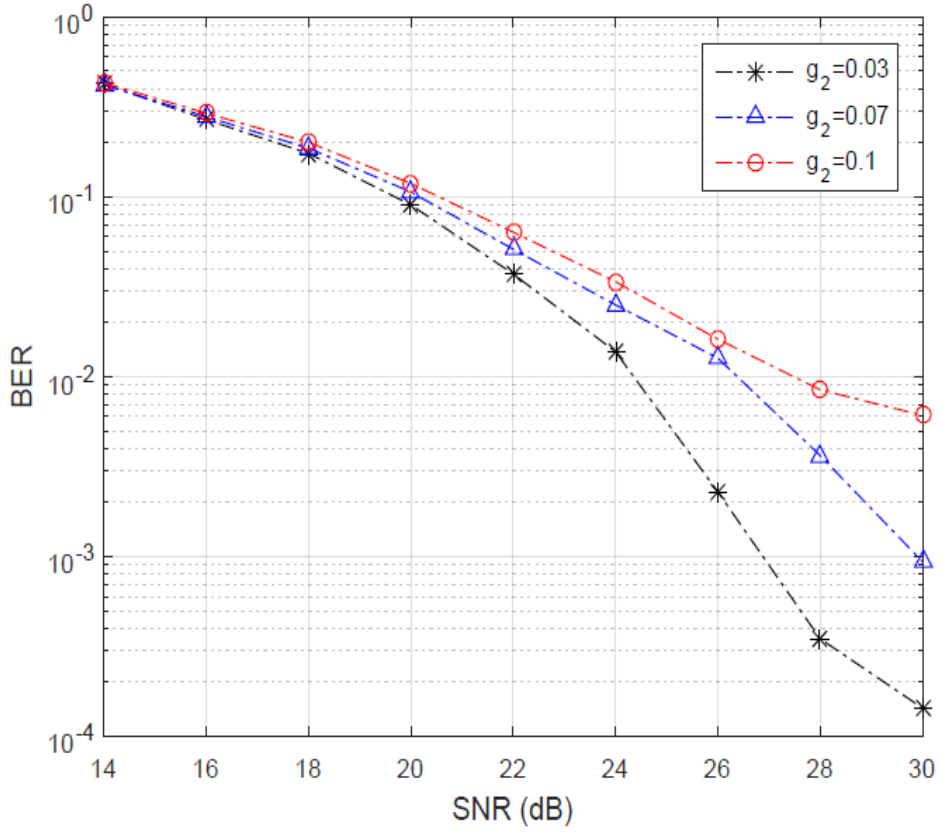

Figure 3.12 BER vs. SNR curve for the strong user $(g_1 = 1.0)$ with several values of the weak channel gain g_2

In Figure 3.13, another comparison of BER vs. SNR for the strong user is studied by defining the propagation path losses of the users as $g_1 = 1.0,\ g_2 = 0.03$ and simulating the system with different values of the RMS delay spread. The RMS delay spread is considered an important parameter in calculating the channel gain coefficient vector per each user.

Figure 3.14 presents a similar comparison as Figure 3.13. Here, the estimation of BER vs. SNR is assessed for the weak user by adjusting the propagation path loss as $g_1 = 1.0,\ g_2 = 0.1$ and simulating the system by using various RMS delay spread values.

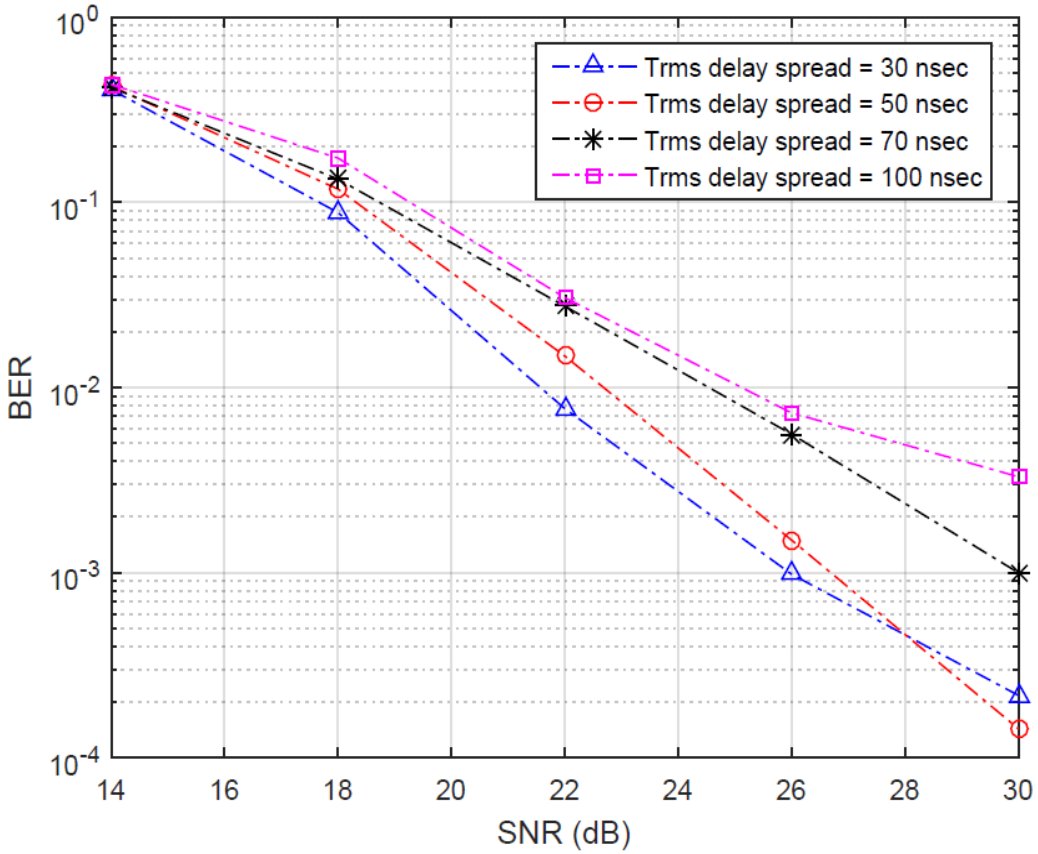

Figure 3.13 BER vs. SNR plot for the strong user$(g_1 = 1.0, g_2 = 0.03)$ with different values of RMS delay spread

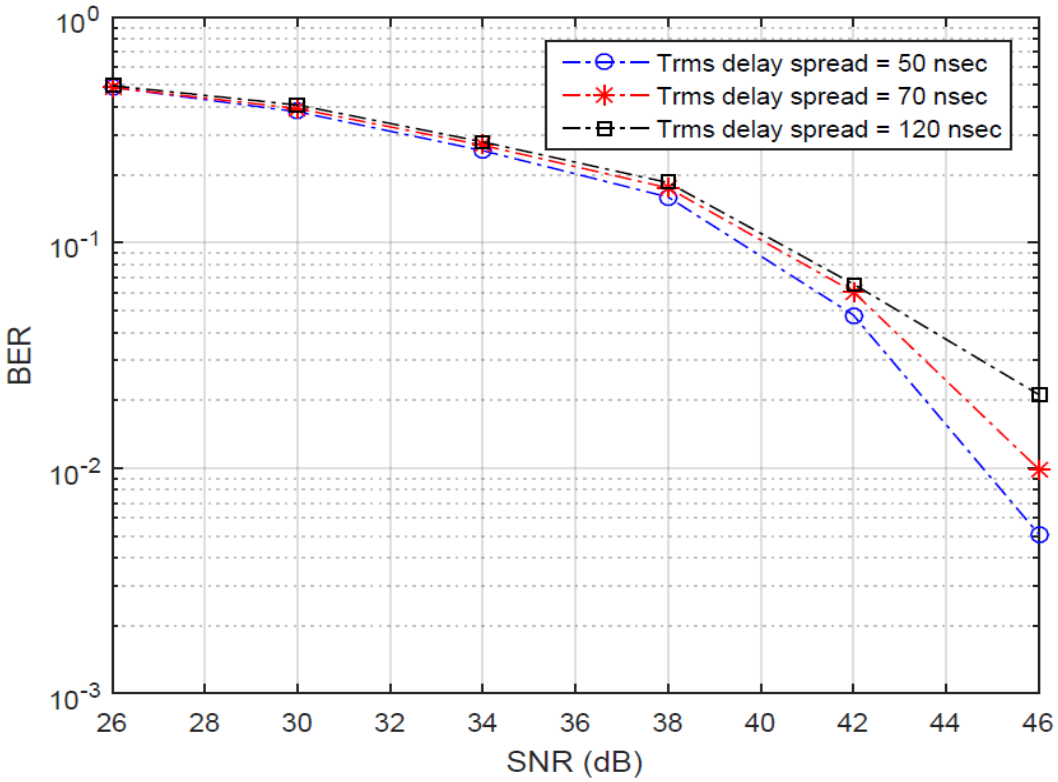

Figure 3.14 BER vs. SNR plot for the weak user ($g_1 = 1.0, g_2 = 0.1$) with several values of RMS delay spread

Based on Figures 3.13 and 3.14, we can conclude that the relationship between system performance and RMS delay spread value is more or less inversely proportional. Better performance can be achieved when a low RMS delay spread value is observed chosen, due to its influence on the channel gain coefficient vector, which in turn decreases the effect of multipath fading.

MATLAB simulation model contained many procedures performed in real Wi-Fi transmitters and receivers typically operating in a single link between a user and an access point. Most of them were described and illustrated in [Sch13]. One of them is the detection of the start of a packet in a receiver. Typically, a certain minimum change in the signal level has to appear at the receiver input to be interpreted as a start of a signal different from noise. In fact, an increase in SNR is detected. In the case of two such signals being the mixture of a strong and a weak one, if their levels differ too much, the receiver of the weak signal working individually can have a

problem with recognizing the packet start if SNR is low for it. Eq. (3.5) is used to explain this problem as:

$$Comparsion\ ratio[j] = \frac{auto\_corr[j]}{var[j]} \tag{3.5}$$

where $auto\_corr[j]$ is the autocorrelation estimate of received signal y_j, while $var[j]$ denotes the variance calculated for the corresponding signal. Comparison between these two quantities represents the primary method of indicating the presence of a valid packet according to the following condition:

$$Valid\ packet \rightarrow if\ auto\_corr[j] \approx\ var[j]$$

$$Invalid\ packet \rightarrow if\ auto\_corr[j] \ll var[j]$$

Comparison ratio acts as a detection threshold and substantially influences the system performance. When the value of this parameter is low, the received packet can be detected with a low power level (low SNR value), however, when the threshold is set sufficiently high, the receiver of a weak signal has a problem with detecting the beginning of the start of a packet. Fortunately, as both receivers for strong and weak signals are physically located at the same place, it is sufficient to use the sufficiently high threshold of the strong signal to start the reasonable operation of both receivers. Certainly, the synchronization of both signals has to be ensured first.

3.5 Summary

This chapter presented some interference cancellation techniques that are utilized to mitigate the interference of multiple users in wireless communications systems. One of them is successive interference cancellation, which was proving to be a one of the key technologies that can be employed to meet the requirements of next generation of wireless communications networks. In this chapter, a brief description of SIC principle as well as its application was introduced. Some simulation results were addressed in order to study the performance of proposed system model.

Chapter 4

Improved SIC Detector and Its Application in NOMA Transmission

A Successive Interference Cancellation (SIC) receiver is one of the important blocks in non-orthogonal multiple access (NOMA) transmission. The quality of detection of the strongest user signals often determines the quality of the whole system and minimizes the error propagation effect. The relative power levels for users sharing the same resources have been the subject of some investigations. Power allocation among users plays an important part in the users' performance, which in turn affects the overall system performance and throughput.

This chapter presents an improved detection algorithm which can be used in NOMA transmission in a much smaller range of power differences between the terminals sharing common radio resources in the uplink, as compared with standard successive cancellation. Its idea is the application of tentative decisions about weaker signals in the detection of stronger ones and then, after improved detection of stronger user signals, causing achievement of more reliable decisions about the weaker ones. The simulation results that have been published by the author in [GW19, GW19a] confirm the idea and show a much higher detection quality of the proposed receiver when compared with the standard solution.

4.1 Model of the Considered System

For the purpose of presenting the proposed detector, the author considers an OFDM system operating in the uplink transmission, shown in Figure 4.1. Binary information block $\mathbf{x}^{(i)}$ $(i = 1,2)$ that is assigned to each OFDM transmitter is subject to channel coding using the principle of convolution code with coding rate $1/2$, thereafter the encoded bit stream is interleaved using the interleaver block with a size equal to the number of coded bits in a single OFDM symbol.

Bits of the resulting codewords are partitioned into groups of bits and mapped onto QPSK/QAM symbols. Users' allocated modulation type (QPSK/QAM) is usually based on the propagation conditions of each user - higher modulation order is assigned to the user facing better

propagation conditions, while lower modulation order is allocated to the user who suffers from worse propagation conditions.

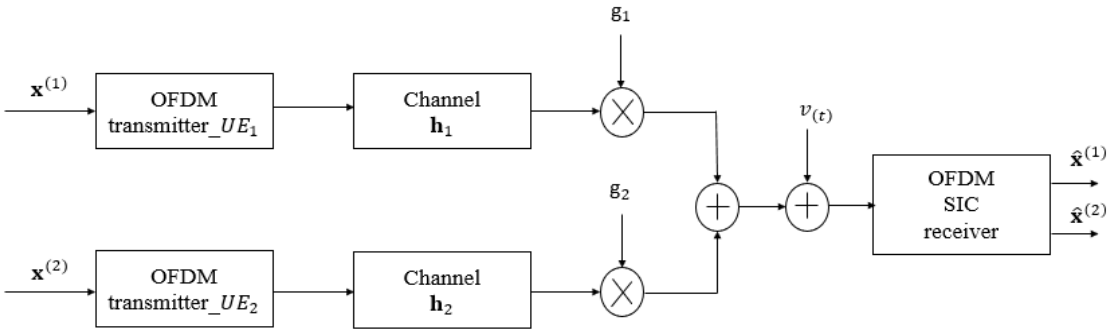

Figure 4.1 System model of uplink NOMA

Subsequently, the resultant symbols constitute subcarrier symbols of the IFFT modulator that consists of 52 subcarriers. Four of them are allocated to pilot signals for assisting the receiver to compensate against frequency offsets and phase noise, and the remaining 48 OFDM subcarriers are dedicated for data transmission. Inverse Fast Fourier Transform (IFFT) has been applied for transforming OFDM symbols from the frequency domain to the time domain and generating time domain samples supplemented by a cyclic prefix that enables system to be robust against multipath propagation. The functional blocks sequence inside each OFDM transmitter can be illustrated by Figure 4.2.

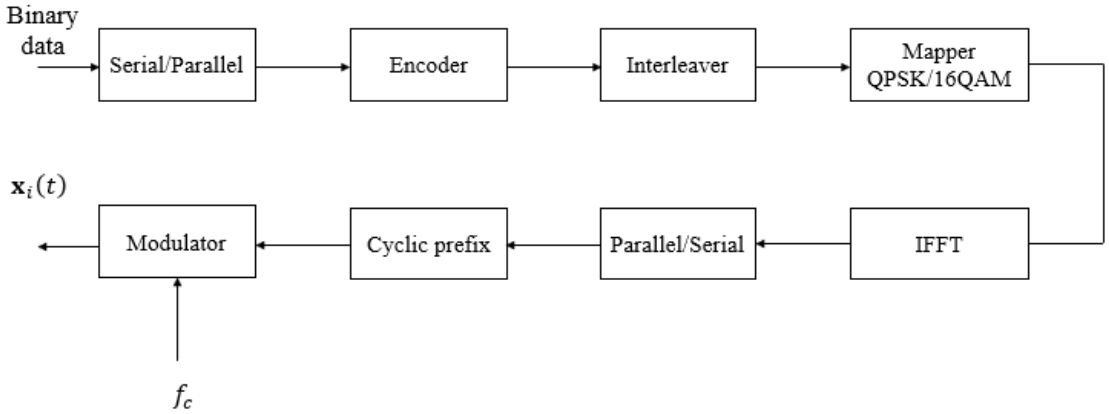

Figure 4.2 Block diagram of an OFDM transmitter [Wes09]

Afterwards, in our system model, the sample baseband sequences generated in a receiver are subject to convolution with the baseband equivalent impulse response of the dispersive radio channel denoted by vector $\mathbf{h}_i$ $(i = 1,2)$. For the sake of simplicity, the author assumes that the mean energy of each channel impulse response is normalized to unity. In order to model the propagation loss, the author assigns the power P_i $(i = 1,2)$ of signals incoming to the receiver from each user by setting the values of the coefficients g_i.

$$g_i = \sqrt{P_i} \qquad i = 1,2 \tag{4.1}$$

The received signal at the reception side is disturbed by the additive white Gaussian noise $v(t)$. It should be taken into consideration that, as assumed previously, signals from both transmitters arrive to the receiver with such a propagation delay difference that the receiver is able to select a common orthogonality period in which OFDM signals from both transmitters are analyzed. Typically, in D2D or V2X communications scenarios, the distances between transmitters and receivers are not large (e.g., up to a few hundred meters), so a coarse synchronization of both transmitters justifies such an assumption. For example, in the case of a typical IEEE 802.11 a/g/n WLAN, the transmission difference in the distance between the transmitter and the receiver equal to 200 m results in a propagation time difference shorter than the length of the OFDM cyclic prefix equal to 0.8 μs.

Based on the principle of an OFDM receiver as shown in Figure 4.3, the author supposes that an OFDM SIC receiver can select a common orthogonality period for the sum of both incoming signals and perform FFT on it.

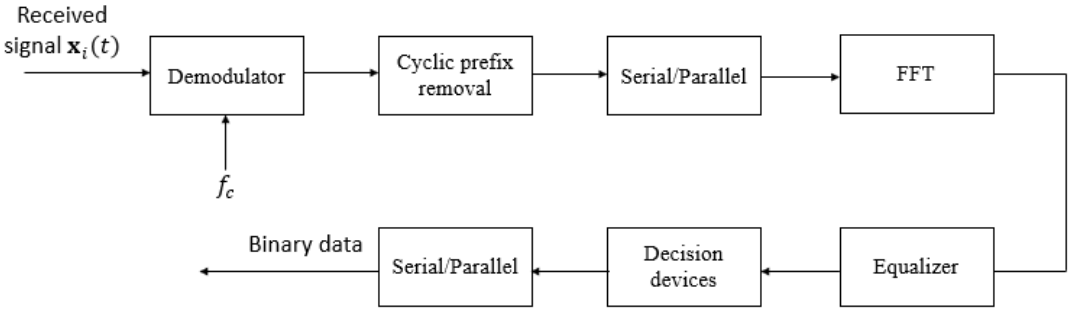

Figure 4.3 Block diagram of an OFDM receiver [Wes09]

As a result, the signal on each OFDM subcarrier output (FFT bin) can be expressed by a simple equation:

$$Y_k = H_k^{(1)} X_k^{(1)} + H_k^{(2)} X_k^{(2)} + N_k \qquad k = 0, \dots, N-1 \tag{4.2}$$

where $X_k^{(1)}, X_k^{(2)}$ represent QPSK/QAM symbols transmitted on the *k*-th OFDM subcarrier $(k = 0, \dots, N-1)$, N is the number of subcarriers in each OFDM symbol, whereas $H_k^{(1)}, H_k^{(2)}$ are channel coefficients on this subcarrier, and

$$\mathbf{H}^{(i)} = \left[H_0^{(i)}, H_1^{(i)}, \dots, H_{N-1}^{(i)}\right] = FFT\{\mathrm{g}_i \mathbf{h}_i\} \qquad i = 1,2 \tag{4.3}$$

where N_k represents a noise sample on the *k*-th subcarrier output. Eq. (4.4) explains the fundamentals of data detection on per-subcarrier basis using the SIC principle. In Figure 4.4, a standard solution resulting from the general rule has been presented. In this approach, first, a strong component of the received signal is detected and the second and third components are jointly treated as noise. Thus, the following operation is performed:

$$\tilde{X}_k^{(1)} = \frac{Y_k}{\widehat{H}_k^{(1)}} \qquad k = 0,1, \dots, N-1 \tag{4.4}$$

Based on the collected samples $\tilde{X}_k^{(1)}, (k = 0,1, \dots, N-1)$, soft-decision de-mapping is typically performed, producing LLR (log-likelihood ratio) samples for each bit of the codeword of the channel code decoder as described in the previous chapter. The result of channel decoding of the strong user (one who experiences better channel propagation) is the information sequence of $\hat{\mathbf{x}}_1$. This procedure can be explained by the following flowchart presented in Figure 4.4.

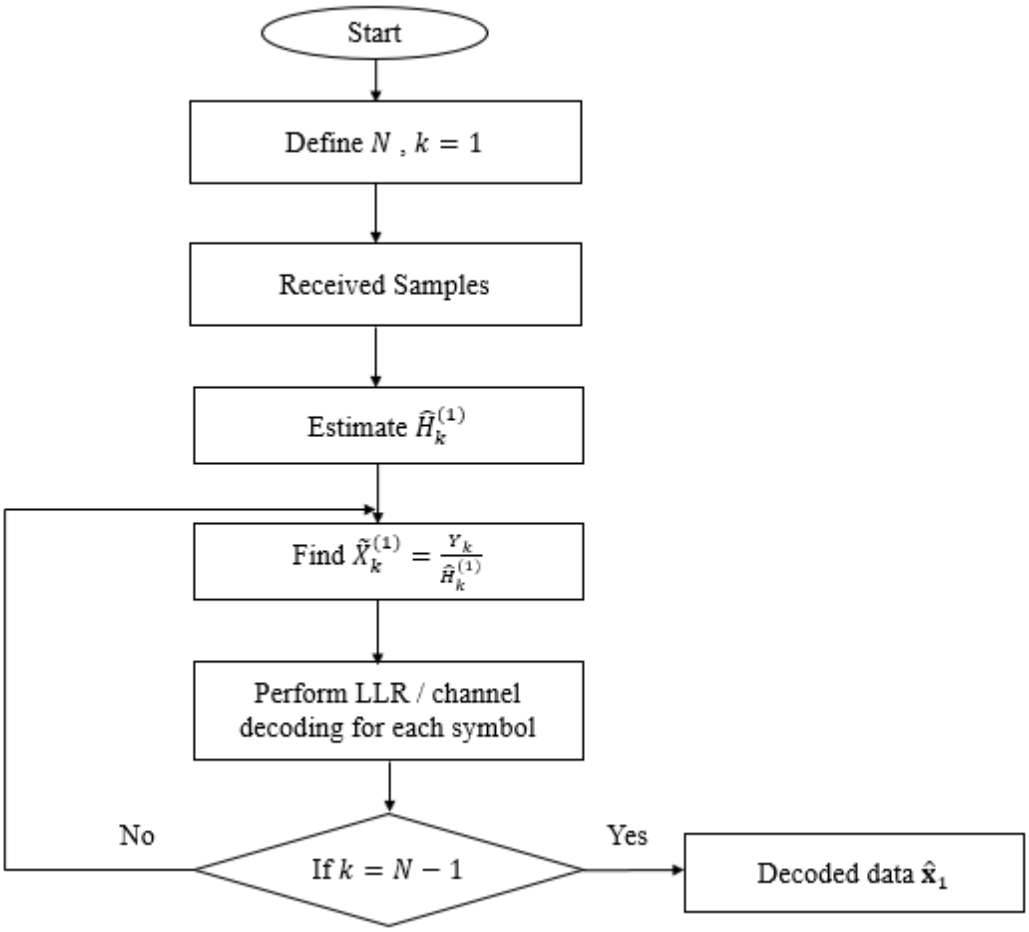

Figure 4.4 Flowchart of strong user's information decoding based on a standard SIC detector

Thereafter, its basic channel coding is performed again and QPSK/QAM re-modulated symbols are produced, namely $\hat{X}_k^{(1)}, (k = 0,1, \dots, N-1)$. They are subsequently used in the cancellation process. Consequently, the weaker user data symbols are produced according to the following formula:

$$\tilde{X}_k^{(2)} = \frac{Y_k - \hat{H}_k^{(1)} \hat{X}_k^{(1)}}{\hat{H}_k^{(2)}} \qquad k = 0,1, \dots, N-1 \tag{4.5}$$

On the basis of the set of samples $\tilde{X}_k^{(2)}, (k = 0,1, \dots, N-1)$, soft de-mapping is performed for the weaker user (one who has worse channel propagation), producing LLR samples for the codeword bits of the channel code used by him. As a result, information block $\hat{\mathbf{x}}_2$ is generated. Figure 4.5 demonstrates the process of information decoding of the weaker terminal.

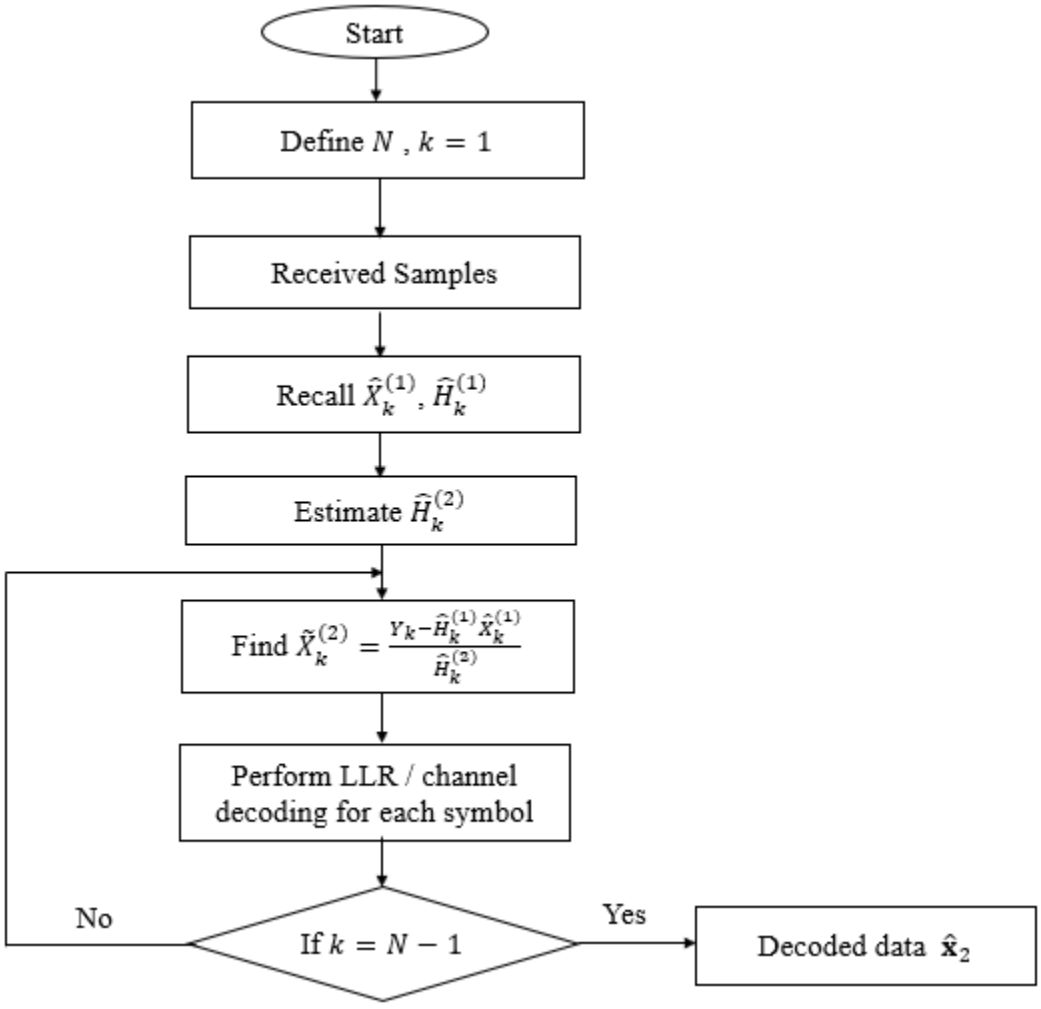

Figure 4.5 Flowchart of weak user's information decoding based on a standard SIC detector

Let us note that in order to make the decisions and perform SIC cancellation, the knowledge of both channel coefficients is required. They have to be estimated on the basis of appropriately designed preambles or pilots purposely placed on the subcarrier-OFDM symbol grid. The particular implementation of a channel estimator depends on the applied system. The existence of a weak signal certainly has a growing negative influence on the quality of the decisions about the strong user.

Simulation results of the proposed detector show that the power level difference between a strong and weak user should be substantial for the reliable operation of a SIC receiver. It was the

motivation behind introducing an improved decision process which extends the range of possible levels of a weaker user and enables reliable detection of both users in a wide range of relative power levels.

4.2 Description of the Proposed Detector

In this section, the author assumes that the channel coefficients' true value or their estimates for weak and strong users are known due to the channel estimation process. Recall Eq. (4.2) of the signal samples received in the FFT demodulator output. For the proposed receiver, tentative hard symbol-by-symbol decisions are first performed on both strong and weak signals concurrently, i.e., in conformance with the maximum likelihood (ML) criterion, the following operation is performed.

$$\left(\bar{X}_k^{(1)}, \bar{X}_k^{(2)}\right) = \arg \min_{X_k^{(1)},\ X_k^{(2)}} \left| Y_k - \hat{H}_k^{(1)} X_k^{(1)} - \hat{H}_k^{(2)} X_k^{(2)} \right|^2 \tag{4.6}$$

for

$$k = 0,1, \dots, N-1$$

To get the tentative decisions according to Eq. (4.6), at this step, the channel coding law is neglected. This way we destroy dependence of QPSK/QAM symbols on each other due to channel coding. The main aim of performing Eq. (4.6) is to obtain $\bar{X}_k^{(2)}, (k = 0,1, \dots, N-1)$ which can be used to improve the quality of samples of the FFT bins of the strong user. This time, instead of Eq. (4.4), the author uses the following samples to calculate the LLR values of codeword bits for the channel code applied by the strong user:

$$\tilde{X}_k^{(1)} = \frac{Y_k - \hat{H}_k^{(2)} \bar{X}_k^{(2)}}{\hat{H}_k^{(1)}} \qquad k = 0,1, \dots, N-1 \tag{4.7}$$

After finding LLR, soft-decision samples that are used in the channel decoder and de-interleaver, the final decision about information block $\hat{\mathbf{x}}_1$of the strong user is made. Figure 4.6 presents the process of information decoding of the strong user.

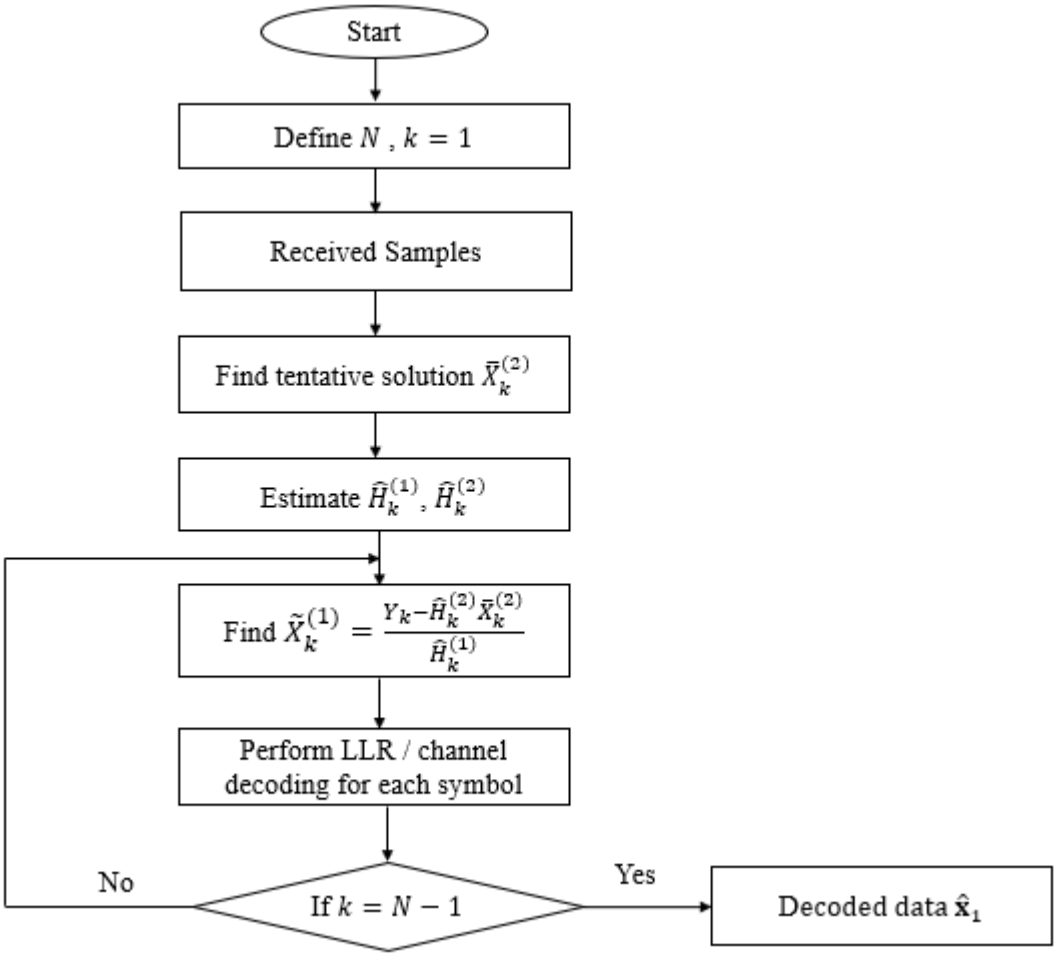

Figure 4.6 Flowchart of strong user's information decoding based on the proposed SIC detector

Based on it, the codeword bits, interleaving and QPSK/QAM mappings are performed, resulting in QPSK/QAM symbols $\hat{X}_k^{(1)}, (k = 0,1, \dots, N-1)$. They are subsequently used in cancellation, as in Eq. (4.5). As previously explained in Figure 4.5, on the basis of the set of samples $\tilde{X}_k^{(2)}, (k = 0,1, \dots, N-1)$, soft de-mapping is performed for the weaker user, producing LLR samples for the codeword bits of the channel code used in this link. As a result, information block $\hat{\mathbf{x}}_2$ is generated.

Summarizing, the main improvement of the SIC cancellation lies in finding tentative decisions about weak user signals in Eq. (4.6) and using them in the calculation of strong user samples Eq. (4.7). The simulation results shown in the next sections indicate that this simple idea

substantially improves the range of possible differences in power between strong and weak users. In consequence, there is much higher tolerance in users' pairing process.

The proposed SIC detector discussed in this chapter is demonstrated on the example of two NOMA users. In general, $K > 2$ users can be considered. For $K = 2$, additional complexity in comparison to the standard SIC detector results from searching for the best pair of data symbols received from the strong and weak users (see Eq. (4.6)). The number of times when Eq. (4.6) is implemented is $M_s M_w$ per OFDM active subcarrier where M_s and M_w represent the signal constellation sizes applied by the strong and weak users, respectively.

In general, if there are *K* NOMA users, each of them applying *M*-array modulation on *N* subcarriers, the additional complexity over the standard SIC solution grows linearly with *N* and exponentially with M^K on each subcarrier.

The proposed scheme can be extended to the NOMA system with $K > 2$ users in the following manner. Let the users be sorted in the descending power order. Then the first two strongest users are treated according to the proposed detection method, whereas the remaining users are treated as distortion. If the detection of both considered user data signals is successful, after the reconstruction of both signals their influence can be cancelled from the joint received signal. The next pair of signals can be considered in the same manner. Such an operation can be repeated till all of them are detected.

Finally, the author is fully aware that much more sophisticated receivers can be considered for several scenarios of future 5G systems. Typically, they are well-matched to particular transmission systems (spreading, channel coding, modulation size, etc.) and are usually based on iterative algorithms using minimum mean square error detectors, parallel or serial interference cancellation, or more sophisticated detection algorithms, such as elementary signal estimators (ESE), the message passing algorithm (MPA) and the expectation propagation algorithm (EPA). Despite that, the author limits her considerations to a simple case of a SIC detector for which the proposed detector improvement can be easily evaluated.

4.3 Theoretical Analysis of Two SIC Detectors

In order to justify the proposed improved detector, an analysis of two simplified cases has been performed. In the first one, a traditional SIC detector described mainly by Eq. (4.4) and (4.5) is

considered, whereas in the second one the author analyzes the proposed SIC detector (Eq. (4.6), (4.7) and (4.5)). An example of a similar analysis performed for a traditional SIC detector can be found in [JS02]. The author analysis is simpler, but leads to fully analytical results.

In both cases the author of this dissertation omits the fact that typically channel coding is applied, as otherwise, the analysis would be much more complicated. At the same time, the author considers signals on a single subcarrier and for the simplicity of this analysis the following equation has been considered for describing a signal on the FFT output (the author neglects the subcarrier number for the sake of clarity of this notation):

$$Y = Y^R + jY^I = X_1 + gX_2 + v \tag{4.8}$$

Let us assume that data symbols $X_1$and X_2 are QPSK-modulated and are selected from a set represented by $\{A + jA, -A + jA,\ A - jA, -A - jA\ \}$. Coefficient g is the weighting factor of magnitude not larger than one. In general, it can be complex, however, let us assume for simplicity that it is real (no phase shift is observed between the stronger X_1 and weaker X_2 (due to g) signals). Let both data symbols be statistically independent and equiprobable. Let us also assume that v is a sample of the white zero mean Gaussian noise of variance σ^2.

4.3.1 Error Probability Analysis of a Regular SIC Detector

First, the symbol error probability for the strong receiver is calculated, aiming at the detection of X_1 symbols. Please recall that it makes a direct decision about X_1 on the basis of the received sample Y (4.8). Denote $P_C(X_1)$ as the probability of correct reception for a particular symbol X_1. Denote $P(X_1)$ as the probability of generation of X_1. Clearly, on the basis of the assumptions, $P(X_1) = 1/4$ for each data symbol X_1. Then the symbol error probability $P_E^{(1)}$for a stronger signal can be described by the equation:

$$P_E^{(1)} = 1 - \sum_{X_1} P_C(X_1)\, P(X_1) \tag{4.9}$$

where

$$P_C(X_1) = \sum_{X_2} P_C(X_1|X_2)\, P(X_2) \tag{4.10}$$

Consider the particular data symbol $X_1 = A + j\,A$. Let us introduce variables b_1^R and b_1^I in the form:

$$b_1^R = A + gX_2^R \tag{4.11}$$

$$b_1^I = A + gX_2^I \tag{4.12}$$

which constitute the in-phase and quadrature components of both received signals without noise, respectively (each of the X_2 data symbol components is equal to $X_2^R = \pm A,\ X_2^I = \pm A$). Taking into account that the in-phase and quadrature noise components have variance $\sigma^2/2$, as a result, the following equation can be written as:

$$P_C(X_1|X_2) = \left(1 - \frac{1}{2}\mathrm{erfc}\left(\frac{b_1^R}{\sigma}\right)\right)\left(1 - \frac{1}{2}\mathrm{erfc}\left(\frac{b_1^I}{\sigma}\right)\right) \tag{4.13}$$

Therefore, recalling that for other symbols X_1 the situation is fully analogous, and $P(X_1) = P(X_2) = 1/4$, the author gets the following formula:

$$\begin{aligned} P_E^{(1)} &= 1 - \tfrac{1}{4}\textstyle\sum_{X_2}\left(1 - \tfrac{1}{2}\mathrm{erfc}(\tfrac{b_1^R}{\sigma})\right)\left(1 - \tfrac{1}{2}\mathrm{erfc}(\tfrac{b_1^I}{\sigma})\right) \\ &= 1 - \tfrac{1}{4}\left[2 - \tfrac{1}{2}\left(\mathrm{erfc}\left(\tfrac{A+gA}{\sigma}\right)\right) + \mathrm{erfc}\left(\tfrac{A-gA}{\sigma}\right)\right]^2 \end{aligned} \tag{4.14}$$

It is important to note that the presence of signal X_2 in sample Y substantially influences the error probability for data symbol X_1. Figure 4.7 illustrates formula (4.14) for several values of the weighting coefficient g.

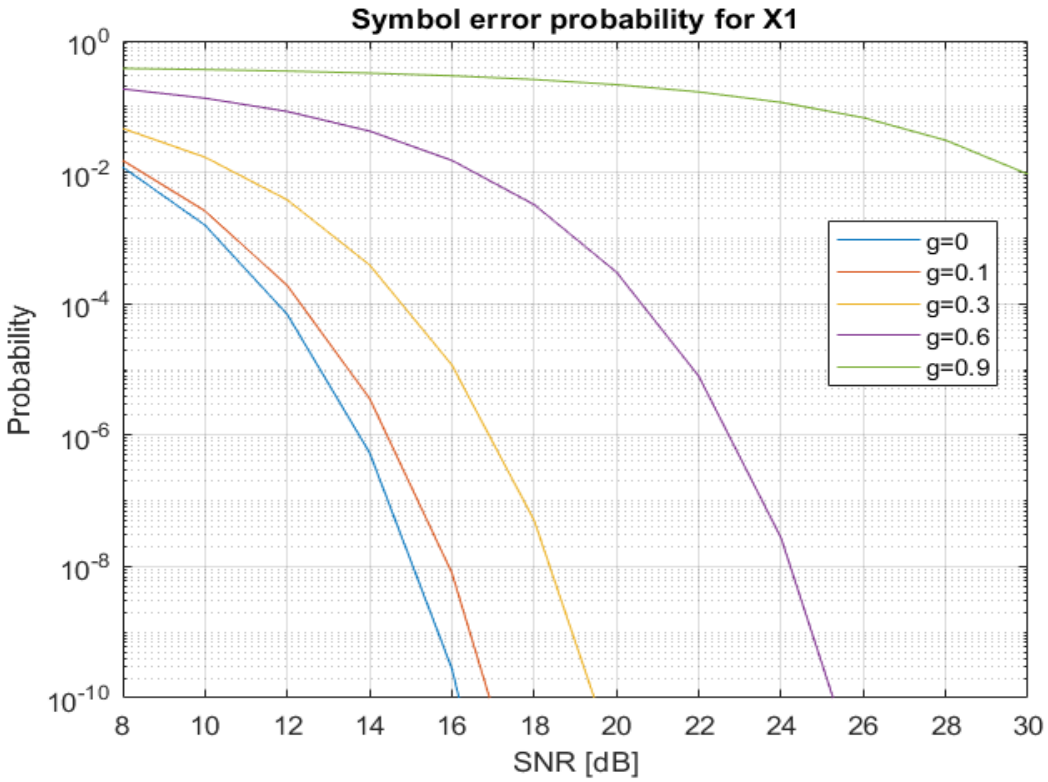

Figure 4.7 Symbol error probability according to Eq. (4.14) for model in Eq. (4.8)

Thereafter, the author focuses her attention on the symbol error probability for the weaker received signal. First, the probability of a correct decision made for symbol X_2 is calculated. It can be expressed in the form:

$$P_C(X_2) = \sum_{X_1} \left[P_C\left(X_2 | \text{correct } \hat{X}_1\right)\left(1 - P_E^{(1)}\right) + P_C\left(X_2 | \text{incorrect } \hat{X}_1\right) P_E^{(1)} \right] P(X_1) \tag{4.15}$$

Certainly,

$$P_E^{(2)} = 1 - \sum_{X_2} P_C(X_2) P(X_2) \tag{4.16}$$

Consider $P_C\left(X_2 | \text{correct } \hat{X}_1\right)$ first. The SIC detector cancels X_1 correctly by subtracting $\hat{X}_1 = X_1$ from Y, so after cancellation the following result is obtained:

$$Z = Y - \hat{X}_1 = gX_2 + v \tag{4.17}$$

In order to apply the threshold detector to X_2, we divide both sides of Eq. (4.17) by g, therefore the following result is obtained:

$$Z' = X_2 + \frac{v}{g} \tag{4.18}$$

Consider signal $X_2 = A + jA$ as the transmitted one. For this case, knowing that $v = v^R + jv^I$, the result is:

$$\begin{aligned} P_c(X_2 = A + jA \big| \text{correct } \hat{X}_1) &= \Pr\left\{\frac{v^R}{g} > -A\right\} \Pr\left\{\frac{v^I}{g} > -A\right\} \\ &= \left[1 - \frac{1}{2}\text{erfc}\left(\frac{Ag}{\sigma}\right)\right]^2 \end{aligned} \tag{4.19}$$

It is worth noting again that for the remaining QPSK-modulated X_2 symbols the situation is analogous, resulting in the same expression for the correct conditional decision Eq. (4.19). Therefore,

$$P_C(X_2 \big| \text{correct } \hat{X}_1) = \left[1 - \frac{1}{2}\text{erfc}\left(\frac{Ag}{\sigma}\right)\right]^2 \tag{4.20}$$

In the case of incorrect detection of X_1, calculations are substantially more complicated. In [JS02] the authors simplify their similar considerations of error calculations for multiuser detectors when a stronger signal is wrongly detected, indicating that error propagation has a disruptive effect on the weaker signal reception quality and the conditional probability $P_c(X_2 \big| \text{incorrect } \hat{X}_1)$ can be well approximated by 1/4 (in the case of QPSK) due to a virtually equally probable guess of the data symbol $\hat{X}_2$. Therefore, recalling that all symbols X_1 are equally probable, Eq. (4.15) can be expressed in the form:

$$P_C(X_2) = \left[1 - \frac{1}{2}\text{erfc}\left(\frac{Ag}{\sigma}\right)\right]^2 \left(1 - P_E^{(1)}\right) + \frac{1}{4}P_E^{(1)} \tag{4.21}$$

Substituting Eq. (4.21) in (4.16), the following formula is obtained:

$$P_E^{(2)} = 1 - \left[1 - \frac{1}{2}\operatorname{erfc}\left(\frac{Ag}{\sigma}\right)\right]^2 \left(1 - P_E^{(1)}\right) - \frac{1}{4}P_E^{(1)} \tag{4.22}$$

4.3.2 Error Probability Analysis for the Proposed SIC Detector

As already mentioned in the previous analysis, the author does not take into account the fact that channel coding is typically applied for both links, assuming the symbol-by-symbol detection is performed at the receiver. According to this proposal, first the detector attempts to find a tentative decision about the weaker symbol X_2. In order to do it, it selects such a pair $(\bar{X}_1, \bar{X}_2)$ that minimizes the metric shown below, which is a simplified version of the metric represented in Eq. (4.6).

$$(\bar{X}_1, \bar{X}_2) = \arg \min_{X_1, X_2} |Y - X_1 - \mathrm{g}X_2|^2 \tag{4.23}$$

A correct guess $\bar{X}_2$ about X_2 will presumably result in decreasing $P_E^{(1)}$ when the final decision about $X_1$is calculated and it will also have a positive impact on the error probability of the weaker signal.

As previously, the author can write:

$$P_E^{(1)} = 1 - \sum_{X_1} P_C(X_1)\, P(X_1)$$

but in the current case

$$\begin{aligned} P_C(X_1) = {} & P_C(X_1|\text{correct}\,\bar{X}_2)\Pr\{\text{correct}\,\bar{X}_2\} \\ & + P_C(X_1|\text{incorrect}\,\bar{X}_2)(1 - \Pr\{\text{correct}\,\bar{X}_2\}) \end{aligned} \tag{4.24}$$

Let us begin the calculations by deriving the expression for $\Pr\{\text{correct}\,\bar{X}_2\}$. This calculation is rather straightforward, but cumbersome. X_1 is assumed again as $X_1 = A + j\,A$. The consideration of all other possible symbols X_1 leads to identical results. Figure 4.8. presents all areas in which the end of the noise vector has to be placed when the tentative decision $\bar{X}_2$ is correct and decisions related to X_1 and X_2 are found according to Eq. (4.23). Such considerations have to be made for each correct symbol X_2. In the sequel, only one such calculation for $X_2 =$

$-A + j\,A$ is shown and presented in Figure 4.8. All the remaining values of X_2 can be considered similarly and these calculations will be omitted.

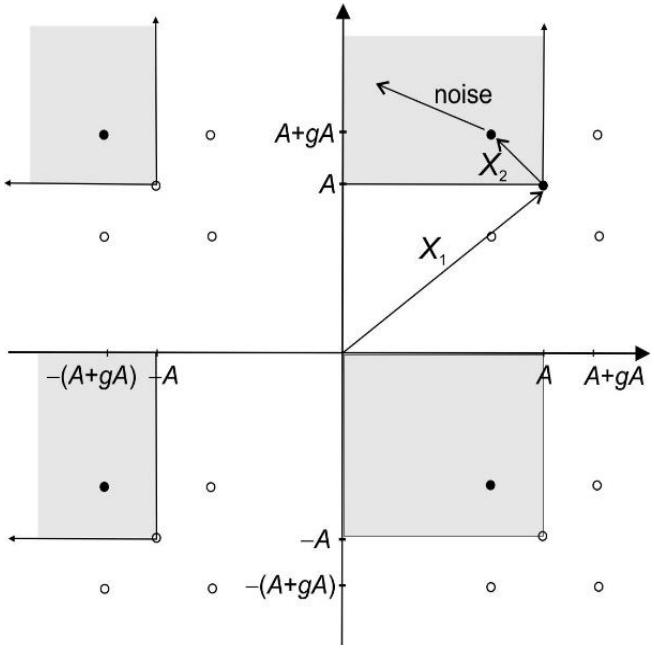

Figure 4.8 Areas determining correct decisions based on Eq. (4.23) about $X_2 = -A + j\,A$ when $X_1 = A + j\,A$

For the case shown in Figure 4.8., the following formula is obtained:

$$\begin{aligned}\Pr\{\text{correct } \bar{X}_2 | X_1 = A + jA,\ X_2 = -A + jA\ \} \qquad (4.25)\\ = \left(\frac{1}{\sqrt{\pi}\sigma}\int_{-(A-gA)}^{gA} e^{-\frac{t^2}{\sigma^2}}\,dt\right)\cdot\left(\frac{1}{\sqrt{\pi}\sigma}\int_{-gA}^{\infty} e^{-\frac{t^2}{\sigma^2}}\,dt\right)\\ + \left(\frac{1}{\sqrt{\pi}\sigma}\int_{-\infty}^{-(2A-gA)} e^{-\frac{t^2}{\sigma^2}}\,dt\right)\cdot\left(\frac{1}{\sqrt{\pi}\sigma}\int_{-gA}^{\infty} e^{-\frac{t^2}{\sigma^2}}\,dt\right)\\ + \left(\frac{1}{\sqrt{\pi}\sigma}\int_{-\infty}^{-(2A-gA)} e^{-\frac{t^2}{\sigma^2}}\,dt\right)\cdot\left(\frac{1}{\sqrt{\pi}\sigma}\int_{-(2A+gA)}^{gA} e^{-\frac{t^2}{\sigma^2}}\,dt\right)\\ + \left(\frac{1}{\sqrt{\pi}\sigma}\int_{-(A-gA)}^{gA} e^{-\frac{t^2}{\sigma^2}}\,dt\right)\cdot\left(\frac{1}{\sqrt{\pi}\sigma}\int_{-(2A+gA)}^{-(A+gA)} e^{-\frac{t^2}{\sigma^2}}\,dt\right)\end{aligned}$$

The upper and lower borders in the integrals in Eq. (4.25) result from the values of in-phase and quadrature noise components which have to occur to make a correct decision about X_2. These calculations lead to the following result:

$$\begin{aligned}\Pr\{\text{correct}\,\bar{X}_2|X_1 = A + jA, X_2 = -A + jA\} \\ = \left[1 - \frac{1}{2}\operatorname{erfc}\left(\frac{A - gA}{\sigma}\right) - \frac{1}{2}\operatorname{erfc}\left(\frac{gA}{\sigma}\right) + \frac{1}{2}\operatorname{erfc}\left(\frac{2A - gA}{\sigma}\right)\right] \\ \cdot \left[1 - \frac{1}{2}\operatorname{erfc}\left(\frac{2A + gA}{\sigma}\right) - \frac{1}{2}\operatorname{erfc}\left(\frac{gA}{\sigma}\right) + \frac{1}{2}\operatorname{erfc}\left(\frac{A + gA}{\sigma}\right)\right]\end{aligned}$$

Considering similarly all the remaining three data symbols X_2, knowing that they are equiprobable ($P(X_2) = 1/4$), the author ends up with the following formula for $\Pr\{\text{correct}\,\bar{X}_2\}$

$$\begin{aligned}&\Pr\{\text{correct}\,\bar{X}_2\} \\ &= \frac{1}{4}\left\{2 - \operatorname{erfc}\left(\frac{gA}{\sigma}\right) - \frac{1}{2}\left[\operatorname{erfc}\left(\frac{A - gA}{\sigma}\right) - \operatorname{erfc}\left(\frac{A + gA}{\sigma}\right)\right]\right. \\ &\left. + \frac{1}{2}\left[\operatorname{erfc}\left(\frac{2A - gA}{\sigma}\right) - \operatorname{erfc}\left(\frac{2A + gA}{\sigma}\right)\right]\right\}^2\end{aligned} \tag{4.26}$$

Returning to Eq. (4.24) it is easy to show that the probability of correct reception of X_1 under the condition of the correct tentative decision $\bar{X}_2$ is simply equal to the probability of the correct reception of the QPSK signal in the presence of additive Gaussian noise, so:

$$P_C(X_1|\ \text{correct}\,\bar{X}_2) = \left[1 - \frac{1}{2}\ \operatorname{erfc}\left(\frac{A}{\sigma}\right)\right]^2 \tag{4.27}$$

Now, the attention is turned to the calculation of $P_C(X_1|\text{incorrect}\,\bar{X}_2)$. Therefore, the following expression is written, in which $\overline{X_2}$ is again a decision about transmitted X_2:

$$P_C(X_1|\text{incorrect}\,\bar{X}_2) = \sum_{X_2} P_C(X_1|\text{incorrect}\,\bar{X}_2, X_2)\,P(X_2) \tag{4.28}$$

In this case calculations are even more lengthy, but still manageable. The author considers again $X_1 = A + jA$ and all possible transmitted X_2 symbols. Considerations for all other X_1 symbols are analogous. For each X_2 the incorrect decision $\bar{X}_2$ has three possible forms that have to

be taken into account. After lengthy calculations similar to those resulting from Figure 4.8, the formula can end up as follows:

$$P_C(X_1|\text{incorrect}\,\bar{X}_2) = (Ca + Db)[(Ca + Db) + 2B(2 - a - b)] \tag{4.29}$$

where

$$B = 1 - \frac{1}{2}\text{erfc}\left(\frac{A}{\sigma}\right), C = 1 - \frac{1}{2}\text{erfc}\left(\frac{A + 2gA}{\sigma}\right) \tag{4.30}$$
$$D = 1 - \frac{1}{2}\text{erfc}\left(\frac{A - 2gA}{\sigma}\right)$$

and

$$a = \frac{1}{2}\text{erfc}\left(\frac{gA}{\sigma}\right) - \frac{1}{2}\text{erfc}\left(\frac{A + gA}{\sigma}\right) + \frac{1}{2}\text{erfc}\left(\frac{2A + gA}{\sigma}\right) \tag{4.31}$$
$$b = \frac{1}{2}\text{erfc}\left(\frac{gA}{\sigma}\right) + \frac{1}{2}\text{erfc}\left(\frac{A - gA}{\sigma}\right) - \frac{1}{2}\text{erfc}\left(\frac{2A - gA}{\sigma}\right)$$

Using Eq. (4.24), (4.26), (4.29) - (4.31), the author is able to plot the error probability for symbol X_1. It turns out the error probability curves as functions of SNR for several coefficient values g are the same as in Figure 4.7. It was also confirmed by a Monte Carlo simulation of the system described by Eq. (4.8). This means that using a modified detector in such a simple scheme as considered in this section does not bring any advantages. As the error probability for X_1 is the same as in a regular detector, the same holds true for X_2 and formula (4.22) is further valid. However, as it is expected, simulations performed for channel-coded systems will prove that a substantial improvement in the performance of the proposed SIC detector is possible as compared with the regular one. The explanation of this fact is the following. By the application of tentative decision $\bar{X}_2$ in the detection of X_1, the receiver is able to calculate more reliable soft LLR values used at the input of the channel code decoder applied in the X_1 link. More errors are corrected as compared with the traditional detector with symbol-by-symbol cancellation and LLRs calculated on its basis. Thus, the regenerated sequence of X_1symbols contains fewer errors, and in consequence, it results in lower error probability of X_2 after the cancellation of the whole block of $\hat{X}_1$.

Unfortunately, an analysis of the system with channel coding would be much more complicated, and therefore the author resorts to simulations.

4.4 Simulation Results

The author has checked the quality of the proposed SIC detection algorithm on the example of a standard IEEE 802.11a system based on the WiFi model analyzed in [Sch13]. In these experiments the system consisted of two users co-operating with an access point. It could also be a model of two terminals sharing common resources and communicating with another terminal in D2D fashion. Let us note that such a model can also be applied in V2V communications, where a system very similar to 802.11a, namely IEEE 802.11p, still prevails.

As it has already been mentioned, OFDM symbols that are transmitted from both terminals are quasi-synchronous, i.e., the receiver is able to find the common orthogonality period needed for OFDM symbol detection, which is located within OFDM symbols generated by each terminal. The convolutional code is used at the transmitting side with coding rate R=1/2. The standard (133,171) code is applied. Different modulation schemes are applied depending on the channel propagation path of each user. Therefore, 16-QAM or QPSK are used in simulation experiments for strong and weak users, respectively. Other modulation choices and coding rates, i.e., modulation and coding schemes (MCS) are also possible, depending on individual channel conditions. The applied channel models were simulating multipath Rayleigh fading channels denoted in the text by vectors $\mathbf{h}_1$and $\mathbf{h}_2$ and they had exponential decay power profile with selected rms delay spread T_{rms}.

4.4.1 System Performance with Ideal Channel Coefficients

To verify the detection quality of the proposed algorithm in comparison to the regular one, first, ideal channel coefficients knowledge is assumed. This shows improvements in the detection abilities of the algorithm itself.

In the simulation experiments the number of packets that was transmitted from each terminal was K=100, 500 or 1000, depending on the required accuracy and level of BER estimation. Every packet contained L=100 payload OFDM symbols. The simulation results consist of two different parts.

The first part shows the estimated bit error rate (BER) vs. signal-to-noise ratio (SNR) measurements for both users when the rms delay spread was set to be $T_{rms} = 50$ ns. In the second part the rms delay spread was $T_{rms} = 100$ ns. In all simulation runs, the author assumes the following definition of SNR:

$$SNR = 10\log_{10}\left(\frac{P_{Tx}(g_1^2 + g_2^2)}{N}\right) \tag{4.32}$$

where P_{Tx} is the reference power transmitted by both terminals, N is the noise power and the channel coefficients $g_1$and g_2 model both propagation loss and change of the power level with respect to the reference one. In all simulation results shown below the author sets $g_1 = 1$ without the loss of generality.

A multipath channel model typical for WiFi was applied [Sch13]. As we have mentioned, the power delay profile was exponentially decaying, depending on the root mean square delay T_{rms}. The energy of the channel impulse response was normalized to unity to better control power by selecting the weighting coefficients g_1 and g_2. The time invariance of the channel impulse response has been assumed within a packet.

Figure 4.9 shows the results of these experiments for the stronger terminal which applied 16QAM. It is clearly seen that the regular SIC detector only works for a relatively low value of the strength of the weak signal. For $g_2 = 0.3$ the BER curve for the strong user is already almost flat and BER does not diminish with increasing SNR anymore. The detection quality of the proposed SIC detector certainly deteriorates with the growth of the relative strength of the weak signal, but the system still works even if $g_2 = 0.1$. This is equivalent to the case when the power of the weaker signal is in fact the same as the stronger one.

Figure 4.10 presents the BER versus SNR plots for the weaker terminal which transmits data using QPSK modulation. The conclusion which can be drawn from this figure is basically the same. The proposed SIC detector operates at much higher powers of the weaker terminal as compared with the stronger one, therefore, it is much more reliable. For the lowest selected power of the weaker signal ($g_2 = 0.03$) it cannot be received in the reasonable range of SNR, as the practical SNR for it is too low to operate reliably. However, already for ($g_2 = 0.1$) reception is possible, although it requires higher SNR.

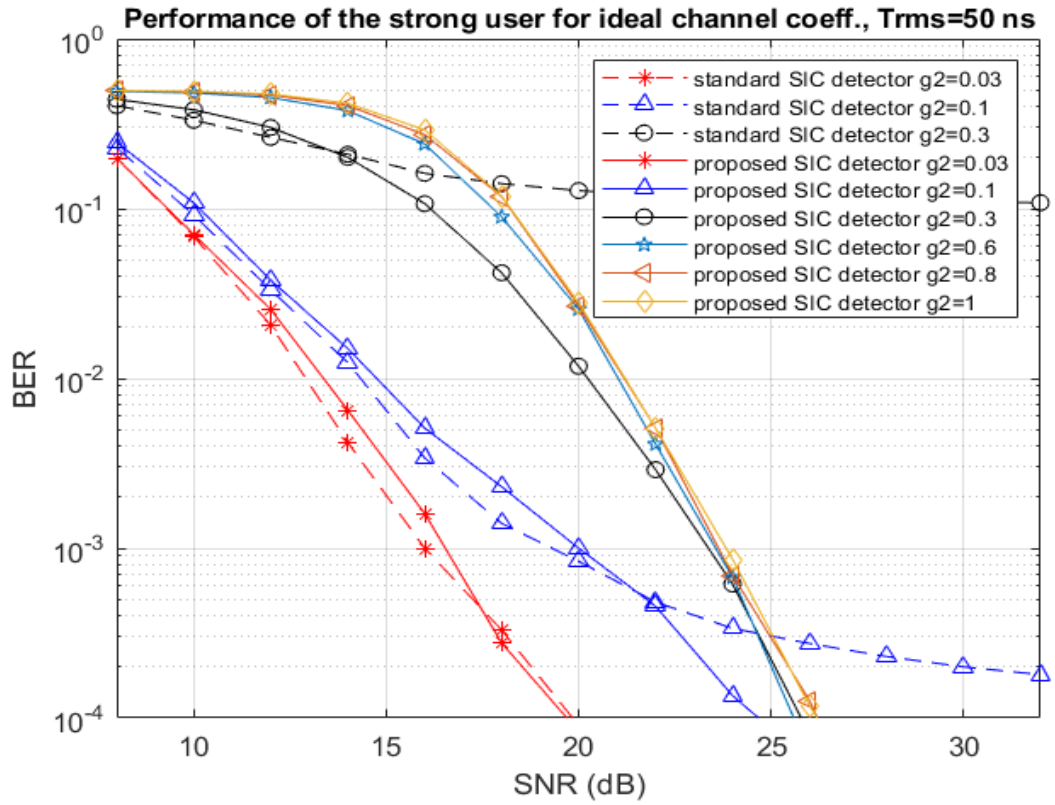

Figure 4.9 Performance of the received data transmitted by the strong terminal for several levels g_2 of the weak signal ($T_{rms} = 50$ ns) when ideal channel coefficients are applied.

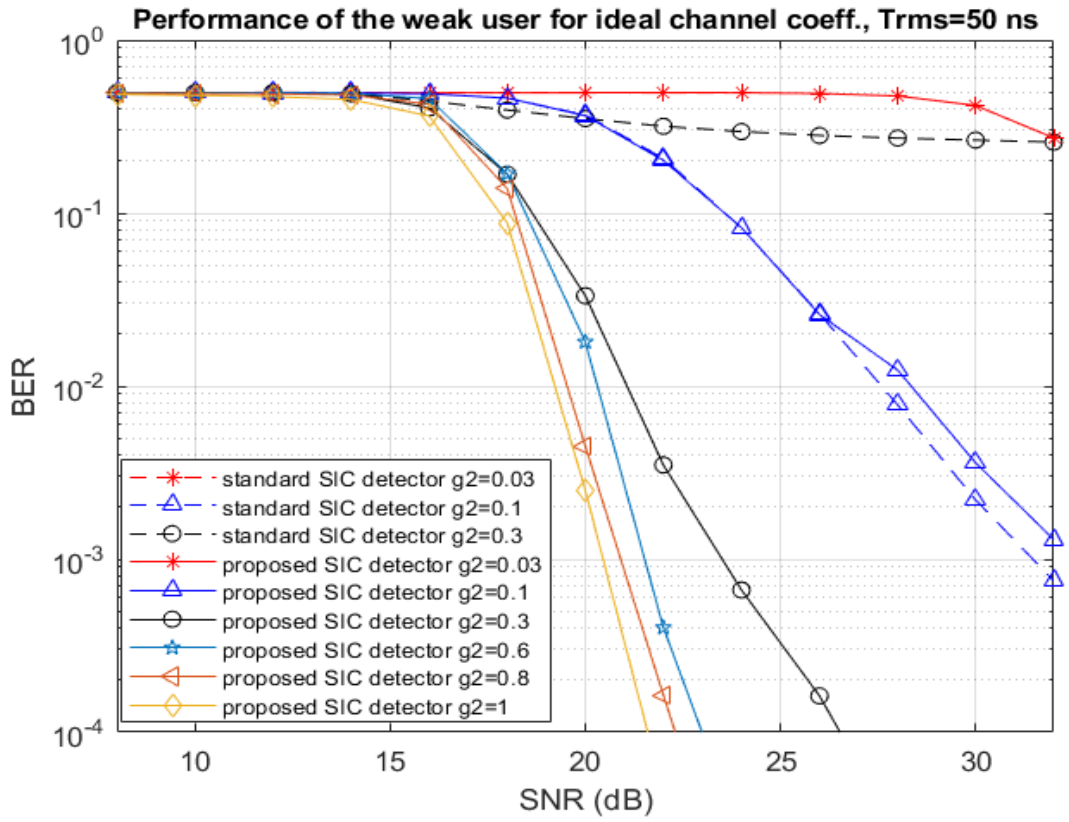

Figure 4.10 Performance of the received data transmitted by the weak terminal for several levels g_2 of the weak signal ($T_{rms} = 50$ ns) when ideal channel coefficients are applied.

Similar experiments have been performed when the channel delay spread was $T_{rms} =$ 100 ns. A more demanding channel, as compared with the previous one, results in similar BER performance. It is shown in Figures 4.11 and 4.12 respectively.

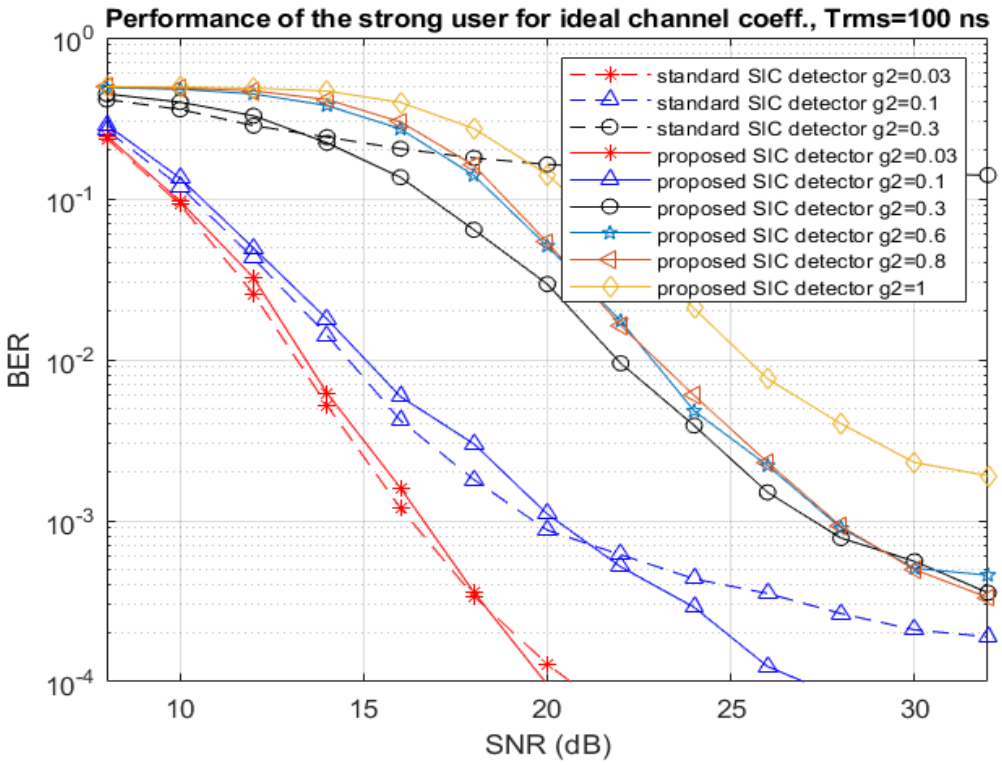

Figure 4.11 Performance of the received data transmitted by the strong terminal for several levels g_2 of the weak signal ($T_{rms} = 100$ ns) when ideal channel coefficients are applied.

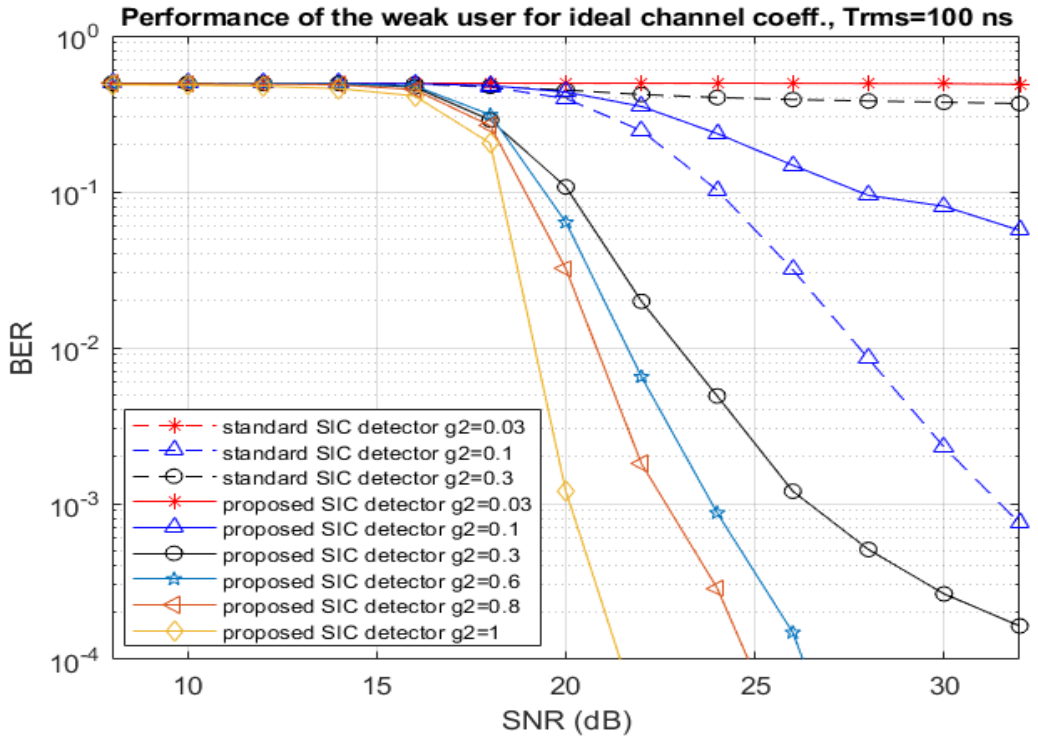

Figure 4.12 Performance of the received data transmitted by the weak terminal for several levels g_2 of the weak signal ($T_{rms} = 100$ ns) when ideal channel coefficients are applied.

Similar conclusions have been drawn as in the case of a very low rms time spread channel. Again, the regular SIC detector operates in a limited range of relative power of the weak signal, whereas the proposed detector can operate in the whole range of values, even in the case of equal power of signals arriving from both terminals.

4.4.2 System Performance with Estimated Channel Coefficients

In the next set of experiments, the channel coefficients in the frequency domain were estimated and the resulting estimates were used in the detection process in both regular and proposed SIC detectors.

As IEEE 802.11a transmission is not fitted to NOMA operation, the author proposes a simple method of channel estimation for both users in the form of the short packet exchange at the start of NOMA operation. Such a procedure can be repeated in appropriate time intervals if needed,

because of the variability of channel characteristics. Figure 4.13 shows the scheme of such operation. First, terminal #1 transmits a short packet consisting of a preamble only. Then, terminal #2, after a passive reception of the preamble from terminal #1, transmits its own preamble as well.

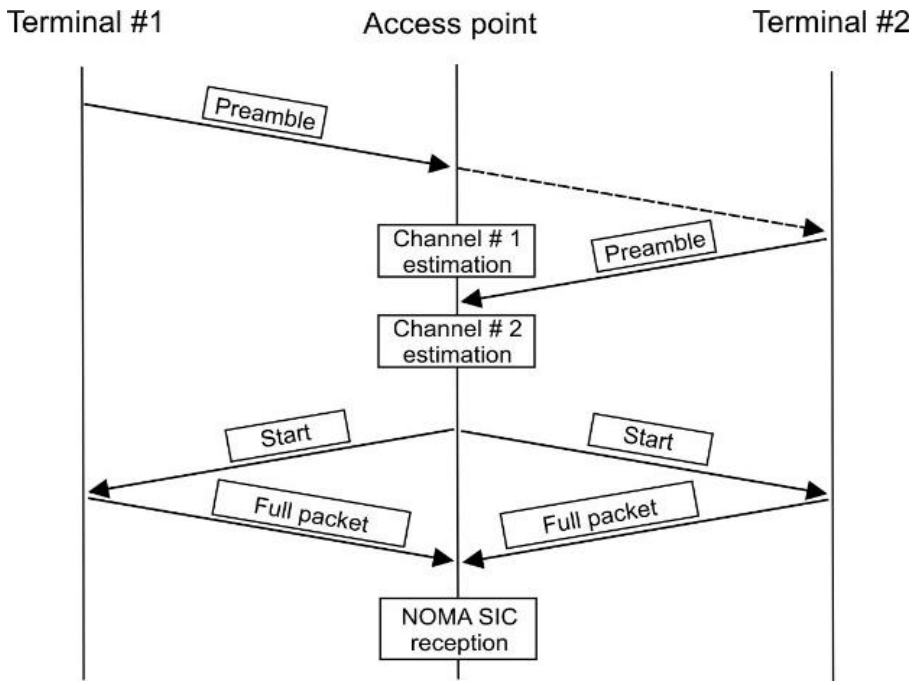

Figure 4.13 Proposed procedure for initial channel estimation and NOMA operation.

After that, the access point transmits the START signal and NOMA operation begins when both terminals transmit their packets concurrently. Initially, channel estimation for both links was based on a standard procedure using two long training sequences of the 802.11a/g preamble. As the samples of both long training symbols are known, the received FFT outputs (being the response of the channel to both training symbols) were averaged and subsequently divided by the ideal tones of both training symbols [Sch13].

However, these experiments indicate that in the case of SIC operation, precise knowledge of both channel characteristics is crucial for the detection process. Direct use of the preamble only causes serious deterioration of performance as compared with the ideal knowledge of channel characteristics. The author has performed experiments in which the proposed SIC detector used

not only two reference symbols in the 802.11a preamble but also some following OFDM symbols acting as additional pilot symbols.

Figures 4.14 and 4.15 show how much gain can be achieved by lengthening the preamble by a few following OFDM pilot symbols. The plots are done for a strong and weak user, respectively. The gain in the performance is clearly visible. It is easily observed that when sufficiently long channel testing packets are applied, the deterioration in the BER performance is about 1 dB as compared with the case of using the ideal coefficients. Certainly, too long preamble causes a loss of transmission efficiency, so some kind of a compromise has to be found.

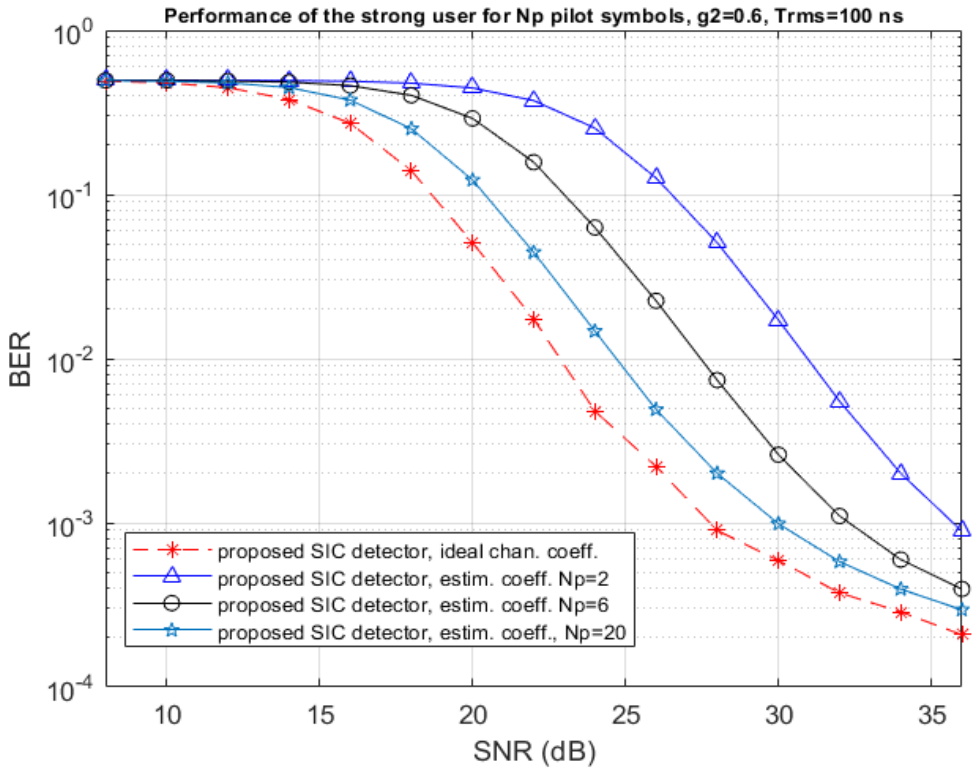

Figure 4.14 BER for the proposed SIC detector for the strong user depending on the number of OFDM pilot symbols N_P compared with the performance when ideal channel coefficients are applied.

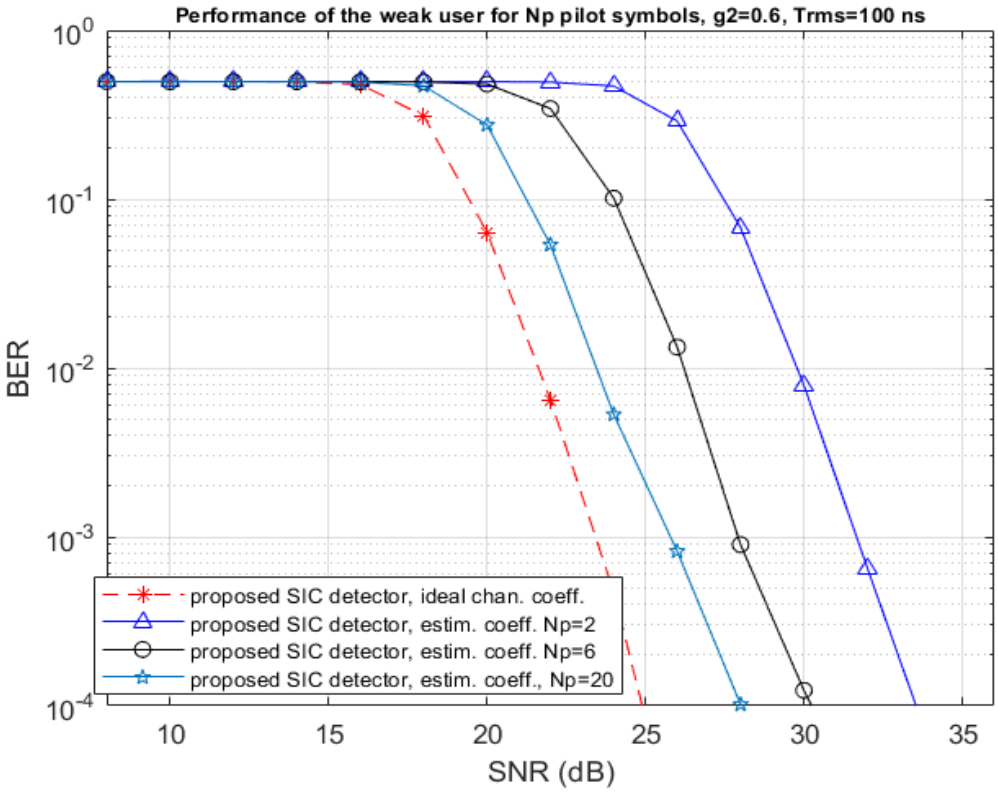

Figure 4.15 BER for the proposed SIC detector for the weak user depending on the number of OFDM pilot symbols N_P compared with the performance when ideal channel coefficients are applied.

In the case of using estimated coefficients, the author applied $N_P = 6$ pilot symbols (including the OFDM symbols C1 and C2 already contained in the preamble). Figures 4.16, 4.17, 4.18 and 4.19 show the BER performance for the system with T_{rms} channel spread equal to 50 and 100 ns when $N_P = 6$ pilot OFDM symbols have been applied.

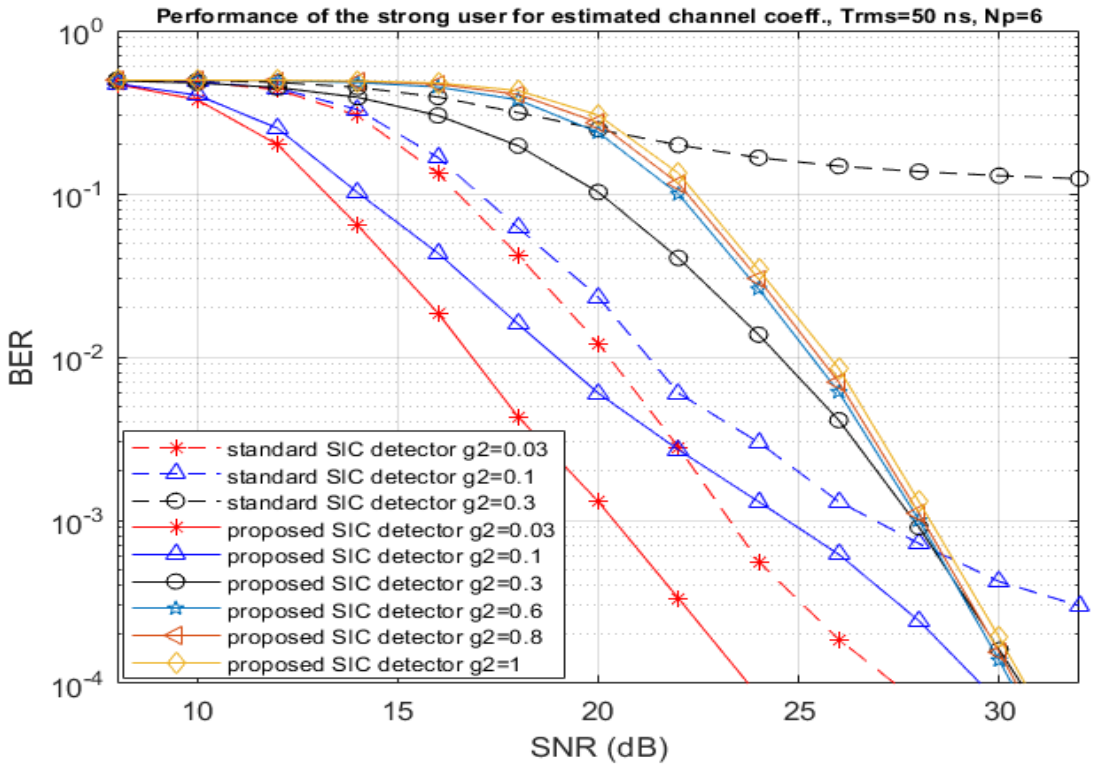

Figure 4.16 Performance of the received data transmitted by the strong terminal for several levels g_2 of the weak signal (T_{rms} = 50 ns) when estimated channel coefficients are applied.

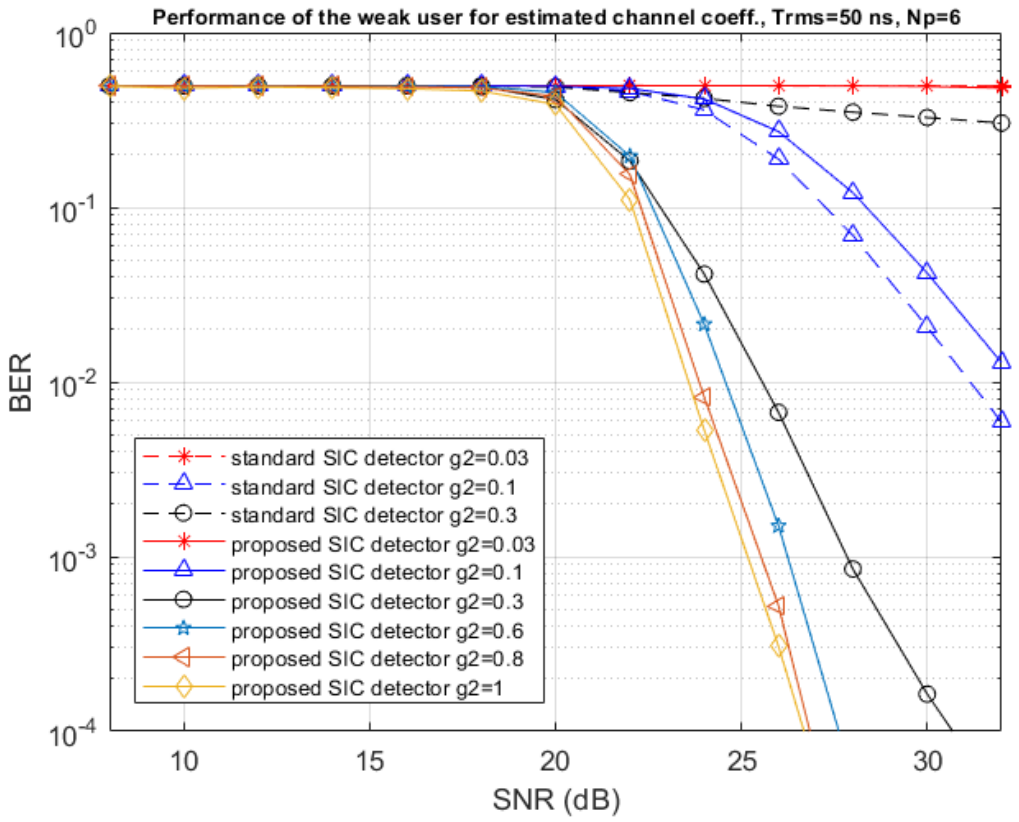

Figure 4.17 BER of the received data transmitted by the weak terminal for several levels g_2 of the weak signal (T_{rms} = 50 ns) when estimated channel coefficients are applied.

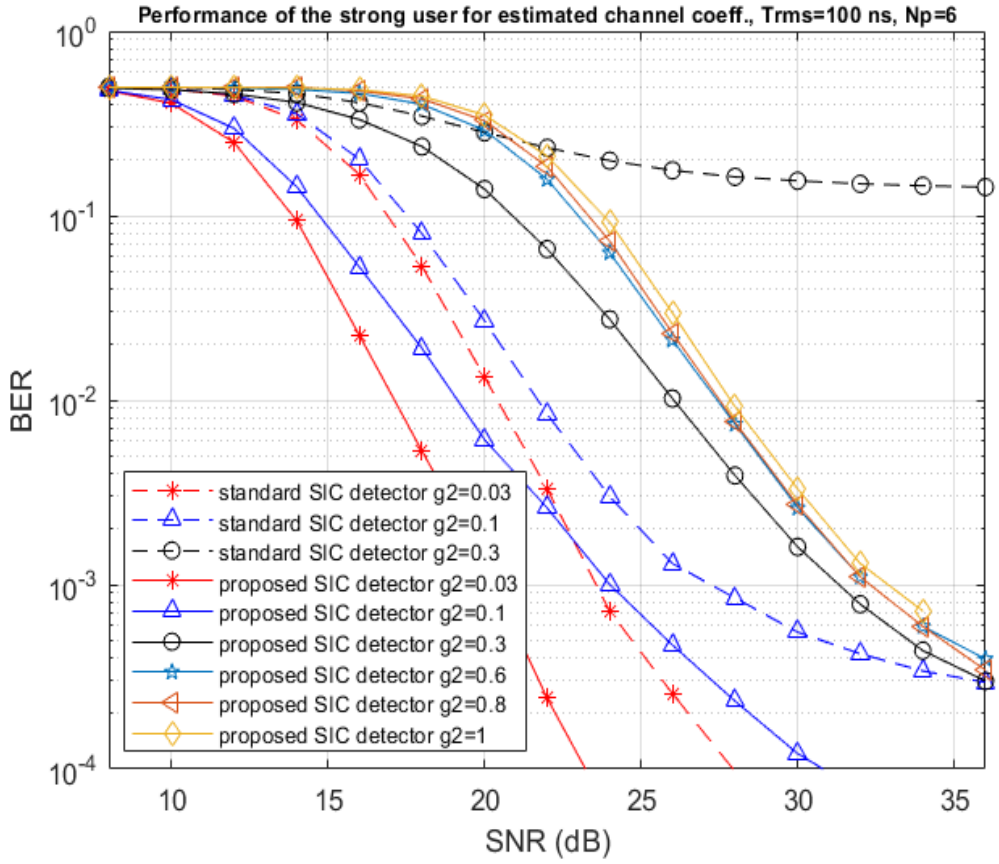

Figure 4.18 BER of the received data transmitted by the strong terminal for several levels g_2 of the weak signal (T_{rms} = 100 ns) when estimated channel coefficients are applied.

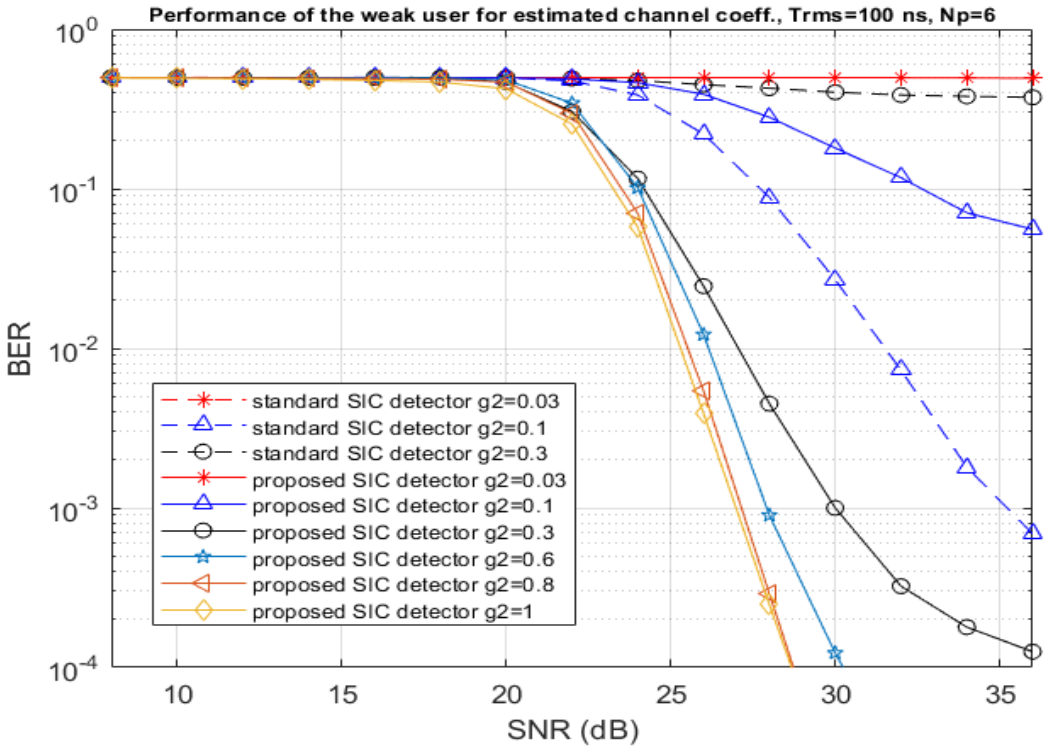

Figure 4.19 BER of the received data transmitted by the weak terminal for several levels g_2 of the weak signal (T_{rms} = 100 ns) when estimated channel coefficients are applied.

4.5 Discussion on MAC Issues

NOMA operation in the WiFi standard has certainly not been foreseen yet. Thus, substantial changes in MAC (medium access control) procedures should be made with channel coding, which is usually applied. Instead of this operation, each data stream after detection using the applied SIC detector can be recovered, including error correction decoding, and then the bit-by-bit modulo-2 sum of information blocks could be re-encoded and transmitted to both terminals in the broadcast phase, enabling the reception of the data stream from the remote terminal with much higher quality.

When two terminals transmit data packets of different length, the proposed detection algorithm can be correctly applied only in that phase when both packets arrive to the AP. Once the shorter one finishes, the AP returns back to its regular operation, i.e. without IC.

4.6 Summary

In this chapter some theoretical considerations supported by intensive simulations were performed for regular and proposed SIC detectors that are applied in NOMA arrangement and shown on the example of a traditional IEEE 802.11a system. The simulation results have proven that the proposed detector can be a valuable alternative to the regular one and it substantially extends the range of relative powers of NOMA users. This approach can be applied to other systems in which access to the transmission medium is based on methods different from CSMA (carrier-sense multiple access). Another possible application of the proposed detector is Physical Layer Network Coding, so a system of that kind will be the subject of a research in the next chapter.

Chapter 5

Application of the Proposed SIC Detector in a Two-Way Relaying System Using Physical Network Coding (PNC)

Future 5G cellular networks, supporting a number of connectivities in the same channel. The degradation in spectral efficiency caused by signal interferences in simultaneous user transmissions is one of these cellular networks' drawbacks; to overcome this problem, many coding and signal processing techniques have been suggested to mitigate multiuser interference.

Physical Layer Network Coding (PNC) was proposed as an effective technique to boost the throughput of multipacket reception systems through exploiting the characteristics of user interference. Moreover, systems designed according to the PNC principle are considered as competitive solutions for 5G networks.

As a result, this chapter introduces a brief description of employing a receiver based on interference cancellation in two-way relaying when the transmission is performed using physical layer network coding. A PNC detector, as well as a proposed SIC detector are designed similarly to that proposed for the NOMA arrangement. The simulation results that have presented by the author in [GW20, GW21] addressed in this chapter in order to examine the system performance and prove the detection quality and achievable gain of employing the proposed SIC receiver as compared with a PNC receiver.

5.1 Wireless Network Coding (WNC)

The interference problem has been recognized as the most significant problem that can limit the performance of future wireless networks, including point-to-multipoint networks, as well as multi-hop systems. It has been mitigated by means of the cellular paradigm which limits the interference level through employing a certain re-use distance [SB18]. In the meantime, the concept of network multiple input, multiple output (NMIMO) has been introduced as a means to overcome inter-cell interference in fifth generation (5G) dense cellular networks, by allowing multiple access points to serve multiple user terminals [PWB18]. This was implemented in the coordinated multipoint (CoMP) approach standardized in LTE-A. This approach results in large

loads on the backhaul network between access points (APs) and the central processing unit (CPU), many times higher than the total user data rate [LSC12], even though some cooperative techniques have been utilized to reduce the backhaul loads, such as Wyner-Ziv compression [LLB13] or iterative interference cancellation [ZY13].

The concept of wireless network coding (WNC) has emerged as one of the hot topics in the research community in recent years, due to several important benefits, such as a decrease in network complexity, increase in throughput, and improvement in the reliability and robustness of the network. Wireless networks are particularly well suited to network coding, as they have a natural capability to send signals to several nodes or terminals concurrently. Numerous researchers have studied the performance of network coding in wireless networks taking into account the properties of omnidirectional transmission, and several other transmission arrangements [WCK04].

Network coding (NC) has been proposed as a promising technique at the network layer for improving network capacity. Furthermore, it was utilized to mitigate the interference in multi hop networks through achieving the following goals:

- A relay node must have the ability to simultaneously modify the received signals into interpretable output signals that are relayed to their final destinations.
- A destination node must have the ability to extract the information addressed to it from the whole relayed signals.

NC can also be used to minimize the delay of data delivery from the source to terminal nodes. As well as, it can be utilized to minimize the number of transmissions in wireless networks [ZLL06]

Network coding was first presented in the work of Ahlswede et al [ACL00] that introduced the possibility of coding of layer-3 packets instead of direct packet forwarding, which resulted in an improvement in the bandwidth efficiency. Originally, it was developed for wired communications. Thereafter, the idea of NC has been extended to wireless communications by Zhang *et al*, by exploiting the additive nature of simultaneously arriving electromagnetic waves and coding in the air [ZLL06].

The key idea of network coding is that the packets transmitted over a network can be represented by combinations of original data packets. This feature can achieve much more flexibility at both intermediate and destination nodes for handling and decoding the original data. The NC

approach allows the intermediate nodes to generate new packets by superimposing the packets that are received and then simultaneously forwarding the mixture to several destinations. In multicast transmission, network coding emerges as a candidate transmission technology for achieving max-flow min-cut capacity [MBC17, Spr10].

The new idea particularly suited for wireless network coding is the application of signal operations on the level of physical layer of a communication system instead of operations on bit streams performed in a regular network coding. This way, inherent features of propagation in wireless media can be efficiently utilized.

The first paper devoted to physical layer network coding (PNC) was presented by Zhang, Liu and Lam in 2006 [ZLL06]. They considered a very idealized communication system in which two terminals transmit their data to the third one, e.g., the latter playing the role of an access point, or a relay. The phase of concurrent transmission to the relay is called (*multiple access phase)*. The authors made some very simplifying assumptions such as the power and phase of the signals received by the relay from both terminals are equal what is hard to achieve. The relay interprets the superposition of the received signals in the form of joint signal constellation and using the appropriate mapping generates the new signal that results from modulo-2 sum of the bit blocks sent from both terminals by the component signals. Such signals broadcasted by the relay are received by both terminals (*broadcast phase*) what allows them to decode the other end terminal signal based on the received one and the knowledge of the own one.

In wireless links, application of channel coding is necessary. If regular or physical layer network coding is applied channel coding has to be used in terminals and often in relays. Therefore, there are two basic concepts which can be applied in a relay: the generation of the relay packet in standard or physical layer network coding is performed on the bit-by-bit or symbol-by-symbol basis, or, alternatively, after channel code decoding (Decode-and-Forward rule). Each concept has advantages and drawbacks. In the first case network coding does not introduce a substantial delay and a relay is more energy efficient. On the other hand, performing network coding operations before channel decoding is more prone to errors and can result in lower link performance.

In the second case, i.e. Decode-and-Forward relaying, the relay introduces substantial delay due to the necessity of channel code decoding carried by both received signals. Computational requirements are also substantially higher as compared with the first case. However, the expected gain is higher performance of a two-way relaying system using such an arrangement.

5.2 Two-Way Relaying Transmission

The two-way relaying channel (TWRC) was first studied by Shannon [Sha61]. It was the first wireless communication scenario where network coding was applied. TRWC is an important information theoretic network structure. Its design and analysis have attracted increasing attention for several reasons. For instance, it gives a simple example of a multi hop wireless network supporting multiple data flows, as well as being an example that clearly demonstrates the benefits of wireless physical layer network coding (WPNC), which has gained some practical interest recently [NCL10].

As depicted in Figure 5.1, the network consists of two user terminals *A* and *B* that are unable to communicate directly and they simultaneously exchange their information with the help of a relay node (Access point).

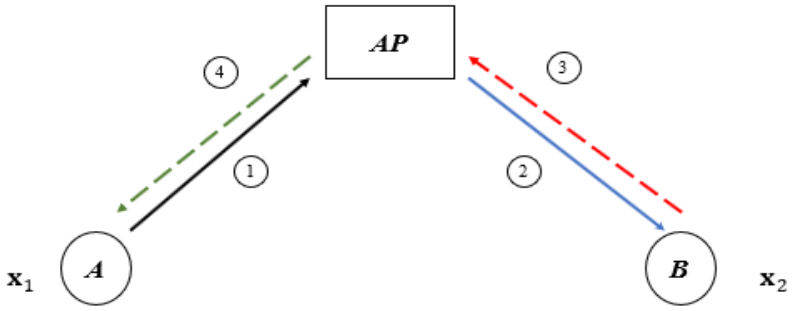

Figure 5.1 Illustrating data exchange in a traditional two-way relaying communication system

There are three configurations that are employed to exchange the information between both terminals. In traditional configuration, the packet exchange consists of four transmission time phases: in the first phase, terminal *A* transmits its own packet to *AP*, in the second - the relay

broadcasts the packet to the receiver of terminal B. In the third phase, terminal B sends its own packet to AP, while the latter in the fourth phase forwards the packet of terminal B to terminal A. Thus, four time slot "ticks" are required for completing the packet exchange [KT12].

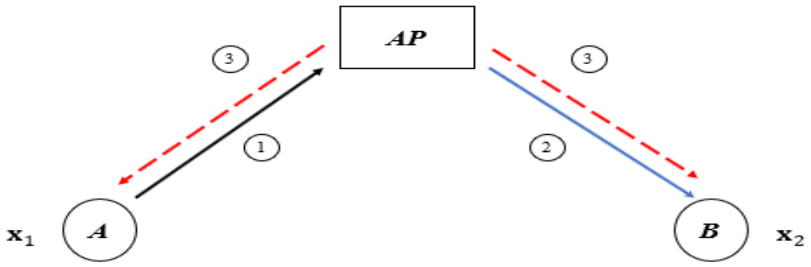

Figure 5.2 Illustrating data exchange using the classical network coding approach

The use of classical network coding reduces the number of the required time phases to three, as depicted in Figure 5.2. In the first phase, terminal A sends its packet to AP, in the second - terminal B does the same. In the third phase, AP simultaneously sends to both terminals a data block which is representing a summed modulo 2 of packets that were received. Based on the knowledge of the own packet transmitted to the relay and the received packet from it, the packet transmitted by the remote terminal can be recovered as the modulo-2 addition of both of them [RBW14].

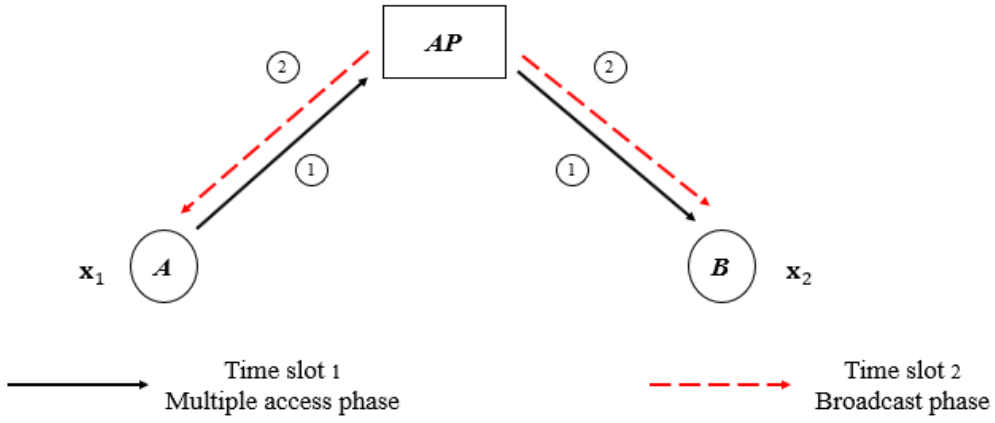

Figure 5.3 Illustrating data exchange using the physical layer network coding approach

The physical network coding (PNC) makes the system even more efficient. Data exchange rate is doubled with respect to a traditional transmission. Both terminals can transmit their

packets at the first transmission phase simultaneously as shown in the generic scheme of system in Figure 5.3. The relay interprets the composite received signal constellations carrying packet data and generates modulo-2 sum of the packets which subsequently determine the packet broadcasted by the relay in the second phase to both terminals. Thus, only two phases (*multiple access (MAC*) and *broadcasting (BC)*) are needed, in contrast to the standard NC requiring three phases. The crucial factor in the PNC is the way how the relay produces the packet to be broadcasted to the terminals participating in the packet exchange.

5.3 Wireless Physical Layer Network Coding Principle (WPNC)

The concept of physical layer network coding (PNC) was originally proposed in [ZLL06] as a novel protocol of network coding, and it has attracted a lot of attention recently. PNC exploits the broadcast nature of wireless communications to exchange information between users when there is no direct signal path between them with a low level of interference [CYX16].

The physical layer network coding technique [HL19] reduces the channel resource usage through performing digital mixing, i.e., XOR operation to superimpose two input signals into one single output signal at the relay node that is in turn forwarding the combined message to participating users who retrieve their own information by performing a similar operation. Moreover, PNC was originally suggested to increase the throughput of a two-way relay network (TWRN) when compared with conventional digital network coding, since it can double the throughput of TWRN as compared to the conventional store-and forward relaying scheme [PLL17, [YLK18].

Due to the additive property of electromagnetic signals at the relay, transmission time phases have been reduced with the PNC scenario as compared to the traditional and classical network coding configurations, as explained in Figure 5.3. As previously mentioned, the overall communication occurs during two phases, namely the MAC and BC phases [KT12]. Moreover, PNC has exploited the previous property (additive property of electromagnetic signals at the relay) in order to achieve the capacity of a wireless network [ATJ13].

As already mentioned, there is a problem how channel coding and other algorithms are managed in the relay of a two-way relaying system. This problem attracted attention of many researchers.

Paper [YML12] is devoted to physical layer implementation of network coding in two-way relay networks. The authors compare the existing network coding schemes such as traditional network coding (NC), physical network coding (PNC), and so called soft network coding (SNC). The latter one is introduced in [ZZL07], however, it is related to traditional NC with channel coding. In this proposal channel decoding at the relay is performed after hard or soft combining of the samples subsequently received from terminals A and B. Then taking advantage of linearity of channel coding and network coding, a single codeword decoding is performed. The authors of [YML12] further change the idea presented in [ZZL07] by proposing combining of the samples of the signals subsequently received from both terminals in front of their demodulators. They show in theoretical analysis that the proposed scheme, similarly to that presented in [ZZL07] saves about 50 percent cost of demodulation and decoding processes as compared with traditional NC with coding. Let us note again that the schemes proposed both in [YML12] and [ZZL07] require three transmission steps, as in a regular NC.

In [HGD07] achievable rates of physical layer network coding schemes are analyzed for two-way relaying channels. The authors propose a new method of PNC inspired by Tomlinson-Harashima precoding [Tom71] in which a modulo operation is used to control the power at the relay. They motivate their proposal by the fact that in the original PNC the relay broadcasts the signal which contains the component which is already known to the destination terminals. In this sense, from the perspective of a given receiver, a portion of the transmit power budget of the relay is wasted in transmitting already known information.

In [ZL09], Zhang and Liew, the inventors of PNC, further develop their PNC idea. They integrate network coding and channel coding by appropriate application of a channel code, called Repeat Accumulate (RA) code [DJM98] at the two end nodes. Thanks to this solution, on the basis of the samples received by the relay the modulo-2 addition of both received source packets can be calculated efficiently. The authors redesign the belief propagation decoding algorithm of the RA code to suit the need of PNC multiple access channel.

In [CHG12] convolutional codes in two-way relay networks with rate diverse network coding are considered. In this arrangement, for a given memory length constraint two source nodes can adopt convolutional codes of different lengths and use reduced-state trellis to reduce decoding complexity. The authors prove that the proposed approach is able to improve system throughput

significantly, offers increased reliability and reduces complexity of decoding of applied convolutional code.

Certainly, other codes than convolutional ones gained interest in application for PNC. In [ATJ13] the authors compare the performance of a two-way relaying network employing PNC with three types of error-correcting codes used at the source and destination nodes. These are iteratively decodable low-density parity check codes (LDPC), turbo codes and bit-interleaved coded modulation with iterative decoding (BICM-ID). The research reported in [ATJ13] indicates that when applied in PNC, the performance of LDPC codes is degraded more than in case of other codes due to the sum-product decoding algorithm which is less robust to unreliable symbols broadcasted from the relay. Another proposal associated with iteratively decodable codes is shown in [CW12]. In this paper a novel joint channel and physical layer network decoding scheme for a two-way relaying communication system is presented. The proposed decoding scheme can be viewed as a serial concatenated decoding scheme with the source codes, not necessary the same, treated as the outer codes and the physical network coding as the inner code.

Bandwidth-efficient coded modulation schemes for PNC with high-order modulations were also a topic of interest. In [CLS17] several soft decision iterative decoding schemes for PNC operated with coded modulations and bit-interleaved coded modulations are presented.

In [CYJ17] Chu, Yoo and Jung consider a PNC coding technique for two-way relaying network which exploits the spatial modulation (SM) with convolutional codes at both source nodes and the relay node. It is assumed that all the nodes are equipped with multiple antennas. The relay node detects signal by utilizing a maximum-likelihood detection technique based on a direct decoding or a separate decoding algorithm. The authors claim that the SM-based PNC outperforms the conventional PNC technique.

In the research devoted to PNC it is often assumed that there are no transmission distortions other than additive Gaussian noise or dispersive channels. However, in real systems we have to face with non-ideal channel estimation or phase and frequency offsets. In [SWY15], Sun, Wang, Yang and Zheng consider low-density parity check codes (LDPC) with PNC for two-way relay channels with different frequency offsets. They propose joint design of PNC and LDPC with compensation of frequency offset in a single node and compensating for an average frequency offset of two nodes and the multiple access phase of the PNC two-way relaying scheme. They

design two corresponding frequency offset filters and analyze their useful signal part and noise distribution.

Finally, channel estimation errors in PNC transmission over fading channels were a subject of research reported in [YRA11]. The authors model channel estimation errors as Gaussian distributed ones and formulate the network coding error by the distance between real and estimated points in the channel coefficients plane. Utilizing this model, the authors present a statistical lower bound on variance of estimation error that can be tolerated by the relay terminal without imposing a network coding error on the system.

Let us remain with the above cited papers, although many other publications could be placed in the presented short overview (see [NG11] as another example). As the main contribution of the research described in the sequel is investigation of the decision making on the basis of two received packets in the physical layer at the relay node, we limit ourselves to relatively simple convolutional codes applied for OFDM transmission which are typical for WiFi IEEE 802.11a. We will also report how channel estimation errors affect the performance of the whole two-way relaying system.

5.4 Investigated System Model

In this section, the principle of employing PNC in wireless communication systems is presented, as well as the application of interference cancellation in the detection performed in two-way relaying when transmission performed using physical layer network coding is investigated. The current section is divided into two parts, the first part illustrates system model of TWRC with PNC transmission, while the second one explains employing of improved SIC detection in TWRC with PNC.

5.4.1 System Model of TWRC with the PNC

In this part, the fundamentals of the application of PNC in two-way relaying is explained. The system model consists of two terminals *A* and *B*. They wish to exchange their information, but they are out of each other's transmission range and they must use *AP* as a relay node, as shown in Figure 5.3. Both terminals are equipped with a single antenna, they are synchronous and mutually independent.

At the transmitting side, the terminals utilize OFDM as a modulation technique with different modulation orders. Figure 5.4. demonstrates the basic concept of data transmission in TWRC.

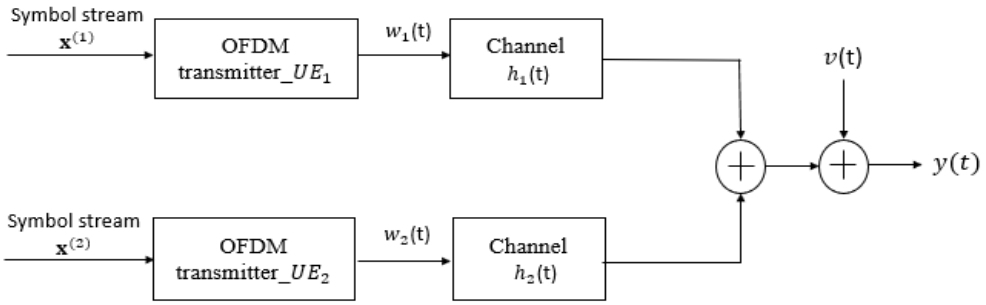

Figure 5.4 Illustrating data exchange using physical layer network coding in TWRC

In the MAC phase, user i $(i = 1,2)$ transmits its individual information $\mathbf{x}_i$ to AP via the multipath channel i that is characterized by the impulse response $h_i(t)$. The latter combines the received signals into one single output signal $y(t)$, which can be formulated as:

$$y(t) = \sum_i w_i(t) * h_i(t) + v(t) \qquad i = 1,2 \tag{5.1}$$

For simplicity we assume that the channel impulse responses have a unit energy and we model unequal power of the signals reaching the relay using the weighting coefficients g_1 and g_2. In order to model the propagation loss we assign the power P_i $(i = 1,2)$ of signals incoming to the receiver from each user by setting the values of the coefficients $g_i = \sqrt{P_i}$. The received signal is disturbed by the additive white Gaussian noise $v(t)$. The transmitted signals from both terminals arrive to the receiver with such a propagation delay difference that the receiver is able to select a common orthogonality period in which OFDM signals from both transmitters are analyzed. Let us assume for simplicity that both terminals use OPSK modulation as a modulation technique. The signal on each OFDM subcarrier output (FFT bin) has been previously presented in Eq. (4.2). By dividing both sides of Eq. (4.2) by the greater of the channel coefficients (let it be $H_k^{(1)}$), a sample can be presented as:

$$\frac{Y_k}{H_k^{(1)}} = X_k^{(1)} + X_k^{(2)} h_k + \frac{N_k}{H_k^{(1)}} \quad , \qquad h_k = \frac{H_k^{(2)}}{H_k^{(1)}} \tag{5.2}$$

By neglecting the additive noise sample for the moment (scaled by the channel coefficient $H_k^{(1)}$), we can get a new composite constellation of the received signal. For example, when using QPSK as a modulation technique during the data transmissions, we will get 16-value modulation, an exemplary constellation of which is shown in Figure 5.5.

Based on the maximum likelihood principle, receiver *AP* tries to decode and retrieve the information of participating users according to the nearest constellation point from the received sample $\mathrm{Y_k}(\, k = 0, \ldots, N-1)$. Let us denote the constellation points of the composite constellation as D_k. Namely,

$$D_k = X_k^{(1)} + h_k X_k^{(2)} \tag{5.3}$$

Then according to the ML criterion we find that D_k from the set $\{D_k\}$ of possible constellation points which fulfills the following rule [GW20, GW21]:

$$\widehat{D}_k = \arg \min_{\{D_k\}} |Y_k - D_k|^2 \tag{5.4}$$

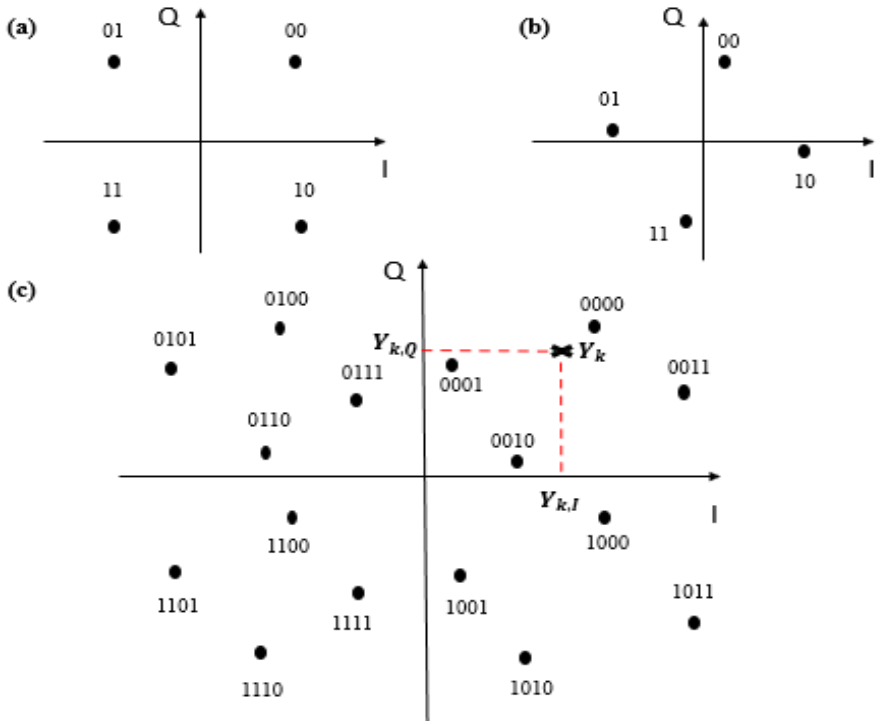

Figure 5.5 Demonstrating constellation diagram: a) QPSK symbol X_1, b) QPSK symbol X_2 scaled by h_k, and c) binary representation of received sample Y_k

Certainly, a unique mapping of constellation points D_k and bit blocks has to be set. Out of many possible mappings that one can be selected for which the first p bits are the same as in the constellation of $X_k^{(1)}$ participating in the creation of a particular D_k and the remaining q bits are the same as in the mapping for $X_k^{(2)}$ participating in that D_k as well. Based on that, let us assume the decided constellation point $\widehat{D}_k$ be assigned to the binary block $b_1 b_2 b_3 b_4$. It can easily be seen that b_1 and b_2 describe the constellation point derived from the symbol X_1, while b_3 and b_4 represent the constellation point derived from the symbol X_2.

After the correct detection of user information, the relay calculates the modulo-2 sum of two bits that have been transmitted by both terminals, as shown in the following equations:

$$d_1 = b_1 \oplus b_3 \tag{5.5}$$

$$d_2 = b_2 \oplus b_4 \tag{5.6}$$

where $\oplus$ denotes the modulo-2 summation performed at the *AP* side.

In the BC phase, *AP* broadcasts QPSK symbols which have a binary representation $d_1 d_2$ simultaneously to both terminals through employing the same channels that are allocated to those users during the MAC phase.

After the whole transmission is completed, both terminals have received QPSK symbols and are trying to convert them into a binary representation in order to detect their transmitted data. The terminals perform the same operation that has previously been performed at the *AP* side, i.e., the first terminal calculates the modulo-2 sum of the two received bits with its own binary block in order to detect information of second terminal located on the other side of transmission.

In order to explain this principle precisely, let us consider the network shown in Figure 5.3 as an example. As a result, terminal *A* estimates the information of terminal *B* as:

$$\hat{b}_3 = d_1 \oplus b_1 \tag{5.7}$$

$$\hat{b}_4 = d_2 \oplus b_2 \tag{5.8}$$

In like manner, terminal *B* detects the transmitted information block from terminal *A* as:

$$\hat{b}_1 = d_1 \oplus b_3 \tag{5.9}$$

$$\hat{b}_2 = d_2 \oplus b_4 \tag{5.10}$$

Table 5.1 Illustrating the timing schedule for MAC/ BC phase

Node	First time slot	Second time slot
A	Transmit	Receive
B	Transmit	Receive
AP	Receive	Transmit

It is important to mention that the above procedure is correctly applied in the case when both terminals do not employ channel coding. Otherwise, the logarithmic likelihood ratio (LLR) calculation of decoded bits is needed. Hence, LLR values are used for soft-decision decoding.

Note that the binary operations in the relay performed to calculate the bits d_1 and d_2 utilized to send relevant QPSK data symbols do not include the existence of channel coding, which affects both the level of wrong decisions at the relay, and later at the receiver of terminals. Additionally, the knowledge of $H_k^{(1)}$and $H_k^{(1)}$ channel coefficients is also required to get a high level of system performance.

5.4.2 Employing Improved SIC Detection in TWRC with PNC

Due to the main described disadvantages of the above solution, the author proposes an improvement that consists in using a combined signal receiver, such as the one the author proposed recently in [GW19, GW19a].

The considered system is an OFDM system composed of two co-operating terminals with the access point operating in the uplink transmission, as shown in Figure 5.6. There is no direct transmission path between both terminals. They communicate and send their independent information via *AP*. Assume that one of them is geographically located closest to *AP*, and it experiences good channel conditions expressed by the value of the coefficient g_1, whereas the other terminal is farther away from the access point so its channel conditions are worse (expressed by a smaller value of g_2), consequently, $g_1 > g_2$.

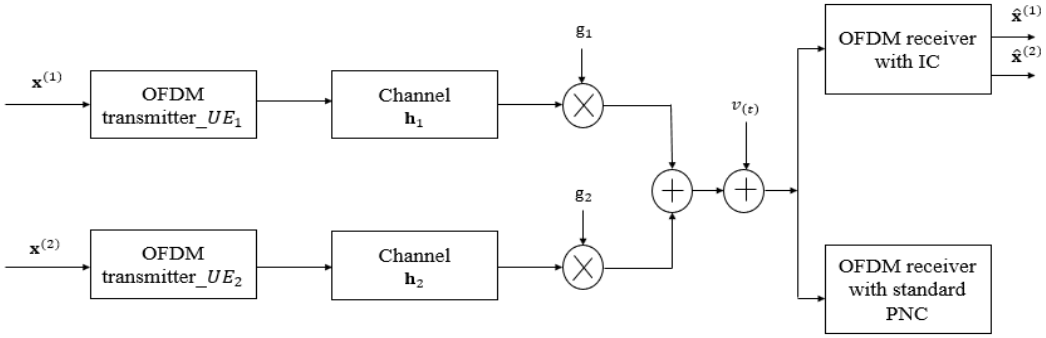

Figure 5.6 General transmission model in the multi-access phase with alternative receivers at relay: proposed (IC) and standard (PNC)

Binary information block $\mathbf{x}_i$ $(i = 1,2)$ that is assigned to each OFDM transmitter is subject to channel coding using the principle of convolutional code with generators [133,171], and coding rate $1/2$. Next, the encoded bit stream is interleaved using the interleaver block with a

size equal to the number of coded bits in a single OFDM symbol. Bits of the resulting codewords are partitioned into groups of bits and mapped onto QPSK symbols. Subsequently, they form subcarrier symbols of the IFFT modulator (of IFFT size equal to 64) that consists of 52 subcarriers in order to convert these OFDM symbols from the frequency domain to the time domain and generate time domain samples supplemented by a cyclic prefix. The latter one enables the system to be robust against multipath propagation. As we have already mentioned, vectors $\mathbf{h}_1$ and $\mathbf{h}_2$ represent the samples of respective impulse responses of the multipath channels.

A simplified diagram of such a receiver is graphically presented in Figure 5.7. The receiver employs interference cancellation (IC) supplemented with additional functional elements specific to the new application.

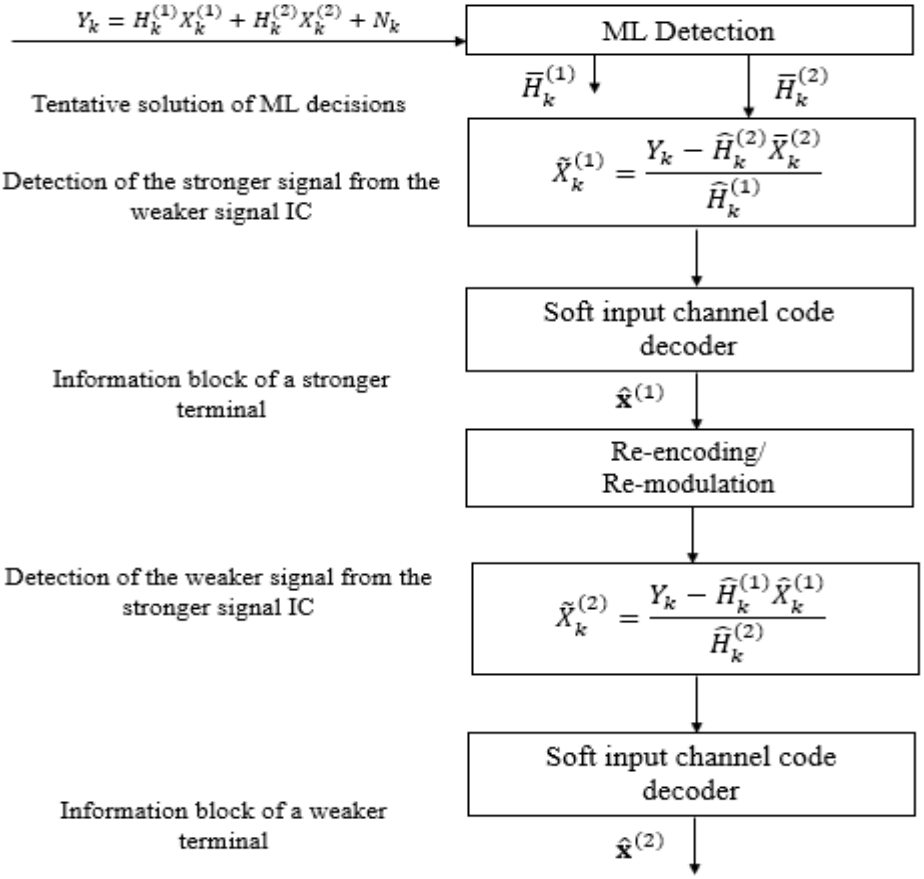

Figure 5.7 Illustrating the simplified receiving method based on interference cancellation (IC) presented in [GW19, GW19a].

The original principle of the proposed IC receiver has been shown in [GW19, GW19a]. The receiver is employed at the relay to determine the estimates of information blocks that are sent by both terminals *A* and *B*, i.e. $\hat{\mathbf{x}}_1, \hat{\mathbf{x}}_2$. Thereafter, the: modulo-2 summation of these two data sequences has been performed bit by bit. The resultant data is subject to the same type of channel coding (convolutional code with generators [133,171], and coding rate 1/2), and this operation is represented by code (.), which is described in Eq. (5.12):

$$\mathbf{w} = \hat{\mathbf{x}}_1 \oplus \hat{\mathbf{x}}_2 \tag{5.11}$$

$$\mathbf{d} = code(\mathbf{w}) \tag{5.12}$$

Bits of the resulting codeword $\mathbf{d}$ are partitioned into groups and mapped again onto QPSK symbols according to the constellation diagram shown in Figure 5.5a. An OFDM symbol (carrying resultant QPSK symbols) is simultaneously sent by *AP* to both terminals during the BC phase. A soft-decision decoding and demodulation process has been implemented at the terminals' side to obtain the estimated information block $\hat{\mathbf{w}}$.

Consequently, terminals *A* and *B* can recreate the terminal's information block located on the opposite side of the link through performing a summed modulo of 2 operations on block $\hat{\mathbf{w}}$ using the locally generated information block, i.e., these operations can be performed as:

$$\bar{\mathbf{x}}_1 = \hat{\mathbf{w}} \oplus \mathbf{x}_2 \tag{5.13}$$

$$\bar{\mathbf{x}}_2 = \hat{\mathbf{w}} \oplus \mathbf{x}_1 \tag{5.14}$$

According to the previous detailed sections, we can easily conclude that the achievable gain of applying the proposed IC detection at the reception side can come from a scenario of receiving information based on interference cancellation in addition to the possibility of reproducing the data signals sent by both terminals at the transmitting side.

Moreover, it is very important to mention the possibility of *AP* to use channel coding, which allows for a significant reduction of the probability of error occurring in the binary sequence sent to terminals when compared with the standard version of network coding in the physical layer. *AP* employs the same previous channel coding for decoding both information blocks, and then

generating their modulo-2 sum, as well as re-encoding, modulating and simultaneously sending the resultant data to participating terminals during the BC phase.

5.5 Simulation Experiments

In this section, some simulation results are addressed to examine the performance of the improved SIC detection algorithm in reducing the interference level in two-way relaying when the principle of physical layer network coding has been applied during the data transmission.

5.5.1 Considered System Model

In the following simulation experiments, a standard IEEE 802.11a system based on the WiFi model analyzed in [Sch13] has been considered. The main parameters of the modelled IEEE 802.11a system have been described in Table 3.1.

As it has already been mentioned, OFDM symbols that are transmitted from both terminals are quasi-synchronous, i.e., the receiver is able to find the common orthogonality period needed for OFDM symbol detection, which is located within OFDM symbols that are generated by each terminal.

A series of simulation experiments were carried out, both assuming the perfect knowledge of the properties of component channels, as well as estimating the channel coefficients at the receivers of the transmitter and terminals. The process of estimating the channel coefficients was previously mentioned in Section 4.4.2.

Note that we assume that these coefficients remained constant during the transmission of a single OFDM packet, as well as the channels in both directions (from and to the terminals) had the same properties (we assume channel reciprocity).

The simulated channels were multipath channel models with an effective 50 ns time dispersion and exponential decaying. It was assumed that signal strengths of individual channels were unitary, but the level of received signals was controlled by the selection of weighting factors g_1 and g_2.

According to the following condition ($g_1 > g_2$), there is an assumption that the stronger signal comes from terminal *A*. For simplicity it assumed that $g_1 = 1$, and g_2 varies in fractional

range, which makes it possible to check the influence of difference in signal levels from both terminals on the quality of system operation.

5.5.2 Simulation Results

In the following simulation experiments, it was assumed that both terminals transmit data blocks of L = 100 OFDM symbols. New channel coefficients are drawn for each new data block. Depending on the level of estimated binary error rate BER as a function of SNR at the output of terminal decoders *A* and *B*, 100, 1000, 2000, 5000 or 10000 OFDM blocks of length L were transmitted to ensure a sufficient level of the quality of estimation. In all simulation runs, the author assumes the definition of SNR as previously illustrated in Eq. (4.32).

In the first part of these simulation results, ideal channel coefficients have been assumed in transmissions from terminal *A* to *B* and in the opposite direction. Figures 5.8 and 5.9 show graphs of estimated BER as a function of SNR when the receiver of the relay or receiver at both terminals are operating in the traditional network coding mode in the physical layer, or when the relay receiver employs the principle of interference cancellation. The parameter in all graphs is the value of the weighting factor g_2, which determines how much weaker was the signal transmitted from the second transmitter (terminal *B*).

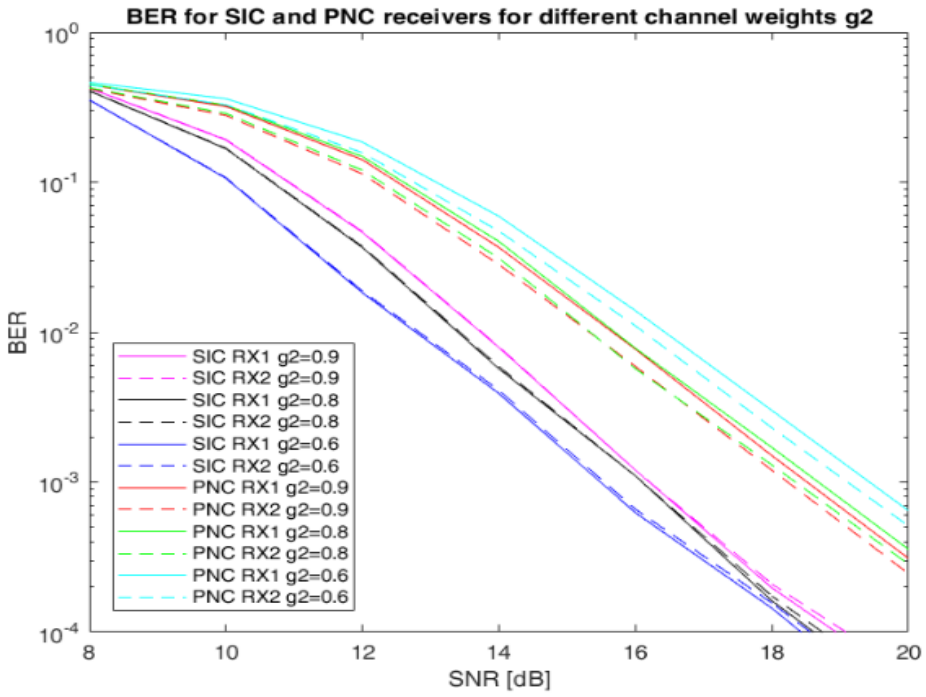

Figure 5.8 Illustrating BER curves as a function of SNR for two types of receivers at the relay and terminals (RX1 and RX2) for large values of the factor g_2 for ideal channel coefficients case

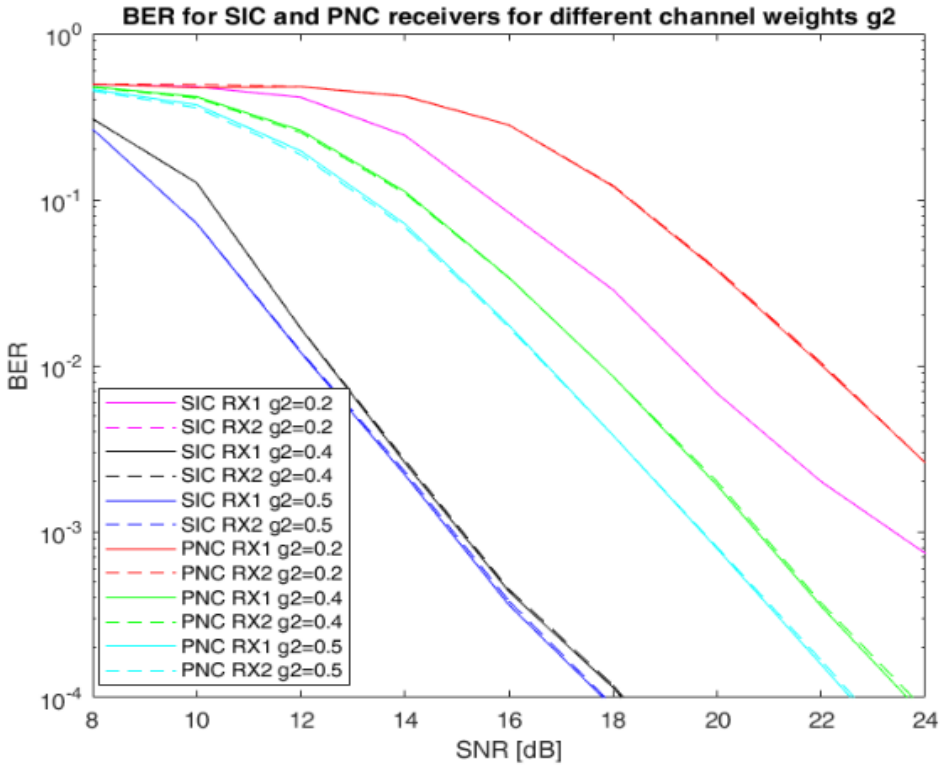

Figure 5.9 Illustrating BER curves as a function of SNR for two types of receivers at the relay and terminals (RX1 and RX2) for small values of the factor g_2 for ideal channel coefficients case

From Figures 5.8 and 5.9 it is easy to conclude that the receiver with IC in the relay proposed for this application significantly improves transmission quality. SNR gain for an error rate of 10^{-3}at the output of channel code decoder for an IC receiver compared to a PNC receiver is of the order of $2.5 - 3$ dB for cases where the signal strengths reaching the relay are comparable (high g_2 values). This gain is significantly higher when the value of g_2 coefficients is much lower than 0.5, as it reaches about 7 dB. Of course, when there is a significant power imbalance between two signals received by the receivers, the error rate significantly increases, but this is inevitable and happens for both types of receivers. Finally, the use of an interference- cancelling receiver in the relay causes better overall system quality.

The next set of experiments refer to the realistic channel situation, where the channel coefficients in the frequency domain were estimated and the resulting estimates were used in the

detection process in both PNC and proposed IC detectors. As previously mentioned in Section 4.4.2, channel estimation for both links was based on a standard procedure using two long training sequences of the 802.11a/g preamble. As the samples of both long training symbols are known, the received FFT outputs (being the response of the channel to both training symbols) were averaged and subsequently divided by the ideal tones of both training symbols [Sch13].

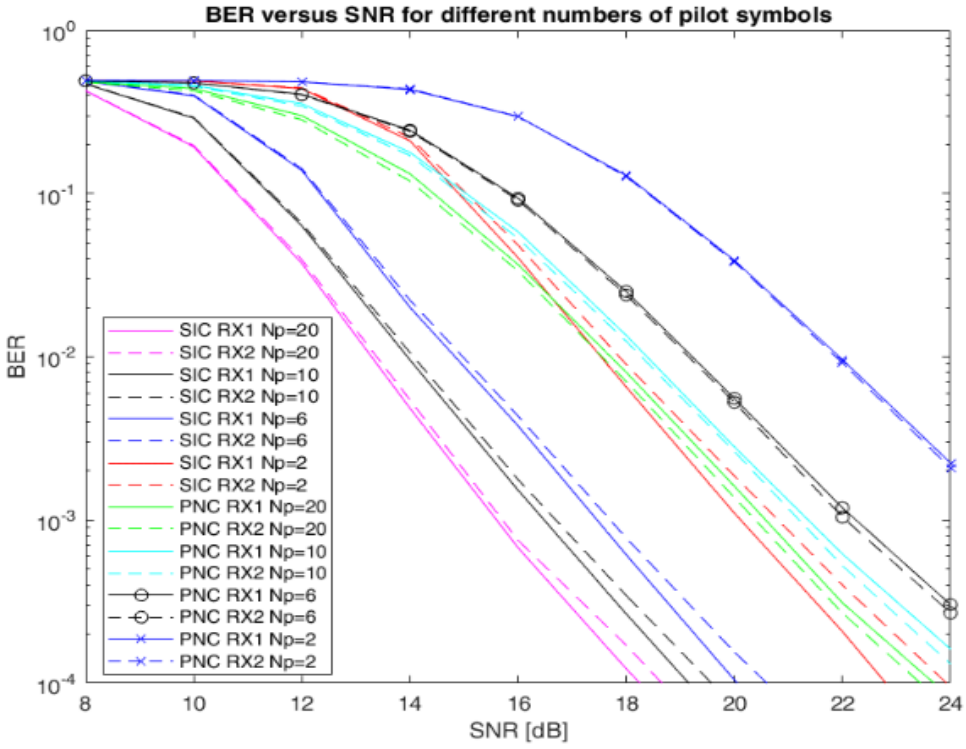

Figure 5.10 BER curves as a function of SNR for the PNC and proposed IC detectors depending on different numbers of OFDM pilot symbols N_P

As already mentioned, the author has performed simulation experiments in which the PNC and proposed IC detectors used not only two reference symbols in the 802.11a preamble, but also some following OFDM symbols acting as additional pilot symbols. Therefore, the direct use of the preamble only causes serious deterioration of performance as compared with the ideal knowledge of channel characteristics.

Figure 5.10 shows how much gain can be achieved by lengthening the preamble by a few following OFDM pilot symbols. The plot is performed for the proposed IC receiver as well as

PNC receiver at both terminals, respectively. The gain in performance is clearly visible. It is easily observed that when sufficiently long channel testing packets are applied, the improvement in the BER performance of about 1 dB is achieved as compared with the case of using short channel testing packets. This conclusion is drawn on the basis of simulation results of two terminals (RX1 and RX2) for both PNC and proposed IC detectors cases.

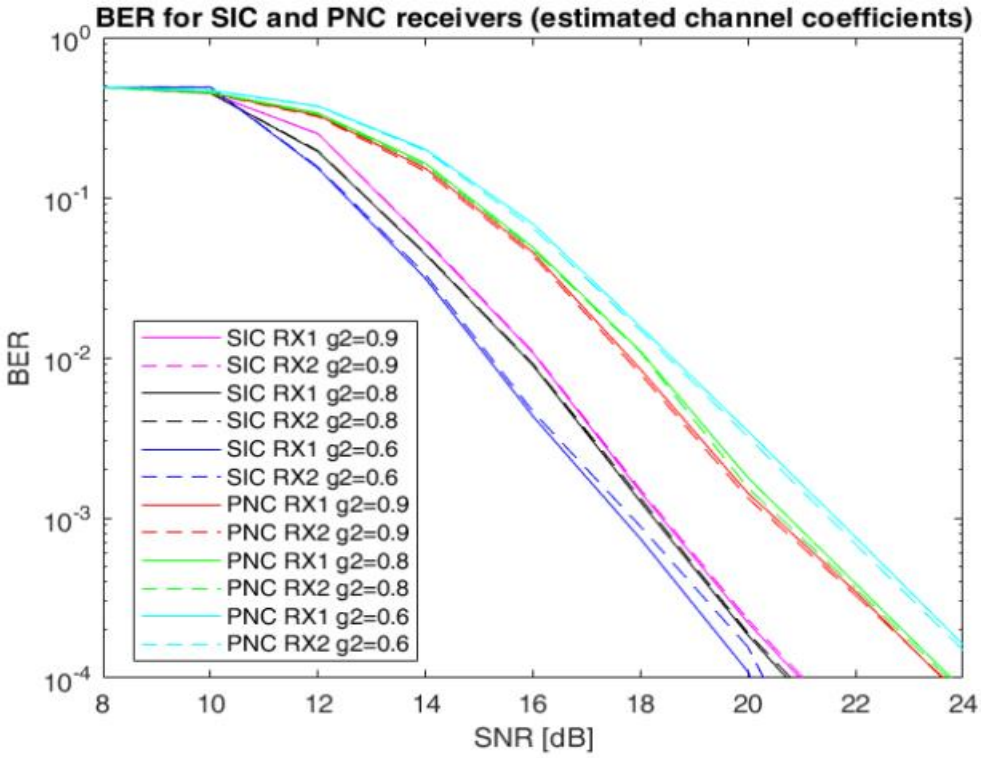

Figure 5.11 Illustrating BER curves as a function of SNR for two types of receivers at the relay and terminals (RX1 and RX2) for large values of factor g_2 for estimated channel coefficients case

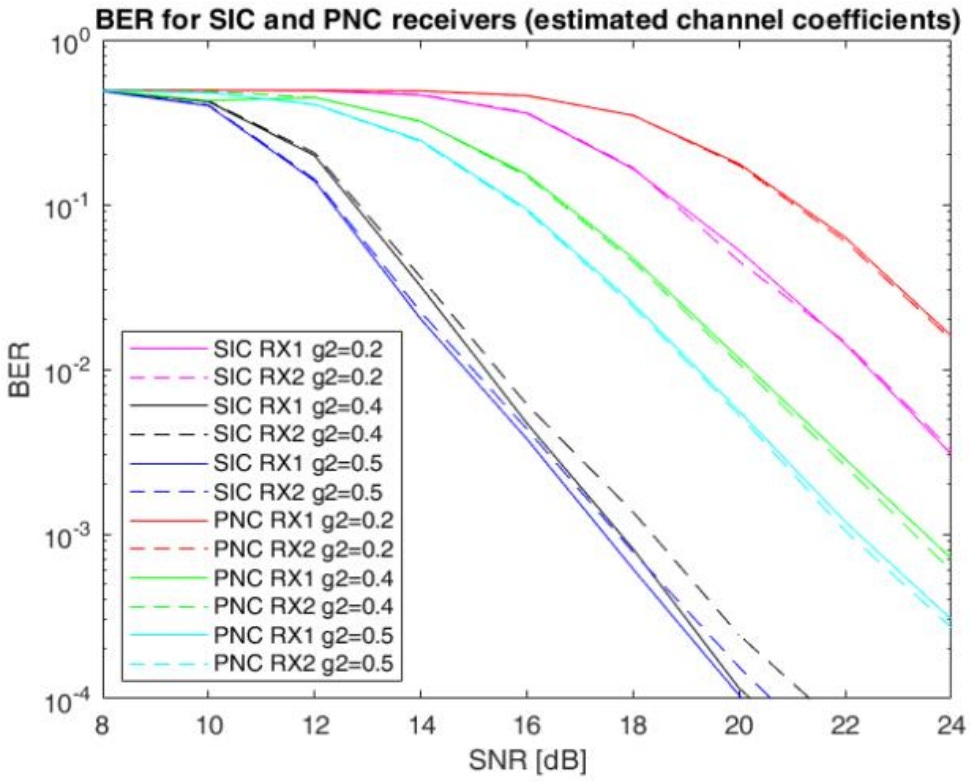

Figure 5.12 Illustrating BER curves as a function of SNR for two types of receivers at the relay and terminals (RX1 and RX2) for small values of factor g_2 for estimated channel coefficients case

From Figures 5.11 and 5.12 we can obviously conclude that a significant improvement in transmission quality can be obtained by using a receiver with IC. The SNR gain for an error rate of 10^{-3} at the output of the decoder for the IC receiver compared to the PNC receiver is of the order of 2.5-3 dB when high values of g_2 are employed. It further increases when the value of g_2 coefficients is much lower than 0.5, as it reaches about 4 dB. At the same time, the error rate is increased when there is a significant power imbalance between two received signals by the transmitter, although this drawback could happen for both types of receivers. Furthermore, better overall system performance can be obtained by utilizing an interference-cancellation receiver in the transmitter. Note that, in these two experiments the author has selected a compromise value of $N_P = 6$.

5.6 Summary

The current chapter presented the application of interference cancellation in the detection process performed in two-way relaying when the transmission is carried out using physical layer network coding. The simulation experiments were performed for PNC and improved IC detectors applied in TWRC transmission. A traditional IEEE 802.11a system was employed as an exemplary system. Some simulation results were investigated to prove the proposed IC detector can achieve better performance in transmission quality as compared to the PNC detector. The applied detection method has produced an improvement in bit error rate as compared to the traditional detection method employed at the relay. Different signal strengths of users participating in a two-way relay transmission were utilized to precisely study the performance of the suggested system.

Chapter 6

Conclusions

This chapter summarizes the objectives and results of the entire research thesis. In the first part of this chapter the author concentrates on the scientific contributions achieved due to her research. Some proposals for future work of this research have been presented in the second part.

6.1 Summary of the main achievements

In the first part of the dissertation, the fundamentals of multiple access techniques employed in wireless communications systems have been studied. Non-orthogonal multiple access has been indicated as one of the promising candidates and a potential component in the fifth-generation mobile systems. A brief introduction of NOMA transmission as well as its main features have been presented.

Some interference management schemes employed to mitigate the interference of multiple users in wireless communications systems have been described. One of them is successive interference cancellation, which represents a considerable approach to meet the functioning of NOMA transmission.

Application of SIC in NOMA transmission could increase the capacity and improve the overall system performance in addition to achieving high spectral efficiency through allowing multiple users with different channel conditions to share the same (time/frequency) resources by allocating several levels of (power/code) to them. As a result, a design of a cooperative scheme for the uplink NOMA multi-carrier OFDM transmission has been investigated on the example of the WiFi IEEE 802.11a system. Various channel models were exploited to examine the system throughput. Convolutional coding in conformance to IEEE 802.11a/g has been applied with different modulation orders to evaluate the user performance. The author hopes that the results achieved for IEEE 802.11a transmission can be easily extended on other multicarrier systems currently standardized in 5G New Radio.

Due to the important role of the SIC receiver in NOMA transmission, as well as the detection quality of the strongest user signals that often decided about the quality of the whole

system and minimized the error propagation effect, an improved detection algorithm has been proposed, which allows for utilizing the NOMA transmission in a much smaller power differences between the participating users sharing common radio resources in the uplink than in a regular arrangement. The achievable gain of employing the proposed SIC detection extends the range of relative powers of the NOMA users and enhances the user throughput as compared with standard successive cancellation methods. The improved SIC detector can also be utilized in the physical layer network coding (PNC) transmission systems.

The application of the proposed SIC detection in two-way relaying with PNC has been investigated. The superiority of the proposed detector has been proven by the apparent improvement in the transmission quality and system performance in comparison with the standard PNC detector.

6.2 Future and unsolved problems

Based on the contributions of this dissertation, it has been proven that NOMA is an advantageous technology for future wireless communications. Much research effort is still needed to develop the performance of NOMA and modify the existing supported techniques. Below there are some suggestions for the future work of this thesis:

- **Channel coding technique**: In this thesis convolutional coding was used as a supporting channel coding in NOMA transmission arrangements. Future work could consider NOMA system based on low density parity check codes (LDPC) or polar codes standardized in 5G new radio. LPDC has been suggested by the 3GPP standardization group to fulfill the requirements of 5G including high throughput, wide coverage, ultra-low latencies, and high flexibility for supporting massive communication connections. LDPC codes have already been adopted into various IEEE standards including wireless LAN (IEEE 802.11n), WiMax (IEEE 802.16e) and digital video broadcasting (DVB-S2 and DVB-T2), because of its remarkable error performance specially for large codeword lengths. Furthermore, low density parity check codes have been considered as an alternative to turbo codes (the primary coding scheme in the third and fourth generation) especially when transmitting long codewords.

- **NOMA applications:** In this thesis, the focus was concentrated on the example of a cooperative scheme for the uplink NOMA Wi-Fi transmission (according to IEEE 802.11 standards) and study the performance of investigated system. Internet of Things (IoT) has become a very interesting technology especially for the industrial and marketing sectors. It represents the proposed expansion of the Internet in the future by achieving a massive increase in the capability of collecting, analyzing and spreading data which can be converted into information, knowledge, etc. In order to connect things to each other or to the cloud, there are several standards and proper devices can be used for this purpose, such as Wi-Fi, Bluetooth, ZigBee, Active RFID, etc. Because of the Wi-Fi features (energy consumption and secure network), it is considered a suitable choice to provide the Internet connection everywhere in the world. The future work could consider the promising application of NOMA technology with the proposed improved SIC detection algorithm in other communications including Device-to-Device (D2D) or Vehicle-to-Vehicle (V2V). Such emerging techniques can improve the spectral efficiency of cellular networks by sharing same spectrum resources among cellular users and (D2D or V2V) pairs.

Bibliography

[RP-18] 3GPP, RP-181403. "Revision of Study on 5G Non-orthogonal Multiple Access".

[ABC14] J.G. Andrews, S. Buzzi, W. Choi, S.V. Hanly, A. Lozano, A.C. Soong, and J.C. Zhang. “What will 5G be?” IEEE Journal on Selected Areas in Communications, vol. 32, no. 6 (2014): pp. 1065–1082.

[ACL00] R. Ahlswede, N. Cai, S.Y. Li, and R.W. Yeung. "Network information flow." IEEE Transactions on Information Theory vol. 46, no. 4 (2000): pp. 1204-1216.

[ADG17] F. AlRabee, K. Davaslioglu, and R. Gitlin. "The optimum received power levels of uplink non-orthogonal multiple access (NOMA) signals." 2017 IEEE 18th Wireless and Microwave Technology Conference (WAMICON), IEEE, 2017.

[AGS18] N. Anugrah, G. Gupta, and K. Srinivas, "Review on Multiple Access Technique Used in Mobile Telecommunications Generations", International Research Journal of Engineering and Technology, vol. 5, no. 10 (2018).

[Ahm13] S. Ahmadi, “LTE-Advanced: a practical system approach to understanding 3GPP LTE releases 10 and 11 radio access technologies”, Academic Press, Oxford, 2014.

[And05] J. G. Andrews. "Interference cancellation for cellular systems: a contemporary overview." IEEE Wireless Communications, vol. 12, no. 2 (2005): pp.19-29.

[ATG18] M. Aldababsa, M. Toka, S. Gökçeli, G.K. Kurt, and O. Kucur. "A tutorial on nonorthogonal multiple access for 5G and beyond." Wireless Communications and Mobile Computing, vol. 2018, Article ID 9713450, 24 pages.

[ATH16] M. S. Ali, H. Tabassum, and E. Hossain. "Dynamic user clustering and power allocation for uplink and downlink non-orthogonal multiple access (NOMA) systems." IEEE Access, vol. 4 (2016): pp. 6325-6343.

[ATJ13] A.A. Al-Rubaie, C.C. Tsimenidis, M. Johnston, and B. Sharif. "Comparison of a physical-layer network coding system with iterative coding schemes." 6th Joint IFIP Wireless and Mobile Networking Conference (WMNC), IEEE, 2013.

[AXI14] M. Al-Imari, P. Xiao, M.A. Imran, and R. Tafazolli, "Uplink non-orthogonal multiple access for 5G wireless networks." 2014 11th International Symposium on Wireless Communications Systems (ISWCS), IEEE, 2014.

[BJ09] J. Blomer, and N. Jindal. "Transmission capacity of wireless ad hoc networks: Successive interference cancellation vs. joint detection." 2009 IEEE International

Conference on Communications, IEEE, June 14-18, Dresden, 2009.

[BSK13] A. Benjebbour, Y. Saito, Y. Kishiyama, A. Li, A. Harada, and T. Nakamura. "Concept and practical considerations of non-orthogonal multiple access (NOMA) for future radio access." 2013 International Symposium on Intelligent Signal Processing and Communication Systems, IEEE, Naha, Japan, Nov. 12-15, 2013.

[CFJ20] C. Chen, S. Fu, X. Jian, M. Liu, X. Deng, and Z. Ding. "NOMA for Energy-Efficient LiFi-Enabled Bidirectional IoT Communication." arXiv preprint arXiv:2005.10104, 2020.

[CHG12] P. Cheng, J. Hao, and Y. Guo, "Convolutional Codes in Two-Way Relay Networks with Rate Diverse Network Coding", 2012 World Congress on Information and Communication Technologies, Trivandrum, India, (2012): pp. 1014-1018.

[CLS17] P. Chen, S. Ch. Liew, and L. Shi, "Bandwidth-Efficient Coded Modulation Schemes for Physical-Layer Network Coding with High-Order Modulations", IEEE Trans. on Communications, vol. 65, no 1 (2017): pp. 147-160.

[Cox12] C. Cox. An introduction to LTE: LTE, LTE-advanced, SAE and 4G mobile communications, John Wiley & Sons, Chichester, 2014.

[CQK12] W. C. Cheung, T. S. Quek, and M. Kountouris. "Throughput optimization, spectrum allocation, and access control in two-tier femtocell networks." IEEE Journal on Selected Areas in Communications, vol. 30, no. 3 (2012): pp. 561-574.

[CS03] D. Chen, and T. Saito. "A new method to reduce the complexity of joint detection algorithm." GLOBECOM'03. IEEE Global Telecommunications Conference, vol. 4, IEEE, San Francisco, Dec. 1-5, 2003.

[CW12] P. Chen, and L. Wang, "A Serial Joint Channel and Physical Layer Network Decoding in Two-Way Relay Networks", IEEE Communications Letters, vol. 16, no. 6 (2012): pp. 769-772.

[CYJ17] E. Chu, J. S. Yoo, and B. Ch. Jung, "Spatial-Modulated Physical- Layer Network Coding in Two-Way Relay Networks with Convolutional Codes", 2017 Ninth International Conference on Ubiquitous and Future Networks (ICUFN), July 4-7, Milan, 2017: pp. 811-813.

[CYX16] F.F. Cao, Q.Y. Yu, W. Xiang, and W.X. Meng. "Ber analysis of physical-layer network coding in the awgn channel with burst pulses.", IEEE Access 4 (2016): pp. 9958-9968.

[DC00] G. A. Dimitrakopoulos, and C. N. Capsalis. "Statistical modeling of RMS-delay spread under multipath fading conditions in local areas." IEEE Transactions on Vehicular Technology, vol. 49, no. 5 (2000): pp. 1522-1528.

[DDC17] Y. Du, B. Dong, Z. Chen, X. Wang, Z. Liu, P. Gao, and S. Li. "Efficient multi-user detection for uplink grant-free NOMA: Prior-information aided adaptive compressive sensing perspective." IEEE Journal on Selected Areas in Communications, vol. 35, no. 12 (2017): pp. 2812-2828.

[DFP15] Z. Ding, P. Fan, and H. V. Poor. "Impact of user pairing on 5G nonorthogonal multiple-access downlink transmissions." IEEE Transactions on Vehicular Technology, vol. 65, no. 8 (2015): pp. 6010-6023.

[DJM98] D. Divsalar, H. Jin, and R. McEliece, "Coding theorems for turbo-like codes" Proc. of Allerton Conference, (1998): pp. 201–210.

[DLC17] Z. Ding, Y. Liu, J. Choi, Q. Sun, M. Elkashlan, I. Chih-Lin, and H.V. Poor. "Application of non-orthogonal multiple access in LTE and 5G networks." IEEE Communications Magazine, vol. 55, no. 2 (2017): pp. 185-191.

[DLK17] Z. Ding, X. Lei, G.K. Karagiannidis, R. Schober, J. Yuan, and V.K. Bhargava. "A survey on non-orthogonal multiple access for 5G networks: Research challenges and future trends." IEEE Journal on Selected Areas in Communications, vol 35, no. 10 (2017): pp. 2181-2195.

[DSJ16] E. Dahlman, P. Stefan, and S. Johan 4G: LTE/LTE-advanced for mobile broadband. Academic Press, London, 2016.

[DWD18] L. Dai, B. Wang, Z. Ding, Z. Wang, S. Chen, and L. Hanzo. "A survey of non-orthogonal multiple access for 5G." IEEE Communications Surveys & Tutorials, vol. 20, no. 3 (2018): pp. 2294-2323.

[DWY15] L. Dai, B. Wang, Y. Yuan, S. Han, I. Chih-Lin, and Z. Wang. "Non-orthogonal multiple access for 5G: solutions, challenges, opportunities, and future research trends." IEEE Communications Magazine, vol. 53, no. 9 (2015): pp. 74-81.

[DYF14] Z. Ding, Z. Yang, P. Fan, and H.V. Poor. "On the performance of non-orthogonal multiple access in 5G systems with randomly deployed users." IEEE Signal Processing Letters, vol. 21, no. 12 (2014): pp. 1501-1505.

[FAG95] D. D. Falconer, F. Adachi, and B. Gudmundson. "Time division multiple access methods for wireless personal communications." IEEE Communications Magazine, vol. 33, no. 1 (1995): pp. 50-57.

[Gol05] A. Goldsmith. Wireless communications. Cambridge University Press, New York, 2005.

[GW18] H.S. Ghazi, and K. Wesołowski. "Uplink NOMA scheme for Wi-Fi applications." International Journal of Electronics and Telecommunications, vol. 64, no.4 (2018): pp. 481-485.

[GW19] H.S. Ghazi, and K. Wesołowski. "Improved Detection in Successive Interference Cancellation NOMA OFDM Receiver", IEEE Access, pp. 103325 –103335, 2019.

[GW19a] H. S. Ghazi, K. Wesołowski, „Metoda odbioru z kompensacją interferencji sygnałów w systemach NOMA," (Method of signal reception with interference cancellation), Przegląd Telekomunikacyjny, Wiadomości Telekomunikacyjne, no. 6, 2019, pp. 193-196.

[GW20] H. S. Ghazi, K. Wesołowski, „Zastosowanie detekcji z kompensacją interferencji w transmisji z przekaźnikiem w trybie kodowania sieciowego w warstwie fizycznej," (Application of interference cancellation in the access point of two-way relaying transmission), Przegląd Telekomunikacyjny, Wiadomości Telekomunikacyjne, no. 7-8, 2020, pp. 382-385.

[GW21] H.S. Ghazi, and K. Wesołowski. "Application of an Interference Cancellation Detector in a Two-Way Relaying System with Physical Network Coding", submitted to IEEE Access, 2021.

[HB15] K. Higuchi, and A. Benjebbour. "Non-orthogonal multiple access (NOMA) with successive interference cancellation for future radio access." IEICE Transactions on Communications, vol. 98, no. 3 (2015): pp. 403-414.

[HGD07] Y. Hao, D. Goeckel, Z. Ding, D. Towsley, and K. L. Leung, "Achievable Rates of Physical Layer Network Coding Schemes on Exchange Channel", IEEE Military Communications Conference, Oct. 29-31, Orlando, (2007).

[HL19] C. Y. Ho, and C. Y. Leow. "Cooperative Non-Orthogonal Multiple Access with Physical Layer Network Coding." IEEE Access 7 (2019): pp. 44894-44902.

[HTD18] J. He, Z. Tang, Z. Dingand, and D. Wu. "Successive Interference Cancellation and Fractional Frequency Reuse for LTE Uplink Communications." IEEE Transactions on Vehicular Technology, vol. 67, no. 11 (2018): pp. 10528-10542.

[IAD16] S. R. Islam, N. Avazov, O. A. Dobre, and K. S. Kwak, "Power-domain non-orthogonal multiple access (NOMA) in 5G systems: Potentials and challenges." IEEE Communications Surveys & Tutorials, vol. 19, no. 2 (2016): pp. 721-742.

[IAT12] M. A. Imran, M. Al-Imari, and R. Tafazolli. "Low density spreading multiple access." Journal of Information Technology and Software Engineering, vol. 2, no. 4 September (2012).

[Ilc13] S. D. Ilcev. "Implementation of multiple access techniques applicable for maritime satellite communications." TransNav: International Journal on Marine Navigation and Safety of Sea Transportation, vol. 7, no. 4 (2013): pp. 529-540.

[JS02] G.J. Janssen, and S. B. Slimane. "Symbol error probability analysis of a multiuser detector for M-PSK signals based on successive cancellation." IEEE Journal on Selected Areas in Communications, vol. 20, no. 2 (2002): pp. 330-338.

[KAS13] A. Kumar, A. Aswal, and L. Singh, "4G Wireless Technology: A Brief Review." International Journal of Engineering and Management Research (IJEMR), vol. 3, no. 2 (2013): pp. 35-43.

[KH14] H. Kayama, and J. Huiling. "Evolution of LTE and new radio access technologies for FRA (future radio access)." 2014 48th Asilomar Conference on Signals, Systems and Computers. IEEE, Nov. 2-5, Pacific Grove, 2014.

[Kha09] F. Khan. “LTE for 4G mobile broadband: air interface technologies and performance.” Cambridge University Press, Cambridge, 2009.

[Kha17] I. Khan. "Performance analysis of 5G cooperative-NOMA for IoT-intermittent communication." International Journal of Communication Networks and Information Security, vol. 9, no. 3 (2017): pp.314-322.

[KHY06] K. S. Kim, K. Hyun, C. W. Yu, Y. O. Park, D. Yoon, and S. K. Park. "General Log-Likelihood Ratio Expression and Its Implementation Algorithm for Gray-Coded QAM Signals." ETRI Journal, vol. 28, no.3 (2006): pp.291-300.

[Kor03] J. Korhonen. “Introduction to 3G mobile communications.” Artech House, Norwood, MA, 2003.

[KT12] I. Krikidis, and J. S. Thompson. "MIMO two-way relay channel with superposition coding and imperfect channel estimation." Journal of Network and Computer Applications, vol. 35, no. 1 (2012): pp. 510-516.

[LBC14] Y. Lan, A. Benjebboiu, X. Chen, A. Li, and H. Jiang. "Considerations on downlink non-orthogonal multiple access (NOMA) combined with closed-loop SU-MIMO." 2014 8th International Conference on Signal Processing and Communication Systems (ICSPCS), Dec. 15-17, Gold Coast, Australia, IEEE, 2014.

[Lee18] S. Lee. "Cooperative non-orthogonal multiple access for future wireless communications." EAI Endorsed Transactions on Industrial Networks and Intelligent Systems, vol. 5, no. 17 (2018).

[LL13] E. Lhetkangas, and H. Lin. "Deliverable D2.1. Requirement analysis and design

approaches for 5G air interface." METIS Deliverable [online] (2013).

[LLB13] T. R. Lakshmana, J. Li, C. Botella, A. Papadogiannis, and T. Svensson. "Scheduling for backhaul load reduction in CoMP." 2013 IEEE Wireless Communications and Networking Conference (WCNC), April 7-10, Shanghai, IEEE, 2013.

[LNL18] M. Liaqat, K. A. Noordin, T. A. Latef, and K. Dimyati, "Power-domain non orthogonal multiple access (PD-NOMA) in cooperative networks: an overview." Wireless Networks vol. 26, (2018): pp.1-23.

[LQE18] Y. Liu, Z. Qin, M. Elkashlan, Z. Ding, A. Nallanathan, and L. Hanzo. "Non-orthogonal multiple access for 5G and beyond." arXiv preprint arXiv:1808.00277 (2018).

[LSC12] D. Lee, H. Seo, B. Clerckx, E. Hardouin, D. Mazzarese, S. Nagata, and K. Sayana. "Coordinated multipoint transmission and reception in LTE-advanced: deployment scenarios and operational challenges." IEEE Communications Magazine, vol. 50, no.2 (2012): pp.148-155.

[MBC17] F.A. Monteiro, A. Burr, I. Chatzigeorgiou, C. Hollanti, I. Krikidis, H. Seferoglu, and V. Skachek. "Special issue on network coding.", 2017.

[MHL19] A. Masaracchia, D.B. Ha, and N.P. Le, "On the optimal user grouping in NOMA system technology." EAI Endorsed Transactions on Industrial Networks and Intelligent Systems, vol. 6, no. 20 (2019).

[Mol12] A. F. Molisch. Wireless communications, vol. 34, John Wiley & Sons, Chichester, 2012.

[Msh12] T. Mshvidobadze, "Evolution mobile wireless communication and LTE networks." 2012 6th International Conference on Application of Information and Communication Technologies (AICT), Oct. 17-19, Tbilisi, 2012.

[MV12] N. I. Miridakis, and D. D. Vergados. "A survey on the successive interference cancellation performance for single-antenna and multiple-antenna OFDM systems." IEEE Communications Surveys & Tutorials, vol. 15, no. 1 (2012): pp. 312-335.

[Nab02] S. M. Nabritt. "Modeling multipath in 802.11 systems." Comms Design online, http://www. commsdesign.com/story/OEG20021 008S0001 (2002).

[NAJ06] N. K. Noordin, B.M. Ali, S.S. Jamuar, T.A. Rahman, and M. Ismail. "Adaptive spatial mode of space–time and space frequency OFDM system over fading channels." Jurnal Teknologi, vol. 45, no. 1 (2006): pp. 59-76.

[NCL10] W. Nam, S.Y. Chung, and Y. H. Lee. "Capacity of the Gaussian two-way relay

channel to within 1/2 bit." IEEE Transactions on Information Theory, vol. 56, no. 11 (2010): pp. 5488-5494.

[NG11] B. Nazer, and M. Gastpar," Reliable physical layer network coding", Proceedings of the IEEE, vol. 99, no. 3 (2011): pp. 438-460.

[PLL17] H. Pan, L. Lu, and S. C. Liew. "Practical power-balanced non-orthogonal multiple access." IEEE Journal on Selected Areas in Communications, vol. 35, no. 10 (2017): pp. 2312-2327.

[PLW06] L. Ping, L. Liu, K. Wu, and W. K. Leung. "Interleave division multiple-access." IEEE Transactions on Wireless Communications, vol. 5, no. 4 (2006): pp. 938-947.

[PMR14] P. Popovski, G. Mange, A. Roos, T., Rosowski, G. Zimmermann, and J. Söder. "Deliverable D6. 3 intermediate system evaluation results." ICT-317669-METIS/D6. 3 (2014).

[Pop13] P. Popovski. " Deliverable D2.2 Novel radio link concepts and state of the art analysis. ", ICT-317669-METIS/D2.2 (2013).

[PWB18] T. Peng, Y. Wang, A. G. Burr, and M. Shikh-Bahaei. "A Physical layer network coding design for 5G network MIMO." 2018 IEEE Global Communications Conference (GLOBECOM). Dec. 9-13, Abu Dhabi, UAE, IEEE, 2018.

[R1-18] 3GPP, R1-1803615. "Key processing modules at transmitter side for NOMA".

[RBK14] R. Rajan, R. Baweja, and R. Kumar, "Review on Different Multiple Access Technique Used in Wireless Communication." International Journal of Research, vol. 1, no. 10 (2014): pp. 1335-1339.

[RBW14] K. Ratajczak, K. Bąkowski, and K. Wesołowski. "Two-way relaying for 5G systems: Comparison of network coding and MIMO techniques." 2014 IEEE Wireless Communications and Networking Conference (WCNC), May 6-9, Istanbul, IEEE, 2014.

[Rum13] M. Rumney (Ed.). "LTE and the evolution to 4G wireless: Design and measurement challenges," John Wiley & Sons, Chichester, 2013.

[SB18] J. Sykora, and A. Burr. "Wireless Physical Layer Network Coding". Cambridge University Press, Cambridge, 2018.

[SBK13] Y. Saito, A. Benjebbour, Y. Kishiyama, and T. Nakamura. "System-level performance evaluation of downlink non-orthogonal multiple access (NOMA)." 2013 IEEE 24th Annual International Symposium on Personal, Indoor, and Mobile Radio Communications (PIMRC), Sep. 8-11, London, IEEE, 2013.

[Sch05] M. Schwartz, "Mobile wireless communications. " Cambridge University Press, 2005.

[Sch13] A. Schwarzinger, “Digital Signal Processing in Modern Communication Systems,” Mary Lake, FL, 2013.

[Sha61] C. E. Shannon. "Two-way communication channels." Proceedings of the Fourth Berkeley Symposium on Mathematical Statistics and Probability, Volume 1: Contributions to the Theory of Statistics. The Regents of the University of California, 1961.

[Sin13] R. Singh, "Multiple access techniques for 4G mobile wireless networks,” International Journal of Engineering Research and Development (IJERD), vol. 5, no. 11 (2013): pp. 86-94.

[SM14] S. Sweta, and P. Malhan, "A Review Paper on Multiple Access Techniques for Mobile Communication.", International Journal of Innovative Research in Technology, vol. 1, no. 6 (2014): pp. 2349-6002.

[Spr10] A. Sprintson. "Network coding and its applications in communication networks." [in:] G. Cormode and M. Thottan (Eds.), Algorithms for Next Generation Networks. Computer Communication Networks, Springer, London, 2010: pp. 343-372.

[Stü17] G.L. Stüber. Principles of mobile communication. Spinger, 2017.

[SSC10] S. Sen, N. Santhapuri, R. R. Choudhury, and S. Nelakuditi. "Successive interference cancellation: A back-of-the-envelope perspective." Proceedings of the 9th ACM SIGCOMM Workshop on Hot Topics in Networks, Oct. 20-21, Monterey, 2010.

[SWY15] B. Sun, G. Wang, W. Yang, and L. Zheng, "Joint LDPC and physical layer network coding for two-way relay channels with different frequency offsets", 10th International Conference on Communications and Networking in China, Aug. 15-17, Shanghai, 2015: pp. 692-696.

[TAH16] H. Tabassum, M. S. Ali, E. Hossain, M. Hossain, and D.I. Kim. "Non-orthogonal multiple access (NOMA) in cellular uplink and downlink: Challenges and enabling techniques." arXiv preprint arXiv:1608.05783 (2016).

[TI15] S. Timotheou, and K. Ioannis. "Fairness for non-orthogonal multiple access in 5G systems." IEEE Signal Processing Letters, vol. 22, no. 10 (2015): pp. 1647-1651.

[Tom71] M. Tomlinson, "New Automatic Equalizer Employing Modulo Arithmetic", Electronics Letters, vol. 7, 1971: pp. 138-139.

[TR38] 3GPP, TR 38.812. "Study on Non-Orthogonal Multiple Access (NOMA) for NR".

[WCC16] C. L. Wang, J. Y. Chen, and Y. Chen. "Power allocation for a downlink non-orthogonal multiple access system." IEEE Wireless Communications Letters, vol. 5, no. 5 (2016): pp. 532-535.

[WCK04] Y. Wu, P. Chou, and S. Kung "Information exchange in wireless networks with network coding and physical layer broadcast," Technical Report MSR-TR-2004-78, Microsoft Research, Redmond WA, 2004.

[Wes09] K. Wesolowski. “Introduction to digital communication systems,” John Wiley & Sons, Chichester, 2009.

[WJP06] P. Wang, X. Jun, and L. Ping. "Comparison of orthogonal and non-orthogonal approaches to future wireless cellular systems." IEEE Vehicular Technology Magazine, vol. 1, no. 3 (2006): pp. 4-11.

[WNY16] Z. Wei, D. W. K. Ng, and J. Yuan. "Power-efficient resource allocation for MC-NOMA with statistical channel state information." 2016 IEEE Global Communications Conference (GLOBECOM), Dec. 4-8, Washington DC, IEEE, 2016.

[WQK13] M. Wildemeersch, T. Q. Quek, M. Kountouris, and C. H. Slump. " Successive interference cancellation in uplink cellular networks." 2013 IEEE 14th Workshop on Signal Processing Advances in Wireless Communications (SPAWC), Jun. 16-19, Darmstadt, IEEE, 2013.

[WQK14] M. Wildemeersch., T. Q. Quek, M. Kountouris, A. Rabbachinand, and C. H. Slump. "Successive interference cancellation in heterogeneous networks." IEEE Transactions on Communications, vol. 62, no. 12 (2014): pp. 4440-4453.

[WYN16] Z. Wei, J. Yuan, D. W. K. Ng, M. Elkashlan, and Z. Ding. "A survey of downlink non-orthogonal multiple access for 5G wireless communication networks." arXiv preprint arXiv:1609.01856 (2016).

[YLK18] X. Yue, Y. Liu, S. Kang, A. Nallanathanand, and Y. Chen. "Modeling and analysis of two-way relay non-orthogonal multiple access systems." IEEE Transactions on Communications, vol. 66, no. 9 (2018): pp. 3784-3796.

[YML12] H. Yang, W. Meng, B. Li and G. Wang, "Physical layer implementation of network coding in two-way relay networks", IEEE International Conference on Communications, Ad-hoc and Sensor Networking Symposium, Jun. 10-15, Ottawa, 2012: pp. 671-675.

[YRA11] K. Yasami, A. Razi, and A. Abedi, "Analysis of Channel Estimation Error in

Physical Layer Network Coding", IEEE Communications Letters, vol. 15, no. 10 (2011): pp. 1029-1031.

[YXP17] Z. Yang, W. Xu, C. Pan, Y. Pan, and M. Chen. "On the optimality of power allocation for NOMA downlinks with individual QoS constraints." IEEE Communications Letters, vol. 21, no. 7 (2017): pp. 1649-1652.

[YYL16] Z. Yuan, G. Yu, W. Li, Y. Yuan, X. Wang, and J. Xu. "Multi-user shared access for internet of things." 2016 IEEE 83rd Vehicular Technology Conference (VTC Spring), May 15-18, Nanjing, China, IEEE, 2016.

[YYY16] Y. Yuan, Z. Yuan, G. Yu, C. H. Hwang, P. K. Liao, A. Li, and K. Takeda. "Non-orthogonal transmission technology in LTE evolution." IEEE Communications Magazine, vol. 54, no. 7 (2016): pp. 68-74.

[ZH14] X. Zhang, and M. Haenggi. "The performance of successive interference cancellation in random wireless networks." IEEE Transactions on Information Theory, vol. 60, no. 10 (2014): pp. 6368-6388.

[ZL09] S. Zhang, and S.-Ch. Liew, "Channel coding and decoding in a relay system operated with physical-layer network coding", IEEE Journal on Selected Areas in Communications, vol. 27, no. 5 (2009): pp. 788-796.

[ZLL06] S. Zhang, S.C. Liew, and P.P. Lam. "Hot topic: Physical-layer network coding." Proceedings of the 12th annual international conference on Mobile computing and networking, Sep. 24-29, Los Angeles, 2006.

[ZMX16] Z. Zhang, Z. Ma, M. Xiao, Z. Ding, and P. Fan. "Full-duplex device-to-device-aided cooperative nonorthogonal multiple access." IEEE Transactions on Vehicular Technology, vol. 66, no. 5 (2016): pp. 4467-4471.

[ZWZ16] Y. Zhang, H.M. Wang, T. X. Zheng, and Q. Yang. "Energy-efficient transmission design in non-orthogonal multiple access," IEEE Transactions on Vehicular Technology, vol. 66, no. 3 (2016): pp. 2852-2857.

[ZY13] L. Zhou, and W. Yu. "Uplink multicell processing with limited backhaul via per-base-station successive interference cancellation." IEEE Journal on Selected Areas in Communications, vol. 31, no. 10 (2013): pp. 1981-1993.

[ZZL07] S. Zhang, Y. Zhu, S.-Ch. Liew and K. B. Lataief, "Joint design of network coding and channel decoding for wireless networks", IEEE Wireless Communications and Networking Conference, Mar. 11-15, Hong Kong, 2007: pp. 780-785.

[ZZM16] H. Zhang, D.K. Zhang, W.X. Meng, and C. Li. "User pairing algorithm with SIC in non-orthogonal multiple access system." 2016 IEEE International Conference

on Communications (ICC), May 23-27, Kuala Lumpur, IEEE, 2016.